NASA Technical Paper 2742

September 1987

Drag Measurements of Blunt Stores Tangentially Mounted on a Flat Plate at Supersonic Speeds

Floyd J. Wilcox, Jr.

NASA

NASA Technical Paper 2742

1987

Drag Measurements of Blunt Stores Tangentially Mounted on a Flat Plate at Supersonic Speeds

Floyd J. Wilcox, Jr.

Langley Research Center
Hampton, Virginia

National Aeronautics and Space Administration

Scientific and Technical Information Office

Summary

An experimental investigation has been conducted to measure the drag of blunt stores tangentially mounted in various arrays on a flat plate at supersonic speeds. The arrays consisted of two and three stores mounted in lateral, tandem, or staggered arrangements. The stores were cylinders with hemispherical noses and afterbodies. The relative positions of the stores in the arrays were varied while the drag of only one store was measured to determine the effect of spacing on the store-on-store interference. The wind-tunnel model consisted of a flat plate, filler plate, pallet, balance, and stores. Part of the filler plate was isolated from the plate and was identified as the pallet. The pallet was mounted on the balance such that the top surface of the pallet was flush with the plate surface. One of the stores was mounted on the metric pallet while the remaining stores were mounted on the nonmetric flat plate, thus allowing the drag of one store to be measured while the positions of the other nonmetric stores were varied. Store-on-store interference was determined by comparing the drag of a single store with the drag of the store in an array. The tests were conducted in the Langley Unitary Plan Wind Tunnel at nominal Mach numbers of 1.60, 1.90, 2.16, and 2.86 and at a nominal Reynolds number of 2×10^6 per foot.

The results of the investigation show the stores in both the two- and three-store lateral arrangements had favorable store-on-store interference (i.e., drag reduction). The drag of the stores was reduced approximately 10 to 20 percent below the store-alone drag at small lateral spacings (less than approximately 0.25 store diameters, store edge to store edge) and approached the store-along drag as the spacing was increased to one store diameter. Analysis of schlieren photographs and shadowgraphs suggests a principal factor in the drag reduction was probably boundary-layer separation ahead of the stores, which puts the stores in a reduced mean dynamic pressure region. In the two-store tandem arrangement, the aft store had a considerably larger drag reduction than the forward store. The drag reduction of the forward store was evident up to a spacing of 4.50 store diameters. The two-store staggered arrangement showed the drag of the stores was reduced approximately 5 to 15 percent below the store-alone drag at certain spacings, and no substantial benefit was obtained by staggering two stores compared with a lateral arrangement. The center store in the three-store staggered arrangements showed a substantial reduction (approximately 50 to 65 percent) in drag over the store-alone drag at certain spacings. Also, a substantial benefit was obtained by staggering three stores compared with a lateral arrangement. Finally, the store drag decreased substantially with Mach number for the tandem arrangement with the metric aft store.

Introduction

Mission requirements for future fighter aircraft will include sustained supersonic cruise capability. This requirement has resulted in the need for supersonic weapons carriage design guidelines to minimize the drag due to external stores. External stores have typically been carried on pylons in either a single mount, a multiple ejection rack (MER), or a triple ejection rack (TER) at subsonic and transonic speeds, but at supersonic speeds these methods cause unacceptable drag increases (ref. 1, 2, and 3). At supersonic speeds, external stores have been carried in conformal arrangements such as tangent or semisubmerged configurations, resulting in large reductions in store drag (refs. 2, 4, and 5). Part of this drag reduction is due to the stores being submerged in the aircraft boundary layer and part is due to the interference between the stores themselves and between the stores and the aircraft. Stores which are carried in tangent and semisubmerged configurations are usually carried in various arrays to take advantage of these effects.

A number of papers have been published which have studied the effects of carrying stores which were conformally mounted in arrays on various aircraft at supersonic speeds. (See refs. 6 to 10.) The typical experimental method used in these references for determining the store carriage drag of an aircraft with stores is to subtract the measured clean-aircraft drag from the drag of the aircraft with stores. One disadvantage of this method is the measured installed store carriage drag contains all the various drag components which contribute to the total installed carriage drag. These various components basically consist of the following terms (see ref. 6): store-on-aircraft interference drag, aircraft-on-store interference drag, isolated store drag, and store-on-store interference drag. Since it is not possible to separately measure these terms, the store-on-store interference cannot be determined. A second disadvantage, which can compromise the accuracy of the measurements, is that the balance used in the test must be chosen to measure the drag of the entire aircraft rather than just the stores. For example, in some semisubmerged configurations, the installed drag of the stores can be of the same magnitude as the balance accuracy, thus making the drag data questionable.

This paper presents the results of an experimental investigation that was conducted to measure the

drag of individual stores tangentially mounted in various arrays on a flat plate at supersonic speeds. In order to minimize or eliminate the disadvantages discussed in the previous paragraph, the present experimental investigation utilized a metric-generic store (a cylinder with a hemispherical nose and afterbody) mounted on a flat plate. The wind-tunnel model allowed the drag of the metric store to be measured with a one-component balance while nonmetric stores were positioned in various arrays around the metric store. In this manner, the measured store drag consisted of only the store-on-store interference drag plus the store-alone (single metric store mounted on flat plate) drag. From these measurements, the store-on-store interference was determined by comparing the store-alone drag with the drag of the store in an array. Accurate store drag measurements were obtained because the balance was chosen to measure the drag of only one store. The flat plate eliminated any interference effects due to the complicated flow field of an aircraft and provided a uniform two-dimensional flow field for all the store arrays tested. The store arrays used in the investigation consisted of either two or three stores mounted in lateral, tandem, or staggered arrangements. The tests were conducted at nominal Mach numbers of 1.60, 1.90, 2.16, and 2.86 and at a nominal Reynolds number of 2×10^6 per foot.

Symbols

A	store cross-sectional area, 0.001963 ft^2
C_D	store drag coefficient, $\frac{\text{Drag force}}{q_\infty A}$
d	store diameter, 0.60 in.
l	store length, 6.00 in.
M_∞	free-stream Mach number
q_∞	free-stream dynamic pressure, lb/ft^2
x	longitudinal distance between stores, in. (see fig. 5)
y	lateral distance between stores, in. (see fig. 5)

Apparatus and Experimental Methods

Model Description

A photograph and drawing of the flat plate are shown in figure 1. The model consisted of a sting-mounted flat plate that was 30.00 in. long with a maximum span of 34.00 in. The leading edge of the plate directly in front of the store models had a 0° sweep angle which provided a uniform two-dimensional boundary layer approaching the stores. The outboard leading edges were swept 30° to decrease the plate planform area to reduce starting loads and to position the tip vortices downstream in order to minimize their effect on the flat-plate flow field. In addition, sweeping the outboard leading edges ensured the Mach lines produced by the tips would propagate downstream of the metric store location. The leading-edge wedge angle (5°) was sufficiently small to allow supersonic attached flow to be maintained at the leading edge throughout the Mach number range.

A cavity which housed the balance and pressure tubing was located on the centerline of the plate and was covered by the filler plate as shown in figure 1(b). A photograph of the filler-plate region is shown in figure 2. A part of the filler plate was isolated from the plate and is identified as the pallet. The pallet was mounted on top of a one-component balance such that the top surface of the pallet was flush with the plate surface. A 0.015-in. air gap between the pallet and the filler plate allowed the plate-balance combination to deflect. Figure 3 is a photograph of the balance cavity with the filler plate and the metric store removed, exposing the pallet, the balance, and the pressure tubes. As shown in figures 1(b) and 3, a foam rubber seal was attached to the filler plate to prevent flow through the pallet and filler-plate gap. Four static-pressure orifices were located in the balance cavity to ensure negligible flow through the gap and the foam rubber seal. Three static-pressure orifices were located on the forward and aft lips of the pallet (as shown in fig. 3) to correct the drag data for pressure forces on the pallet. The tare for the foam rubber seal and the pressure tubes is discussed in the *Measurements and Corrections* section of this report. The balance cavity was vented to the plate surface with four multihole vent plates (see fig. 1(b)) to reduce the starting load normal force on the pallet and balance.

A sketch of the store shape tested is shown in figure 4. The store was a cylinder with a hemispherical nose and afterbody and had a length-to-diameter ratio of 10. The attachment screws for the nonmetric stores were inserted through machined slots, which aided in positioning the stores. The slots were covered with balsa wood inserts during the test. (See fig. 2.) Also shown in figure 2 are small holes in the filler plate and the surrounding plate which were used to mount the nonmetric stores in various positions. These holes were filled prior to testing.

The store arrays which were tested consisted of two and three stores mounted tangentially in lateral,

tandem, and staggered arrangements. Sketches of the various arrangements and listings of the spacings which were tested are shown in figure 5. Photographs of the various arrangements are shown in figure 6. Photographs of the devices used to align the stores in the various arrangements are shown in figure 7. The alignment bars and blocks enabled the stores to be aligned in yaw to within $\pm 0.05°$ and in lateral-longitudinal spacing to within ± 0.003 in.

Wind Tunnel and Test Conditions

The tests were conducted in the low Mach number test section of the Langley Unitary Plan Wind Tunnel (UPWT), which is a continuous flow, variable-pressure, supersonic wind tunnel with two test sections. The test sections are approximately 4 ft square and 7 ft long. The nozzle leading to the test section consists of an asymmetric sliding block which permits continuous variation of Mach number from 1.50 to 2.90 in the low Mach number test section. A complete description of the tunnel and its calibration can be found in reference 11.

The tests were conducted at the following conditions:

Mach number	Reynolds number, per foot	Stagnation pressure, lb/ft^2	Stagnation temperature, °F	Dynamic pressure, lb/ft^2
1.60	2×10^6	1079	125	455
1.90	↓	1154	↓	435
2.16	↓	1349	↓	439
2.86	↓	1934	↓	372

The tunnel air dew point was maintained below $-20°F$ to prevent condensation effects. The angle of attack of the flat plate was held constant at 0° throughout the entire test.

To ensure a fully turbulent boundary layer on the flat plate, grit-type boundary-layer transition strips were applied to the plate leading edge. The transition strips consisted of no. 35 sand grit (0.0215-in. nominal height) individually spaced along a line 0.4 in. aft of the leading edge measured streamwise. The distance between the sand grit particles was approximately 0.09 in. measured parallel to the plate leading edge. The grit size and location were selected using unpublished data from another similar flat-plate experiment conducted at the UPWT. Transition strips were not applied to the stores.

Measurements and Corrections

The store drag was measured with a one-component (axial force) electrical strain-gage balance. (See fig. 8.) All drag data have been corrected for the pressure drag on the pallet forward and aft lips, as discussed in the *Model Description* section. The tare from the foam rubber seal and the pressure tubes attached to the pallet was determined through two balance calibrations. The first balance calibration determined the sensitivity for the balance without any tare from the foam rubber seal or the pressure tubes. The second balance calibration determined the sensitivity for the balance with the pallet, the filler plate, and the pressure tubes installed in the test configuration. The balance sensitivity obtained during this calibration was linear and repeatable. From a comparison of the sensitivities from both balance calibrations, the tare from the foam rubber seal and the pressure tubes was determined to be 1.42 percent. All data have been corrected for this tare.

The pallet lip pressures and the balance cavity pressures were measured with a pressure scanner which was connected to a single pressure transducer. The tunnel stagnation pressure was measured independently with mercury manometers.

The uncertainty of the drag measurements was calculated with the method discussed in the appendix and are approximately as follows (in terms of drag coefficient):

M_∞	Uncertainty in C_D
1.60	± 0.017
1.90	$\pm .019$
2.16	$\pm .021$
2.86	$\pm .026$

The drag data are contained in table I.

Results and Discussion

The results from this investigation are divided into three major areas: lateral spacing effects, tandem spacing effects, and staggered spacing effects. Each of the three major areas is discussed in the following sections. The first section discusses the effects of lateral spacing on a two-store arrangement, on a three-store arrangement with the metric store in the middle position, and on a three-store arrangement with the metric store in the side position. (See fig. 5(a).) The second section discusses the effects of tandem spacing on a two-store arrangement with the metric store in the forward position and with the metric store in the aft position. (See fig. 5(b).) The final section discusses the effects of staggered spacing on a two-store arrangement and on a three store arrangement with the metric store in the middle position. (See fig. 5(c).) In the data figures, except where noted, the solid line represents the store-alone

(i.e., single metric store mounted on flat plate) drag while the symbols represent the drag of the metric store in the presence of the nonmetric stores.

Lateral Spacing Effects

Two stores. Figure 9 shows the effects of lateral spacing on the store-on-store interference for a two-store arrangement. The trend of the C_D data with increasing y/d at all Mach numbers shows a significant drag reduction at the smallest spacing tested ($y/d = 0.125$) and an increase in drag as the stores are separated. At a separation distance of one store diameter ($y/d = 1.000$), the drag of the metric store is approximately the store-alone value. The maximum percentage drag reduction with respect to the store-alone drag occurs at the smallest spacing tested ($y/d = 0.125$) for all Mach numbers, and the reductions are as follows:

M_∞	y/d	Drag reduction, percent
1.60	0.125	13
1.90	↓	20
2.16	↓	22
2.86	↓	23

The favorable store-on-store interference obtained during this test is contrary to past published data for empirical prediction factors such as those used in the DATCOM/Hoerner method (described in appendix C of ref. 6). This result is probably due to the store shape differences between the present test and the test data used to obtain some of the empirical prediction factors used in the DATCOM/Hoerner method.

Figure 10 shows the effects of Mach number on C_D range from a maximum C_D decrease of 6 percent with increasing M_∞ at $y/d = 0.125$ to a minimum C_D decrease of 2 percent at $y/d = 0.400$. The effect of Mach number on C_D for the store alone is an 8-percent increase as M_∞ increases.

A typical schlieren photograph (knife-edge horizontal) and shadowgraph are shown in figure 11 to illustrate the various points discussed in the flow visualization photographs which are presented in this report. Schlieren photographs of the two-store lateral spacing arrangement are shown in figure 12. Comparison of the schlierens shows the separation shock ahead of the store nose bow shock is stronger and originates farther upstream for the two-store lateral spacing arrangement than for the store alone. This indicates more extensive boundary-layer separation farther upstream of the stores positioning a larger percentage of the store height in the reduced mean dynamic pressure region and thus reducing the store drag. As the separation distance is increased, the separation shock origination point moves downstream, an indication the boundary-layer separation point moves downstream. This reduces the percentage of the store height submerged in the reduced mean dynamic pressure region, thus increasing the store drag. A reattachment shock forms aft of the stores as the flow expands over the store afterbody and flows parallel with the flat-plate surface. At $M_\infty = 1.60$ and 2.86 for store separation distances of $y/d \leq 0.500$ and for the store alone, the reattachment shock appears to be formed at some distance from the plate surface by a coalescing of weak compression waves. At the larger store spacings ($y/d = 0.750$ and 1.000), the reattachment shock appears to form near the plate surface aft of the stores and does not appear to be formed from a series of weak compression waves. At $M_\infty = 1.90$ and 2.16, the reattachment shock appears to form near the plate surface aft of the stores for all spacings. In addition, the store-alone schlierens at these two Mach numbers do not show any clear reattachment shock formation. Finally, the drag of the store alone and the metric store in the two-store lateral spacing arrangement ($y/d = 1.000$) are approximately equal whereas their schlieren photographs are different.

Three stores with metric middle store. Figure 13 shows the effects of lateral spacing on the store-on-store interference for a three-store arrangement with the metric store in the middle position. The trend of the C_D data with increasing y/d shows a relatively flat curve at small spacings ($y/d \lessapprox 0.300$), then an increase in C_D as the separation distance increases followed by an apparent leveling off to approximately the store-alone C_D at $y/d \approx 1.000$. At $M_\infty = 1.60$, the drag of the middle store is slightly higher than that of the store alone for $y/d \gtrapprox 0.750$, whereas at all other Mach numbers the drag is still slightly below the store-alone drag. The maximum percentage of drag reduction with respect to the store-alone drag occurs at a spacing of $y/d = 0.250$ at all Mach numbers, as shown below:

M_∞	y/d	Drag reduction, percent
1.60	0.250	8
1.90	↓	17
2.16	↓	21
2.86	↓	26

The effects of Mach number on C_D range from a maximum C_D reduction of 15 percent for $y/d = 0.250$ to a minimum C_D reduction of 2 percent at $y/d = 0.750$, as shown in figure 14.

Three stores with metric side store. Figure 15 shows the effects of lateral spacing on the store-on-store interference for a three-store arrangement with the metric store in the side position. The general trend and magnitude of the data are similar to the data for the three-store lateral spacing arrangement with the metric store in the middle position. At small spacings ($y/d \lessapprox 0.300$), the data show a relatively flat curve before increasing and apparently leveling off to the store-alone drag at $y/d \approx 1.000$. Although additional data for $y/d > 1.000$ would be helpful in determining where the metric store drag reaches the store alone value, the flat plate used in this investigation was not configured for three-store lateral spacings of $y/d > 1.000$. The maximum percentage of drag reduction with respect to the store-alone drag occurs at a spacing of $y/d = 0.125$ at all Mach numbers, as shown below:

M_∞	y/d	Drag reduction, percent
1.60	0.125	12
1.90	↓	18
2.16		21
2.86		23

As shown in figure 16, the effects of Mach number on C_D range from a maximum C_D decrease of 6 percent with increasing M_∞ for $y/d = 0.125$ to a minimum C_D decrease of 2 percent for $y/d = 0.400$.

Schlieren photographs of the three-store lateral spacing arrangement are shown in figure 17. The effects seen in the schlierens for the three-store lateral spacing arrangement are similar to those seen in the two-store lateral spacing arrangement.

Lateral arrangement comparisons. Shown in figure 18 are typical shadowgraphs of the store-alone and the two- and three-store lateral spacing arrangements. These shadowgraphs show basically the same results as the schlieren photographs, except that more detail of the flow at the store nose is provided for comparison. The separation shock ahead of the store nose bow shock is stronger for the three-store lateral spacing arrangement than for the two-store lateral spacing arrangement, both of which are stronger than the store-alone separation shock. This indicates more extensive boundary-layer separation ahead of the three-store lateral spacing arrangement than the two-store lateral spacing arrangement. The more extensive boundary-layer separation ahead of the three-store lateral spacing arrangement generally reduces the drag of these stores slightly more than it reduces the drag of the stores in the two-store lateral spacing arrangement. Thus, the shadowgraphs and the previous schlieren photographs indicate one of the principal factors influencing the favorable store-on-store interference for the lateral spacing arrangements is probably the boundary-layer separation ahead of the stores.

Tandem Spacing Effects

Two stores with metric forward store. Figure 19 shows the effects of tandem spacing on the store-on-store interference for a two-store arrangement with the metric store in the forward position. The drag of the forward store is less than the store-alone drag for a longitudinal spacing of $x/d \leq 3.000$, indicating favorable interference, and is approximately the store-alone value at $x/d = 4.500$. The C_D data generally show a slight increase as the stores are separated from $x/d = 0.250$ to 3.000, although the data show some scatter. The reason for this scatter is unknown, although it could be due to unsteady flow around the forward store. Since no other data contained in this report show this type of scatter, it is probably not due to the balance instrumentation. The maximum percentage of drag reduction of the forward store with respect to the store-alone drag occurs at $x/d = 0.500$ at all Mach numbers except $M_\infty = 2.86$, for which it occurs at $x/d = 2.000$ (probably because of data scatter), as shown below:

M_∞	x/d	Drag reduction, percent
1.60	0.500	15
1.90	.500	14
2.16	.500	12
2.86	2.000	12

The favorable store-on-store interference is probably caused by the reduced base pressure drag due to the presence of the aft store. In figure 20 the effects of Mach number on C_D show the same trends at all values of x/d. The value of C_D increases with increasing M_∞ a maximum of 12 percent for $x/d = 0.500$ to a minimum of 7 percent for $x/d = 4.500$.

Two stores with metric aft store. Figure 21 shows the effects of tandem spacing on the store-on-store interference for a two-store arrangement with the

metric store in the aft position. Because the forward store was positioned in front of the metric store, the nose of the forward store moved closer to the plate leading edge as x/d increased, thereby varying the height of the boundary layer approaching the forward store for each spacing tested. The drag of the aft store is reduced substantially from the store-alone drag at $x/d = 0.250$, as shown below (percentage based on store-alone drag):

M_∞	x/d	Drag reduction, percent
1.60	0.250	70
1.80	↓	76
2.16		79
2.86		85

The drag increases slightly from $x/d = 0.250$ to 2.000 before increasing at a faster rate between $x/d = 2.000$ and 3.000. The drag of the aft store is still substantially below the store-alone drag at $x/d = 3.000$, as shown below (percentage based on store-alone drag):

M_∞	x/d	Drag reduction, percent
1.60	3.000	47
1.90	↓	57
2.16		62
2.86		57

The drag reduction of the aft store is probably due to the store being in the wake (reduced mean dynamic pressure region) of the forward store and also to insufficient spacing between the stores to allow the flow to expand into the gap between the stores, thereby eliminating the bow shock and the associated high pressures on the nose of the aft store. This can be seen in the schlieren photographs which are discussed in the next paragraph. As shown in figure 22, the effects of Mach number on C_D range from a maximum C_D decrease of 46 percent with increasing M_∞ for $x/d = 1.000$ to a minimum C_D decrease of 22 percent for $x/d = 3.000$. Although the magnitude of the drag variation for a given store spacing as M_∞ varies is approximately the same as for the other store arrangements, the large percentage of drag reduction is mainly due to the relatively small drag of the metric store in the aft position of the tandem arrangement.

Schlieren photographs of the two-store tandem spacing arrangement are shown in figure 23. As the stores are separated, the flow begins to expand into the gap between the stores before exiting the gap through a series of weak compression waves which coalesce into a shock wave above the stores. Since a bow shock does not form on the aft store at any spacing, the high pressures on the nose of the aft store associated with a bow shock are eliminated, thereby reducing the store drag.

Staggered Spacing Effects

Two stores. Figure 24 shows the effects of staggered spacing on the store-on-store interference for a two-store arrangement which had a constant lateral spacing of 0.5 store diameters. The trend of the C_D data with increasing x/l is a sinusoidal shape with decreasing amplitude as M_∞ increases. At all Mach numbers except 2.86, the minimum drag occurs at a longitudinal spacing of $x/l = -0.50$ and the maximum drag, which is approximately equal to the store-alone drag, occurs at $x/l = 0.50$. At $M_\infty = 2.86$, the drag of the metric store is slightly less than the store-alone drag for $x/l \leq 0$ before increasing to approximately the store-alone drag at $x/l = 0.500$ followed by a slight decrease in drag at $x/l = 1.000$. The maximum percentage of drag reduction with respect to the store-alone drag occurs at $x/l = -0.5$ for all Mach numbers except $M_\infty = 2.86$, as shown below:

M_∞	x/l	Drag reduction, percent
1.60	−0.500	12
1.90	−.500	14
2.16	−.500	12
2.86	1.000	7

For longitudinal spacings of $x/l > 0$, the drag of the metric store is probably affected by a reduction in base drag whereas for $x/l \leq 0$ the drag of the metric store is probably influenced by boundary-layer separation ahead of the stores, as indicated in the schlieren photographs discussed in the next paragraph. The effects of Mach number on C_D range from a maximum C_D decrease of 13 percent for increasing M_∞ at $x/l = -0.500$ to a minimum C_D decrease of 5 percent for $x/l = 0.500$, as shown in figure 25.

Schlieren photographs of the two-store staggered spacing arrangement are shown in figure 26. At $M_\infty = 1.60$ and $x/l = -0.500$, the intersection of the separation shock with the nose bow shock of the metric store can be seen. At the higher Mach numbers, the separation shock is probably hidden by

the nonmetric store. Similar to the lateral spacing arrangements, the boundary-layer separation ahead of the metric store for $x/l \leq 0$ probably is a factor in the drag reduction.

Three stores with metric middle store. Figure 27 shows the effects of staggered spacing on the store-on-store interference for a three-store arrangement with the metric store in the middle position and which had a constant lateral spacing of 0.5 store diameters. The data are similar to those of the two-store staggered spacing arrangement except the amplitude of the sinusoidal shape is much larger. At all Mach numbers, the minimum drag occurs at $x/l = -0.500$ and the maximum drag occurs at $x/l = 0.500$. The maximum drag is approximately the store-alone drag at all Mach numbers except $M_\infty = 1.60$, for which the maximum drag is greater than the store-alone drag. The maximum percentage of drag reduction with respect to the store-alone drag occurs at $x/l = -0.500$, as shown below:

M_∞	x/l	Drag reduction, percent
1.60	−0.500	53
1.90	↓	58
2.16		61
2.86		66

Figure 28 shows the effects of Mach number on C_D range from a maximum C_D decrease of 26 percent with increasing M_∞ for $x/l = -1.000$ and -0.500 to a minimum C_D decrease of 6 percent for $x/l = 0.500$. The large percentage of drag variation for $x/l = -1.000$ to -0.500 is mainly due to the small drag of the metric store.

Schlieren photographs of the three-store staggered spacing arrangement are shown in figure 29. At $M_\infty = 1.60$ and 1.90 and $x/l = -1.000$ and -0.500, the intersection of the separation shock with the nose bow shock of the metric store can be seen. At the higher Mach numbers, the separation shock is probably hidden by the nonmetric stores. Similar to the two-store staggered spacing arrangement, the schlieren photographs indicate boundary-layer separation is probably a principal factor in the drag reduction of the metric store for $x/l \leq 0$. In addition, the bow shocks from the two side stores intersecting ahead of the metric store could affect the boundary layer and therefore be a factor in the drag reduction. Schlieren photographs for $M_\infty = 2.86$ and $x/l = -1.000$ and -0.500 show a second shock directly behind the bow shocks of the forward stores. The second shock indicates the intersection of the two bow shocks.

Total configuration drag. The drag of each individual store in an arrangement can be summed, and thus the total drag of the arrangement can be determined and the lowest drag arrangement identified. Inspection of the lateral (two and three stores) and tandem spacing plots (figs. 9, 13, 15, 19, and 21) shows the lowest total configuration drag arrangement would occur at the smallest lateral spacing ($y/d = 0.125$) and the smallest tandem spacing ($x/d = 0.250$). Since the two- and three-store staggered arrangements have a sinusoidal variation in the metric-store drag, it is difficult to determine the arrangement which has the lowest drag strictly from the inspection of the drag plots.

Figure 30 shows the total configuration drag of the two-store staggered spacing arrangement with a constant lateral spacing of 0.5 store diameters. The data are obtained from figure 24 by summing the drag for $x/l = 1.000$ and -1.000 and for $x/l = 0.500$ and -0.500 and by doubling the drag for $x/l = 0$. These data are shown compared with the drag of two stores which had no store-on-store interference; this is indicated as "double store alone." The results indicate that, at all Mach numbers except $M_\infty = 1.60$, staggering two stores ($x/l = 1.000$ and 0.500) increases the total configuration drag compared with a lateral arrangement ($x/l = 0$), as shown below (percentage reduction based on the lateral arrangement drag):

M_∞	x/l	Drag reduction, percent
1.60	1.000	2
1.90	1.000	−1
2.16	1.000	−3
2.86	.500	−2

Figure 31 shows the total configuration drag of the three-store staggered spacing arrangement with a constant lateral spacing of 0.50 store diameters. The data are obtained by summing the drag of the middle store from the three-store staggered spacing arrangement (see fig. 27) and doubling the values from the two-store staggered spacing arrangement (see fig. 24) to account for the side stores. The two-store staggered data are used because the drag of the side stores in the three-store staggered spacing arrangement were not measured during this investigation. The use of the the two-store staggered data is probably a reasonable assumption because the side stores

were two store diameters apart and their influence on each other is small, as shown in the results for the two-store lateral spacing arrangement (fig. 9). These results show that, at one store diameter, the stores have virtually no effect on each other. These data are compared with the drag of three individual stores which have no store-on-store interference, and this is indicated as "triple store alone." The results indicate that at a longitudinal spacing of $x/l = -1.000$ (i.e., noses of side stores forward of the nose of the middle store), a significant percentage of drag reduction is obtained with respect to the lateral spacing arrangement ($x/l = 0$), as shown below:

M_∞	x/l	Drag reduction, percent
1.60	−1.000	13
1.90	↓	11
2.16	↓	11
2.86	↓	15

These large drag reductions are principally due to the low drag of the middle store rather than the drag of the side stores.

Conclusions

An experimental investigation has been conducted to measure the drag of blunt stores (cylinders with hemispherical noses and afterbodies) tangentially mounted in various arrays on a flat plate at supersonic speeds. The arrays consisted of either two or three stores mounted in lateral, tandem, or staggered arrangements. The relative positions of the stores in the arrays were varied while the drag of only one store was measured to determine the effect of spacing on the store drag. Store-on-store interference was determined by comparing the drag of a single store with the drag of the store in an array. The tests were conducted at nominal Mach numbers of 1.60, 1.90, 2.16, and 2.86 and at a nominal Reynolds number of 2×10^6 per foot.

The following is a summary of the significant results:

1. All the stores in both the two- and three-store lateral spacing arrangements had favorable interference for spacings less than one store diameter, and the drag was nearly equal to the store-alone drag at a spacing of approximately one store diameter.

2. In the three-store lateral spacing arrangement, both the middle and side stores had approximately the same drag for all spacings.

3. Boundary-layer separation, as evidenced from schlieren photographs and shadowgraphs, was probably a principal factor in the drag reduction for the two- and three-store lateral spacing arrangements.

4. The drag reduction of the aft store in the two-store tandem spacing arrangement was significantly greater than the drag reduction of the forward store at all spacings.

5. The drag reduction of the stores in a two-store staggered spacing arrangement had a sinusoidal shape and was relatively small at most spacings, whereas the drag reduction of the middle store in the three-store staggered spacing arrangement also had a sinusoidal shape but with a significant drag reduction at most spacings.

6. For the total configuration drag (sum of the drag of all the individual stores), no significant drag reduction was obtained by staggering two stores (with 0.50 store diameter lateral spacing) when compared with a lateral arrangement.

7. Significant reduction in total configuration drag was obtained by staggering three stores (with 0.50 store diameter lateral spacing) compared with a lateral arrangement when the noses of the two side stores were forward of the middle store nose.

8. The effects of Mach number on the store drag showed a substantial percentage decrease in drag for the tandem arrangement with the metric aft store. For the other arrangements, there was generally less than a 15-percent variation in drag over the Mach numbers tested.

Appendix

Experimental Data Uncertainty Analysis

The uncertainty of the drag measurements was calculated with the method discussed in reference 12. For this investigation, the experimental drag coefficient was calculated from five variables as follows:

$$C_D = C_D(p_t, D, p_{fl}, p_{al}, M)$$

$$= \frac{D + (p_{al} - p_{fl})A_l}{0.7M^2 p_t(1 + 0.2M^2)^{-3.5}A}$$

where

A store cross-sectional area, 0.001963 ft^2

A_l pallet lip area, 0.001304 ft^2

D drag force, lb

M Mach number

p_{al} static pressure on pallet aft lip, lb/ft^2

p_{fl} static pressure on pallet forward lip, lb/ft^2

p_t free-stream stagnation pressure, lb/ft^2

The uncertainty in C_D because of the uncertainty in each of the five variables used to calculate C_D is

$$\omega_{C_D} = \left[\left(\frac{\partial C_D}{\partial p_t}\omega_{p_t}\right)^2 + \left(\frac{\partial C_D}{\partial D}\omega_D\right)^2 + \left(\frac{\partial C_D}{\partial p_{fl}}\omega_{p_{fl}}\right)^2 + \left(\frac{\partial C_D}{\partial p_{al}}\omega_{p_{al}}\right)^2 + \left(\frac{\partial C_D}{\partial M}\omega_M\right)^2\right]^{1/2} \quad \text{(A1)}$$

where

ω_{C_D} uncertainty in C_D

ω_{p_t} uncertainty in the measured p_t, ± 1.0 lb/ft^2

ω_D uncertainty in the measured D, ± 0.0125 lb

$\omega_{p_{fl}}$ uncertainty in the measured p_{fl}, ± 3.6 lb/ft^2

$\omega_{p_{al}}$ uncertainty in the measured p_{al}, ± 3.6 lb/ft^2

ω_M uncertainty in M (from ref. 11), ± 0.02

The uncertainty in C_D was calculated for each data point with equation (A1), and the largest uncertainty in C_D at each Mach number is as follows:

M_∞	Uncertainty in C_D
1.60	± 0.017
1.90	$\pm .019$
2.16	$\pm .021$
2.86	$\pm .026$

References

1. Haines, A. B.: Prospects for Exploiting Favourable and Minimising Adverse Aerodynamic Interference in External Store Installations. *Subsonic/Transonic Configuration Aerodynamics,* AGARD-CP-285, Sept. 1980, pp. 5-1–5-25.
2. Bradley, Richard G.: Practical Aerodynamic Problems—Military Aircraft. *Transonic Aerodynamics*, David Nixon, ed., American Inst. Aeronaut. & Astronaut., c.1982, pp. 149–187.
3. Poisson-Quinton, Ph.: Parasitic and Interference Drag Prediction and Reduction. *Aircraft Drag Prediction and Reduction,* AGARD-R-723, July 1985, pp. 6-1–6-27.
4. Agnew, J. W.; and Weber, W. B.: Tangential Weapons Carriage on a High Performance Fighter Aircraft. *Store Airframe Aerodynamics,* AGARD-CP-389, Aug. 1986, pp. 21-1–21-9.
5. Nichols, James H., Jr.; and Martin, C. Joseph: *Conformal Weapons Carriage—Joint Service Development Program.* NSRDC-4027, U.S. Navy, Dec. 1971. (Available from DTIC as AD 909 716L.)
6. Wilcox, Floyd J., Jr.: *Store Carriage Drag Measurements for an Advanced Fighter Aircraft at Supersonic Speeds.* NASA TP-2521, 1985.
7. Brigulio, J. A.; Halt, G. E.; Dyer, R. D.; and Grove, J. E.: Effects of Air-to-Air Missile Integrations on Longitudinal Aerodynamic Characteristics of a Delta Wing Fighter. *Store Airframe Aerodynamics*, AGARD-CP-389, Aug. 1986, pp. 28-1–28-8.
8. Mathews, Charles B.; Korn, Stephen C.; and Studwell, Victor E.: *Evaluation of the Conformal Carriage Concept on the Performance and Basic Static Longitudinal Stability of the F-4E Aircraft.* AFATL-TR-71-76, U.S. Air Force, July 1971. (Available from DTIC as AD 889 648L.)
9. Dollyhigh, Samuel M.; Sangiorgio, Giuliana; and Monta, William J.: *Effects of Stores on Longitudinal Aerodynamic Characteristics of a Fighter at Supersonic Speeds.* NASA TP-1175, 1978.
10. Monta, William J.: *Effect of Conventional and Square Stores on the Longitudinal Aerodynamic Characteristics of a Fighter Aircraft Model at Supersonic Speeds.* NASA TM-81791, 1980.
11. Jackson, Charlie M., Jr.; Corlett, William A.; and Monta, William J.: *Description and Calibration of the Langley Unitary Plan Wind Tunnel.* NASA TP-1905, 1981.
12. Holman, J. P.: *Experimental Methods for Engineers, Third ed.* McGraw-Hill Book Co., c.1978.

Table I. Drag Data

(a) Two-store lateral spacing (see fig. 5(a))

Spacing, y/d	C_D at Mach numbers of—			
	1.60	1.90	2.16	2.86
Store alone	0.944	1.009	1.028	1.009
.125	.823	.812	.802	.774
.250	.851	.861	.871	.873
.400	.897	.903	.912	.904
.500	.906	.922	.932	.946
.750	.934	.952	.981	.984
1.000	.949	.965	.989	.990

(b) Three-store lateral spacing with metric store in middle position (see fig. 5(a))

Spacing, y/d	C_D at Mach numbers of—			
	1.60	1.90	2.16	2.86
Store alone	0.944	1.009	1.028	1.009
.125	.876	.840	.819	.750
.250	.873	.836	.815	.746
.400	.882	.845	.833	.812
.500	.899	.886	.879	.836
.750	.959	.950	.951	.937
1.000	.980	.977	.987	.952

(c) Three-store lateral spacing with metric store in side position (see fig. 5(a))

Spacing, y/d	C_D at Mach numbers of—			
	1.60	1.90	2.16	2.86
Store alone	0.944	1.009	1.028	1.009
.125	.827	.826	.812	.774
.250	.840	.825	.821	.814
.400	.873	.868	.872	.855
.500	.878	.888	.897	.914
.750	.914	.933	.956	.950
1.000	.957	.975	.999	.989

Table I. Continued

(d) Two-store tandem spacing with metric store in forward position (see fig. 5(b))

Spacing, x/d	C_D at Mach numbers of—			
	1.60	1.90	2.16	2.86
Store alone	0.944	1.009	1.028	1.009
.250	.820	.879	.920	.906
.500	.803	.863	.903	.917
1.000	.827	.888	.924	.912
1.500	.828	.886	.923	.925
2.000	.819	.879	.912	.891
2.500	.881	.928	.956	.955
3.000	.899	.963	.971	.975
4.500	.963	1.014	1.037	.999

(e) Two-store tandem spacing with metric store in aft position (see fig. 5(b))

Spacing, x/d	C_D at Mach numbers of—			
	1.60	1.90	2.16	2.86
Store alone	0.944	1.009	1.028	1.009
.250	.281	.243	.212	.152
.500	.302	.257	.228	.166
1.000	.357	.308	.271	.192
2.000	.395	.334	.292	.214
3.000	.501	.434	.389	.431

(f) Two-store staggered spacing ($y/d = 0.500$) (see fig. 5(c))

Spacing, x/l	C_D at Mach numbers of—			
	1.60	1.90	2.16	2.86
Store alone	0.944	1.009	1.028	1.009
−1.000	.882	.934	.969	.969
−.500	.832	.863	.908	.955
.000	.906	.922	.932	.946
.500	.957	.997	1.010	.982
1.000	.889	.933	.956	.943

Table I. Concluded

(g) Three-store staggered spacing with metric store in middle position ($y/d = 0.500$) (see fig. 5(c))

Spacing, x/l	C_D at Mach numbers of—			
	1.60	1.90	2.16	2.86
Store alone	0.944	1.009	1.028	1.009
−1.000	.571	.557	.531	.421
−.500	.464	.426	.402	.345
.000	.899	.886	.879	.836
.500	.997	1.037	1.042	.977
1.000	.740	.870	.841	.827

L-87-3154

(a) Model mounted in wind tunnel.

Figure 1. Flat-plate model description.

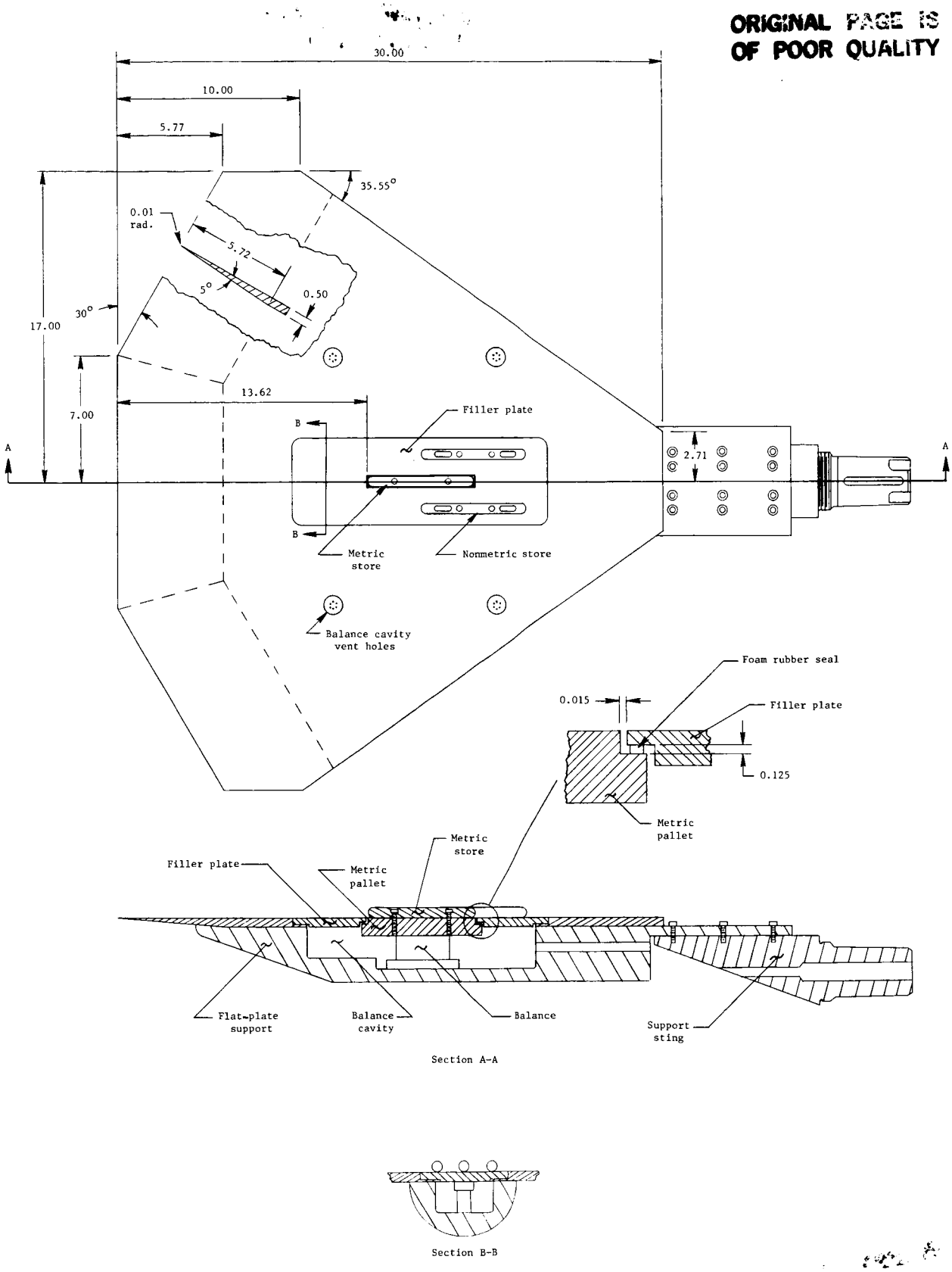

(b) Flat-plate dimensions. All linear dimensions are in inches.

Figure 1. Concluded.

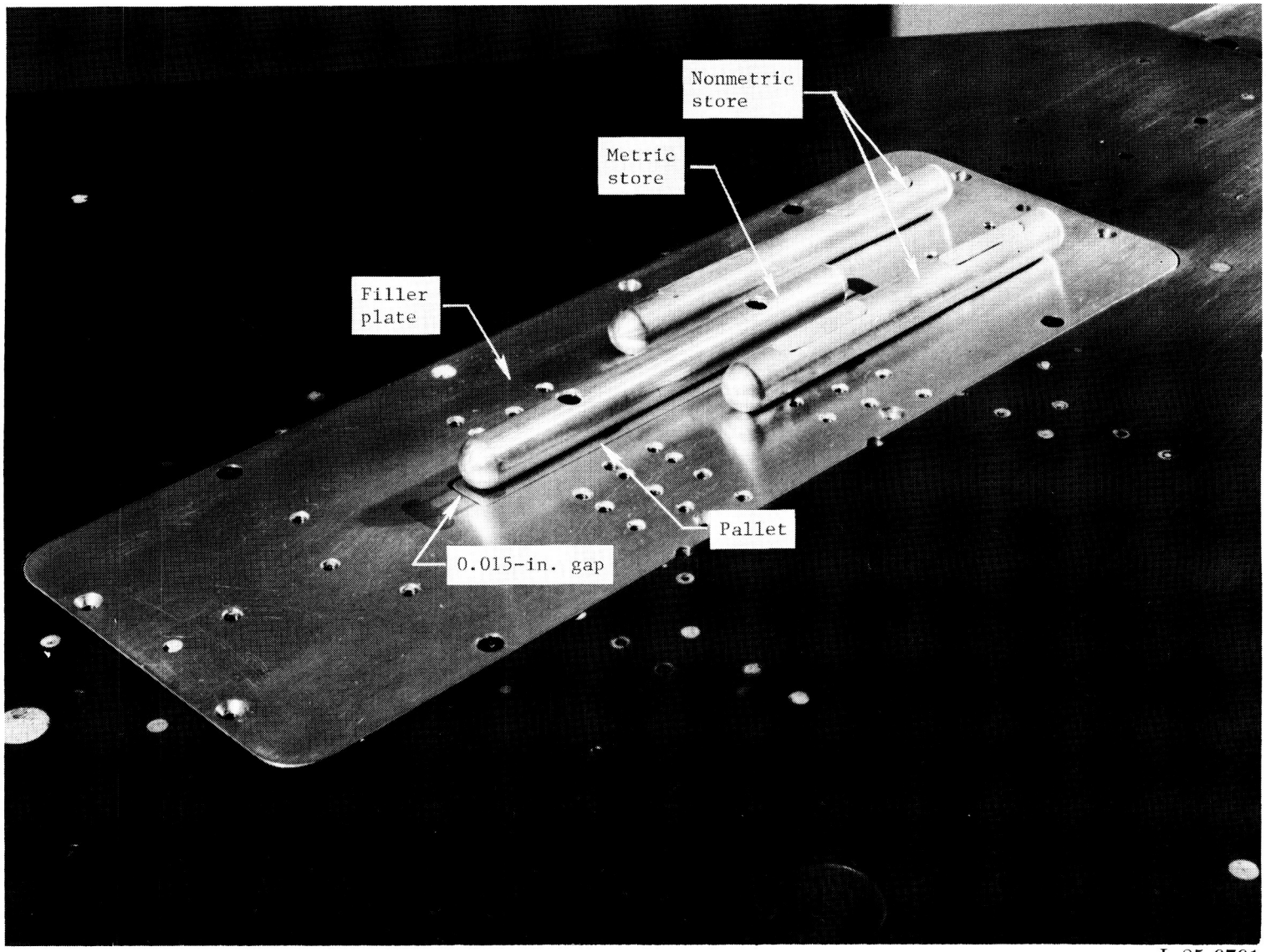

L-85-6761

Figure 2. Stores and filler-plate area.

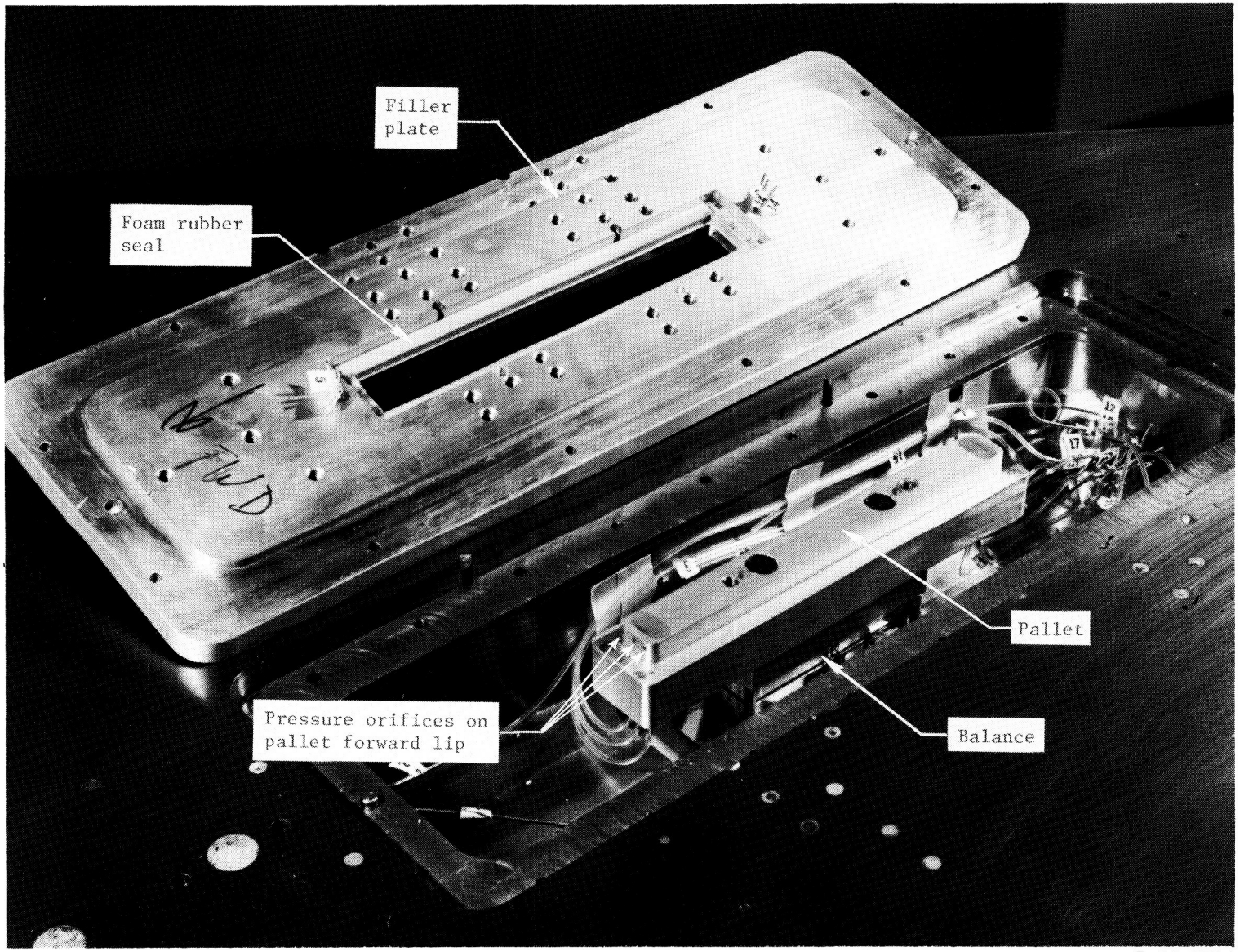

L-85-6764

Figure 3. Balance cavity with filler plate removed.

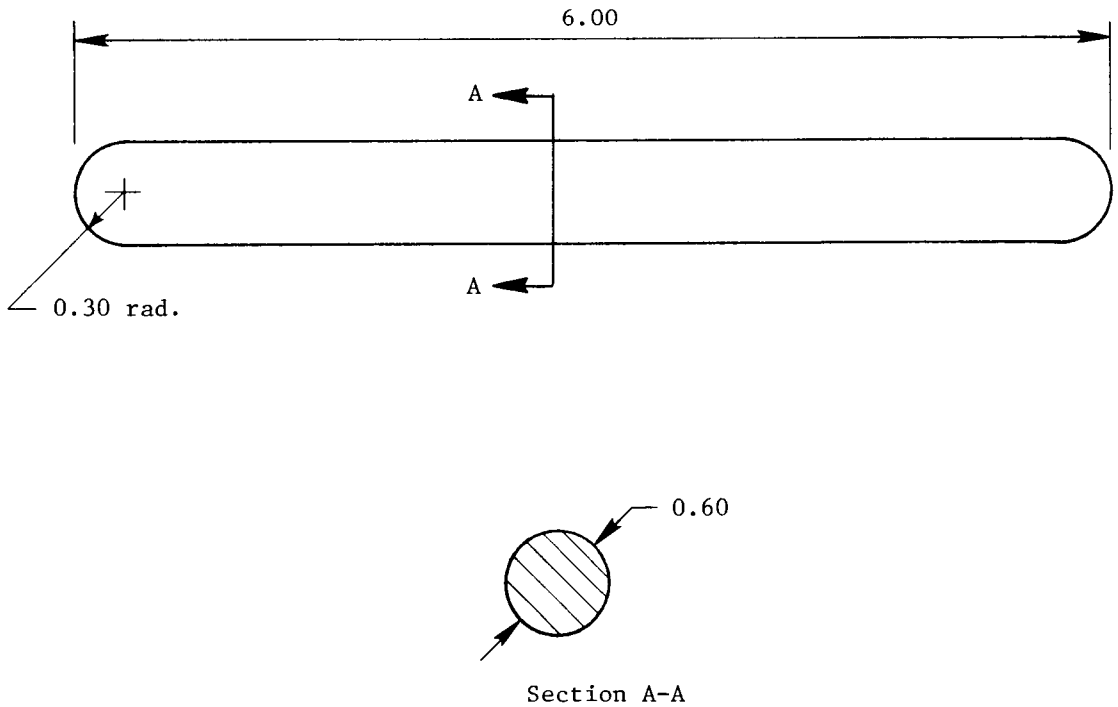

Figure 4. Sketch of store geometry. All dimensions are in inches.

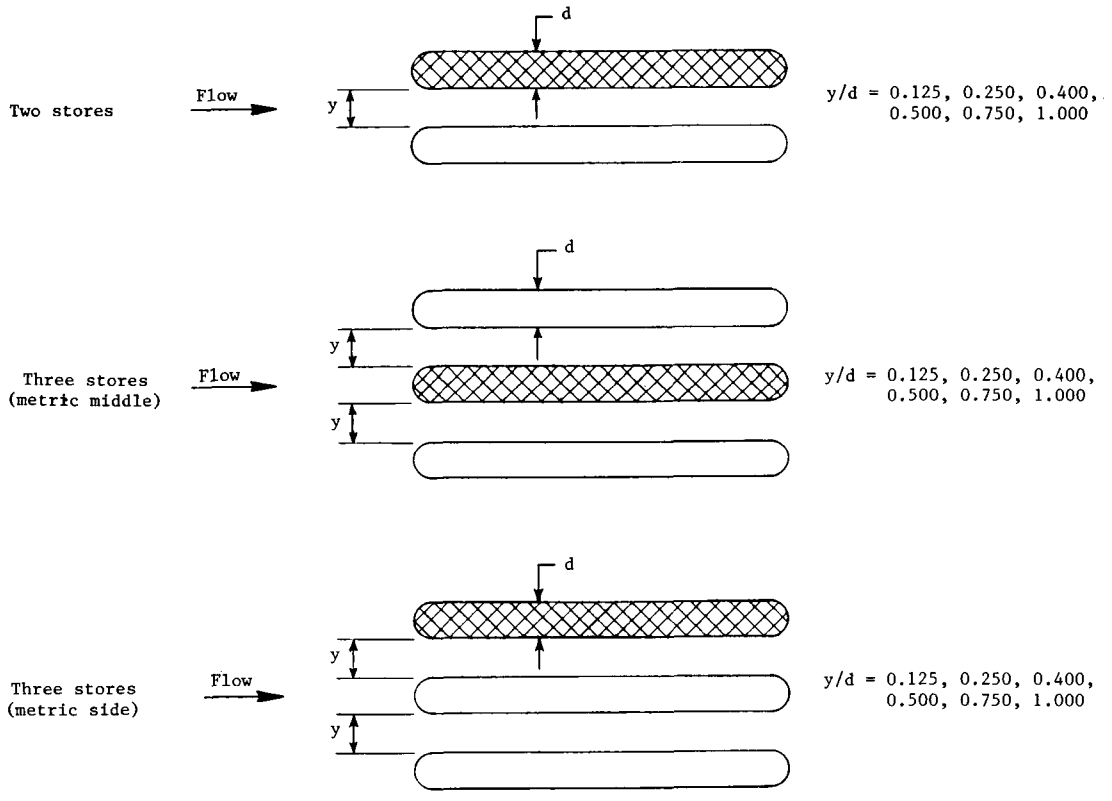

(a) Lateral spacing arrangements.

Figure 5. Store arrangement details. Metric store is shaded.

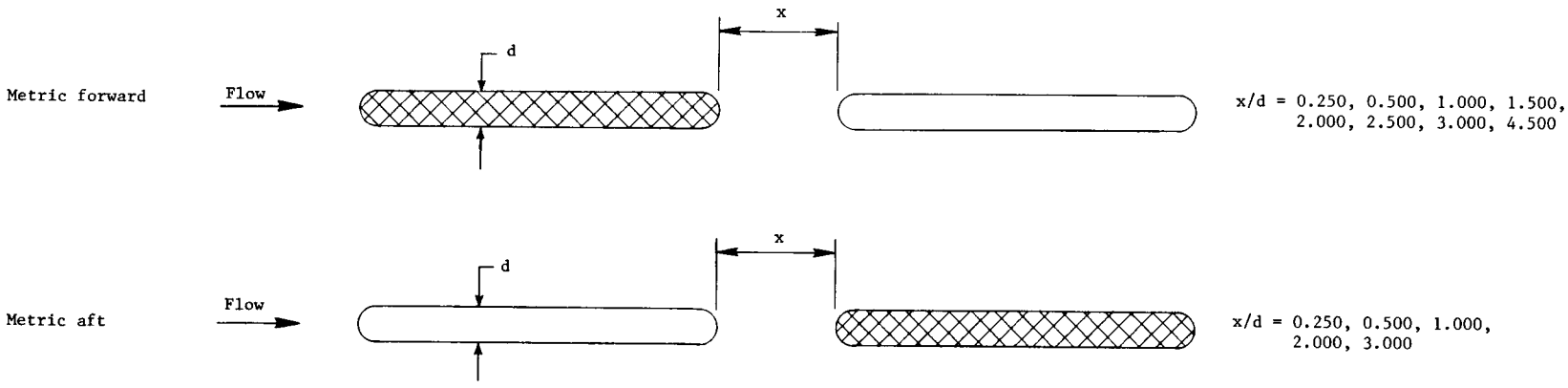

(b) Tandem spacing arrangements.

Figure 5. Continued.

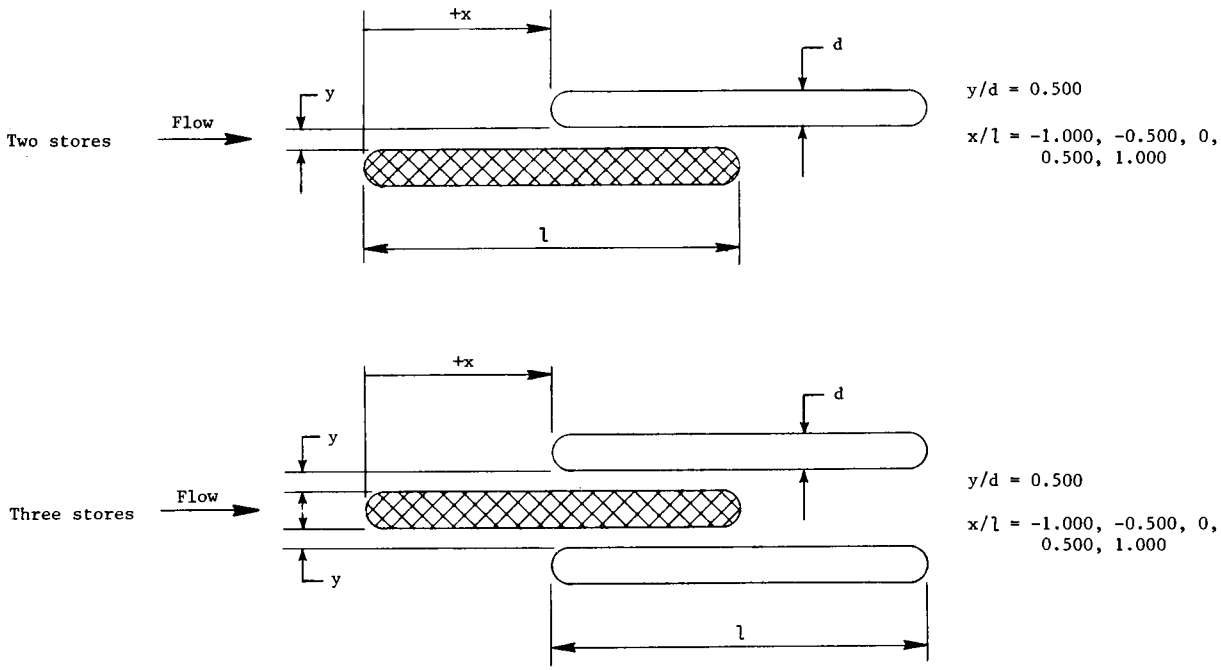

(c) Staggered spacing arrangements.

Figure 5. Concluded.

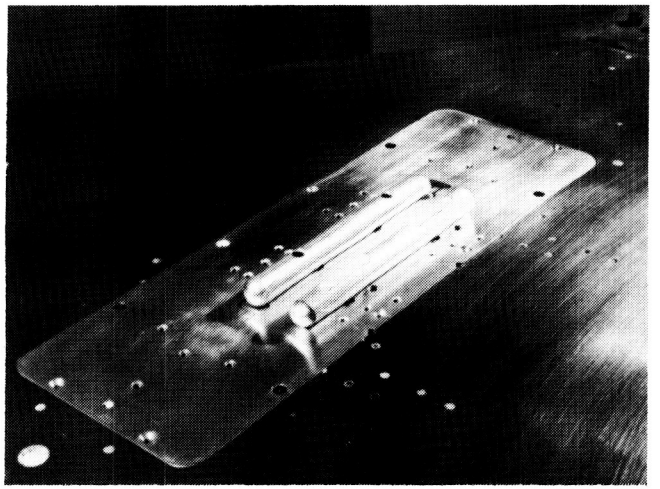

L-85-6759

Two stores

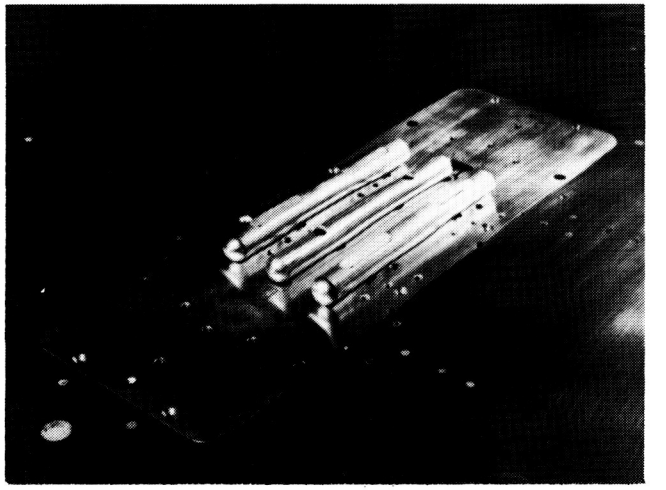

L-85-6763

Three stores with metric middle store

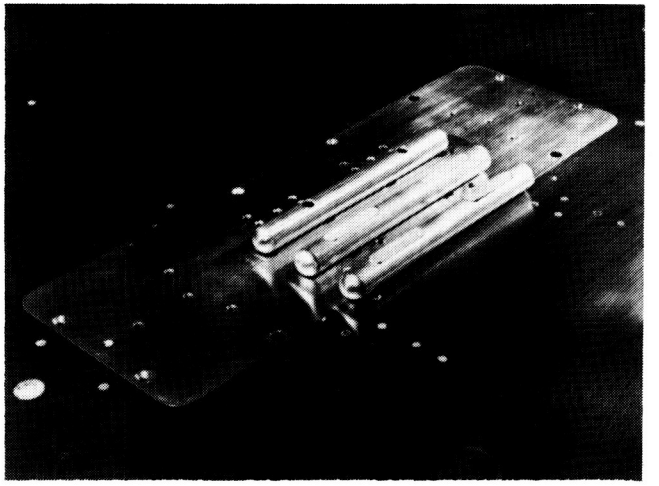

L-85-6762

Three stores with metric side store

(a) Lateral spacing arrangements.

Figure 6. Store arrangements on model.

L-85-6771

Metric aft store

L-85-6772

Metric forward store

(b) Tandem spacing arrangements.

Figure 6. Continued.

L-85-6767

Two stores ($x/l = -0.500$)

L-85-6761

Three stores ($x/l = 0.500$)

L-85-6769

Two stores ($x/l = -0.500$)

L-85-6768

Three stores ($x/l = -0.500$)

(c) Staggered spacing arrangements.

Figure 6. Concluded.

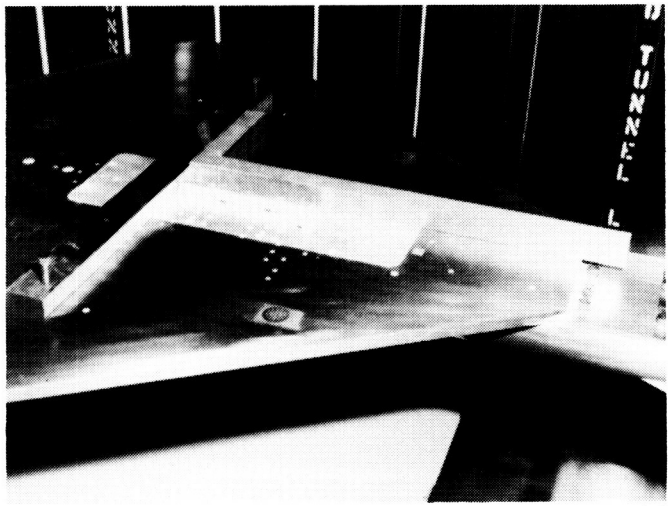

L-85-6679

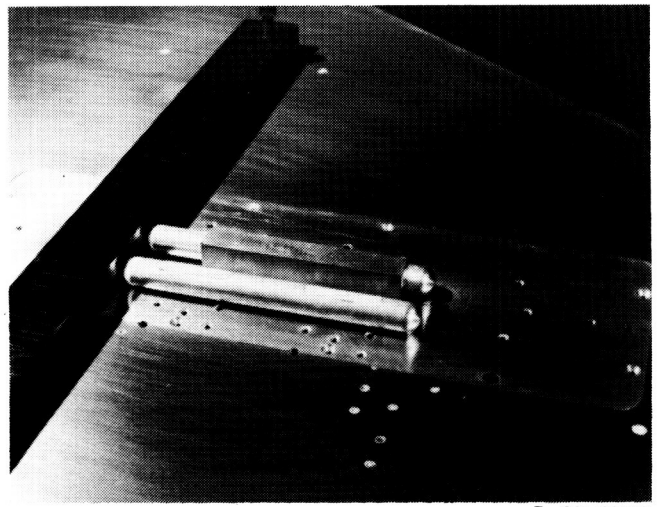

L-85-6760

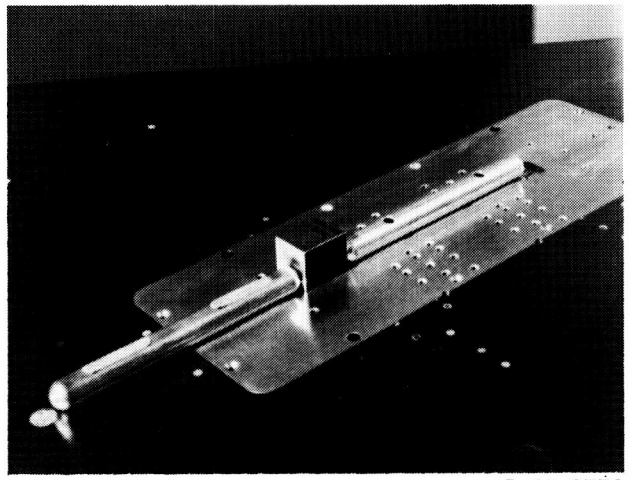

L-85-6770

Figure 7. Alignment bars and blocks used to position the stores.

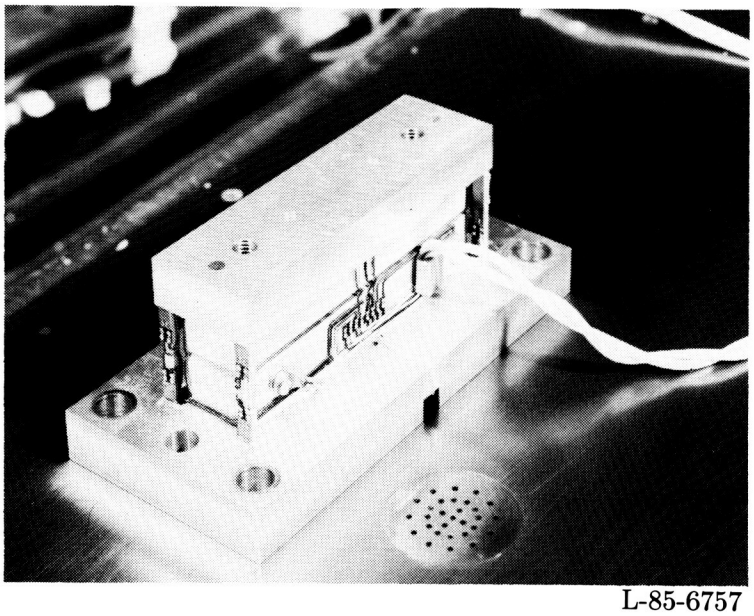

L-85-6757

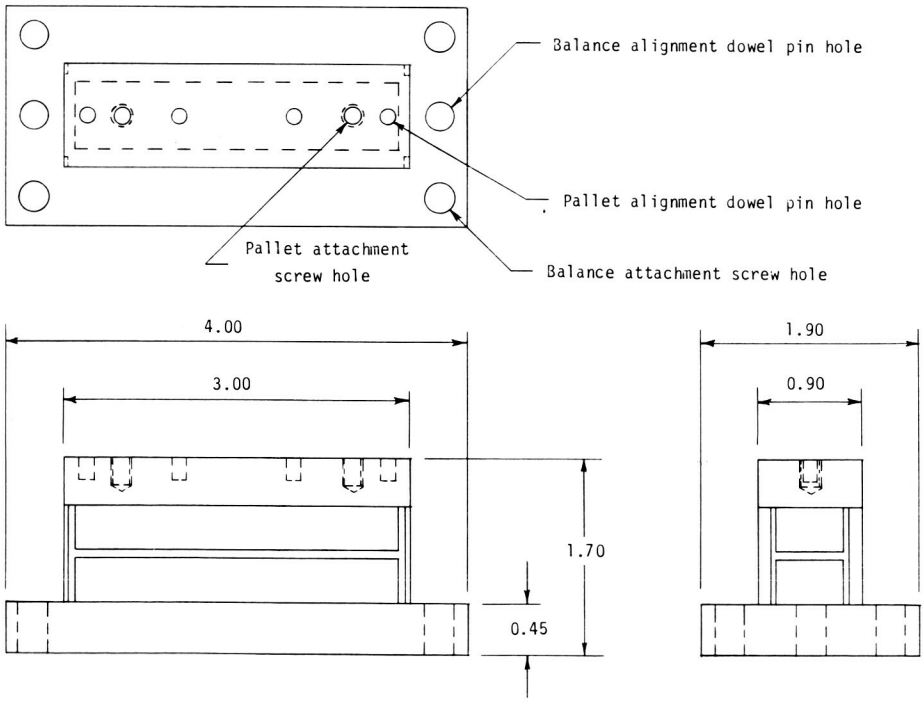

Figure 8. Details of strain-gage balance. All dimensions are in inches.

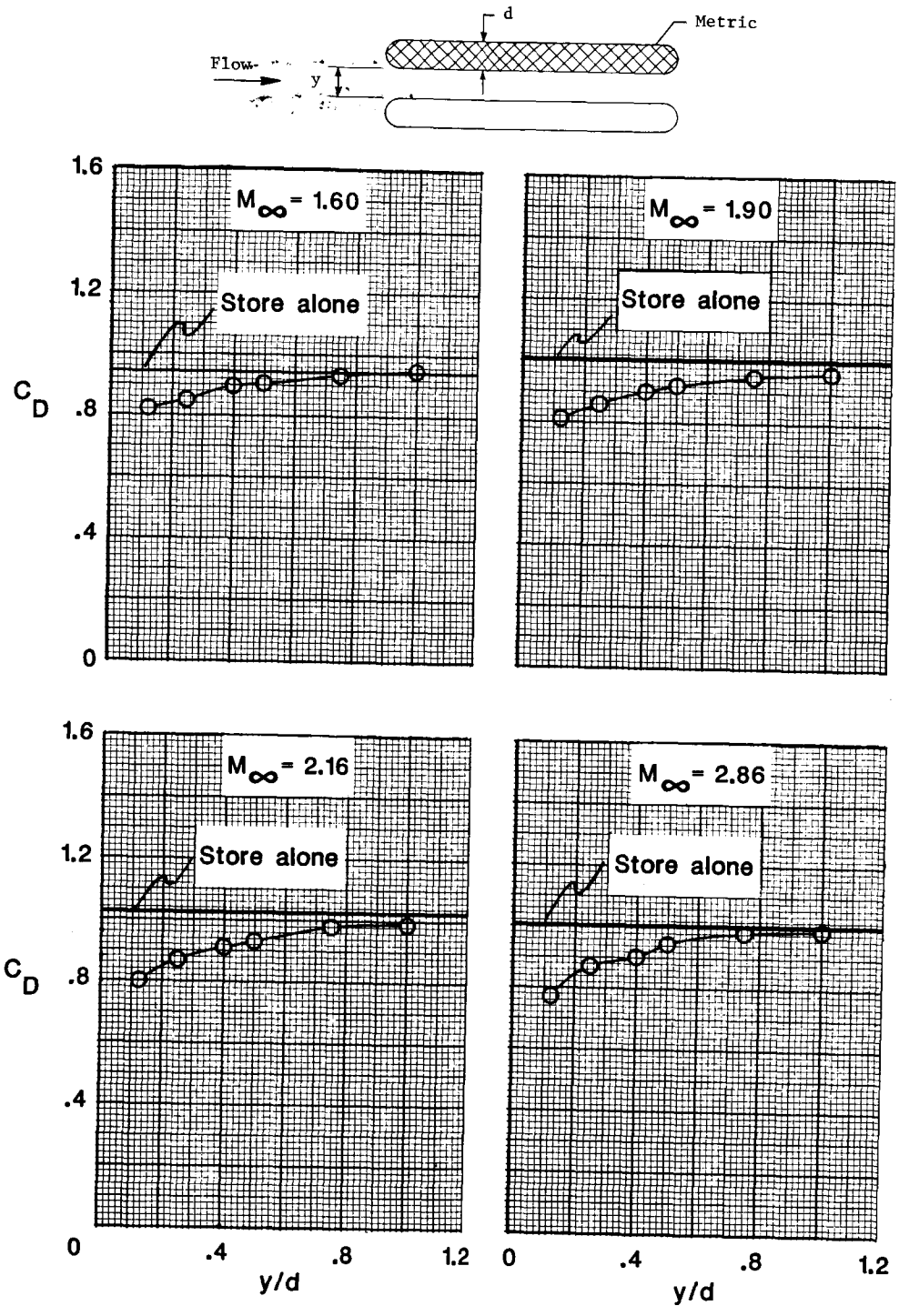

Figure 9. Lateral spacing effects for two-store arrangement.

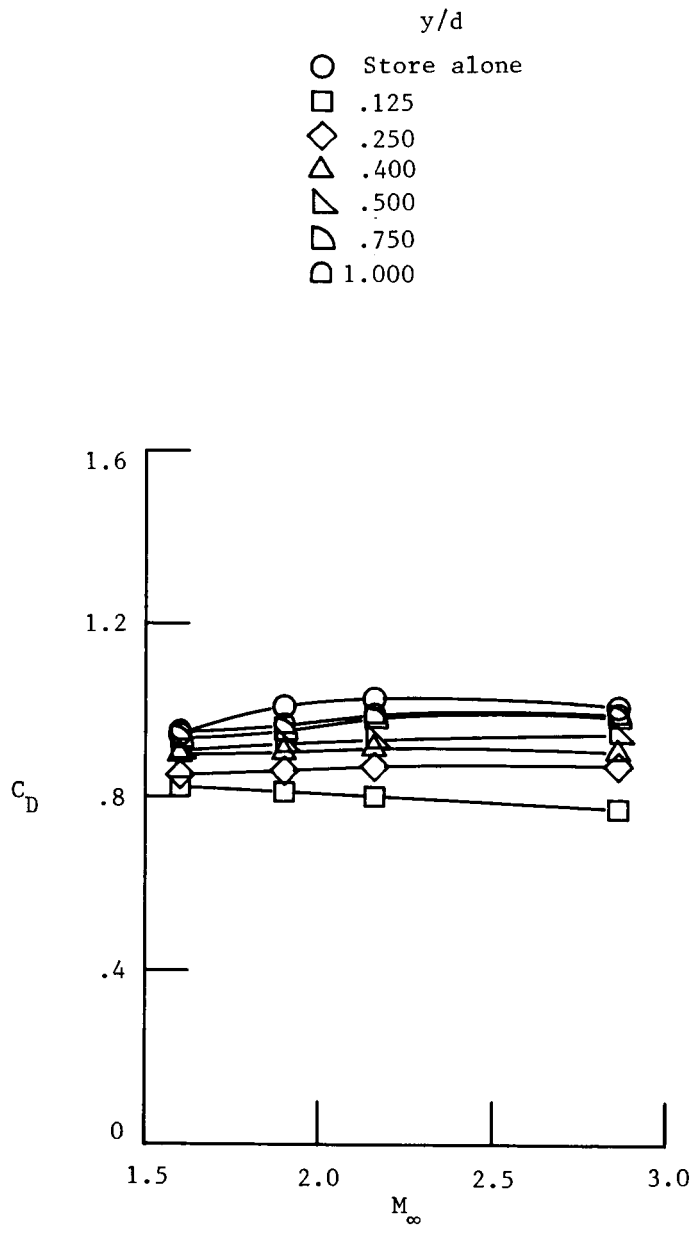

Figure 10. Mach number effects for two-store lateral spacing arrangement.

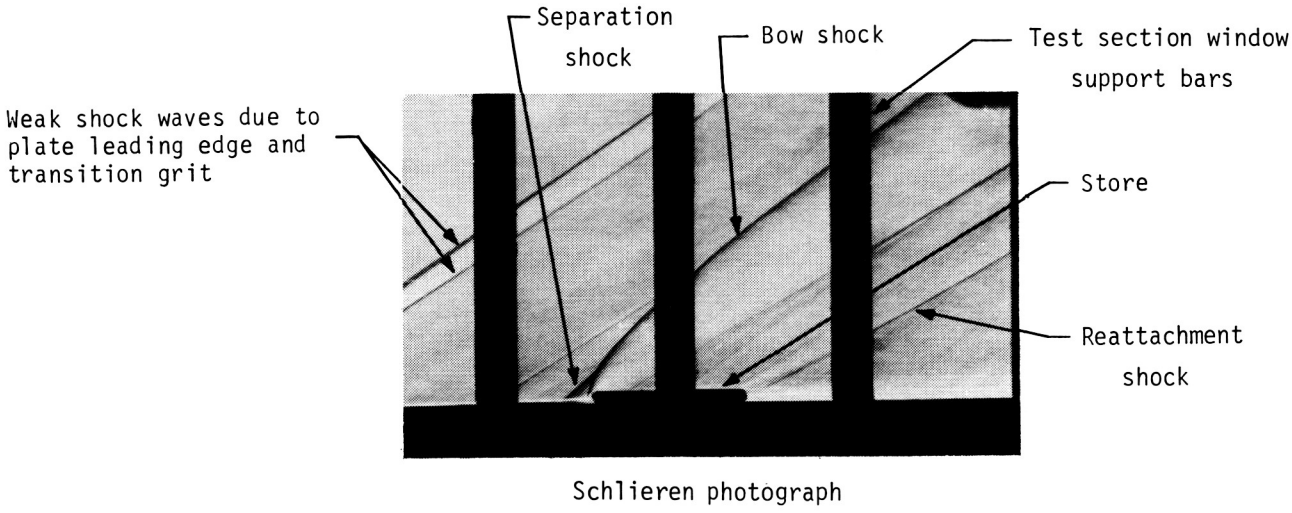

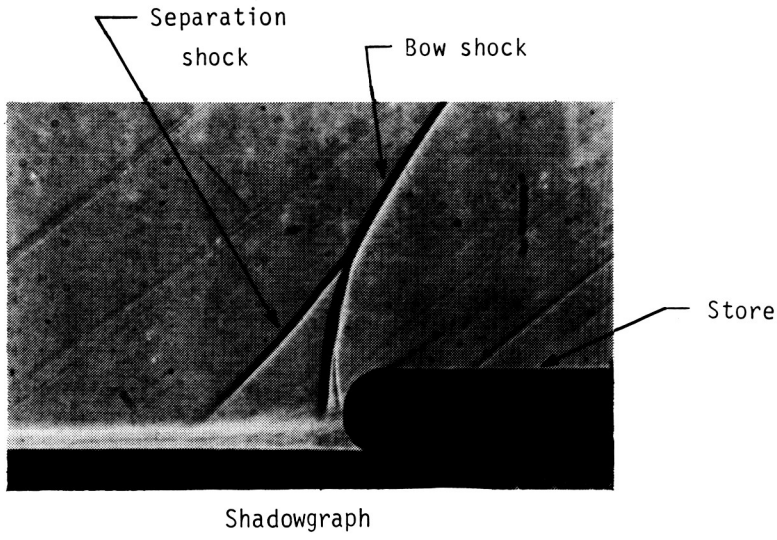

Figure 11. Typical schlieren photograph and shadowgraph.

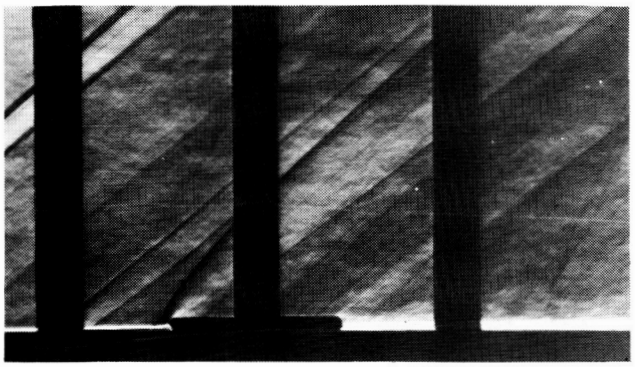

Store alone

NO DATA

$y/d = 0.500$

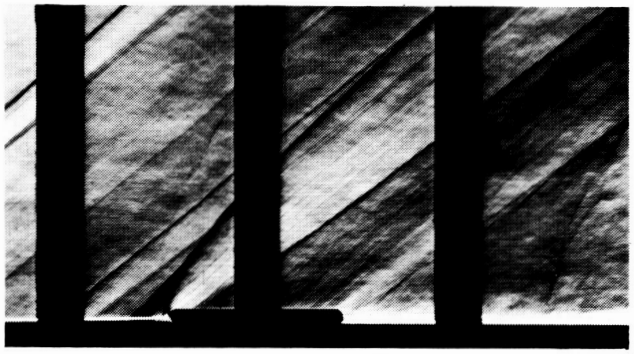

$y/d = 0.125$

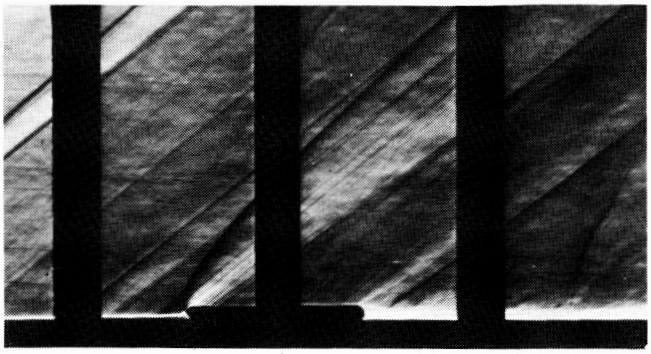

$y/d = 0.750$

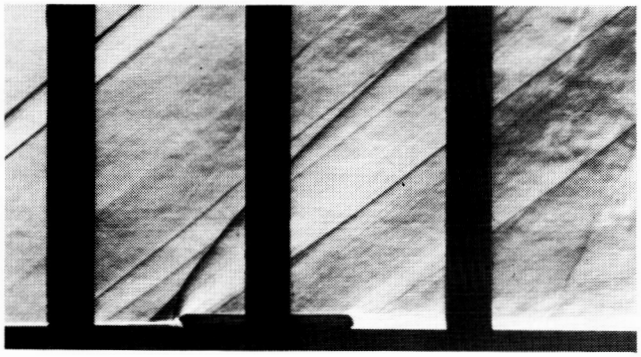

$y/d = 0.250$

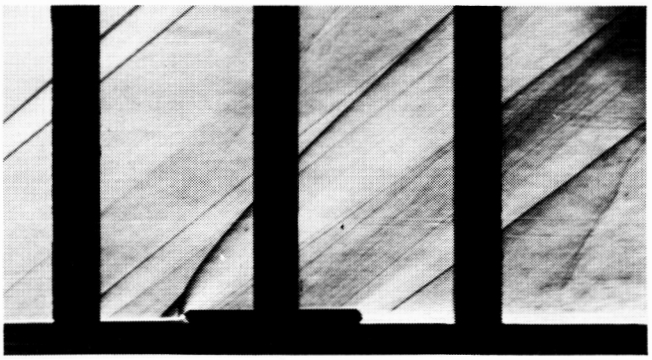

$y/d = 1.000$

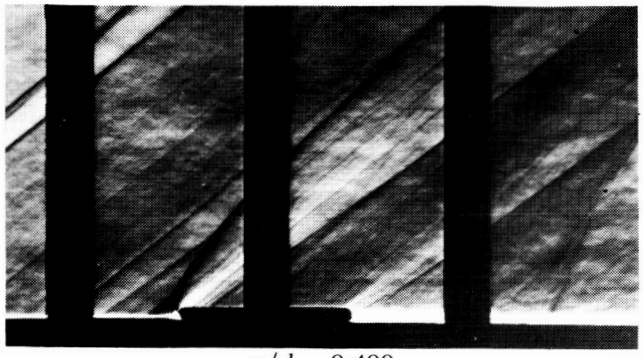

$y/d = 0.400$

(a) $M_\infty = 1.60$.

Figure 12. Schlieren photographs of two-store lateral spacing arrangement.

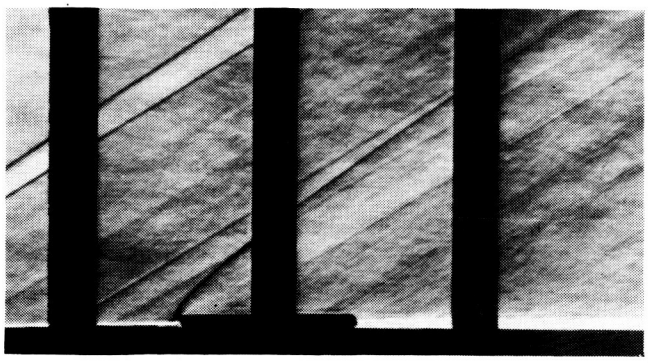

Store alone

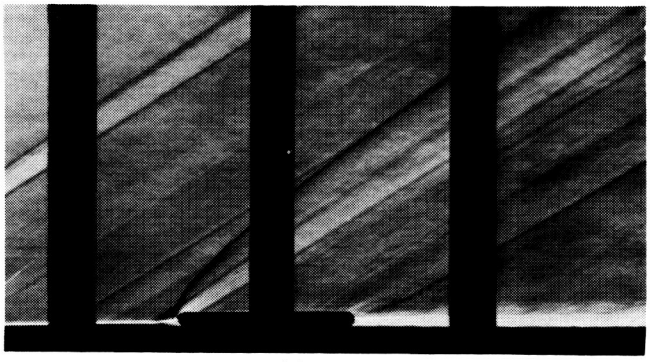

$y/d = 0.500$

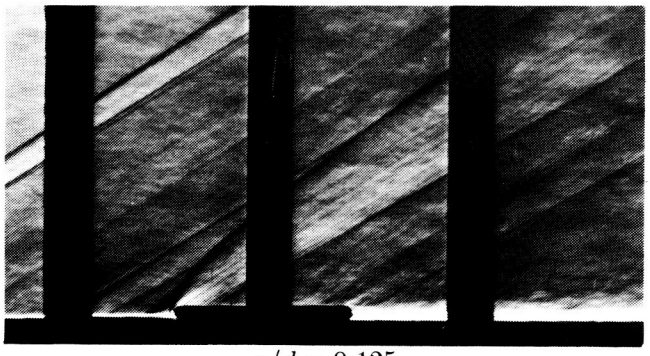

$y/d = 0.125$

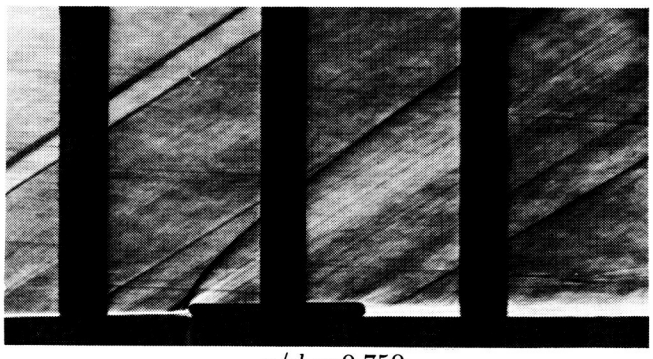

$y/d = 0.750$

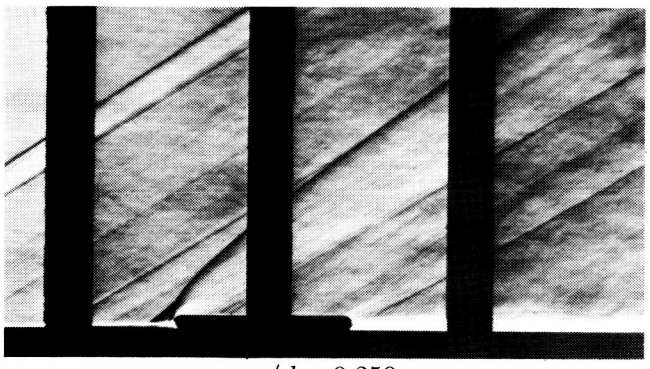

$y/d = 0.250$

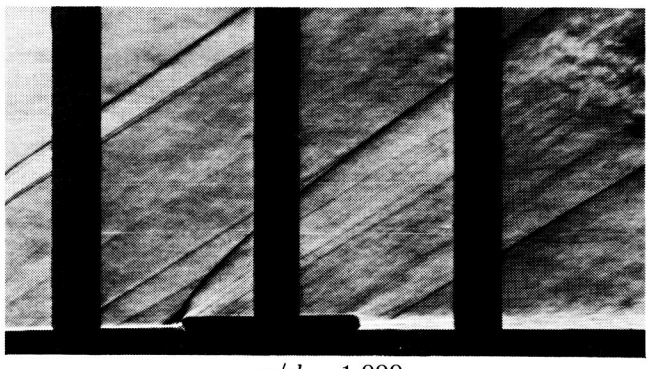

$y/d = 1.000$

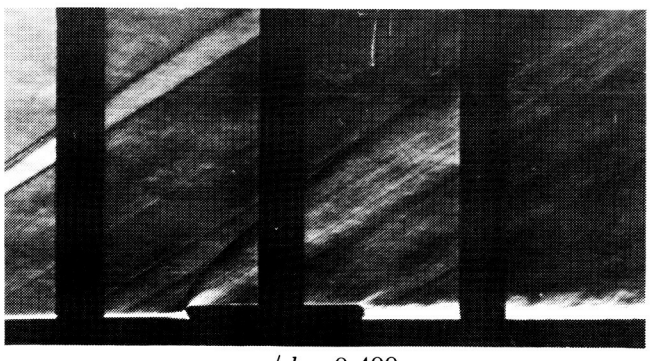

$y/d = 0.400$

(b) $M_\infty = 1.90$.

Figure 12. Continued.

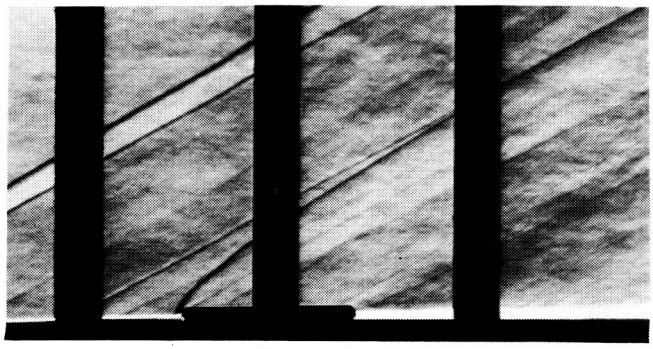

Store alone

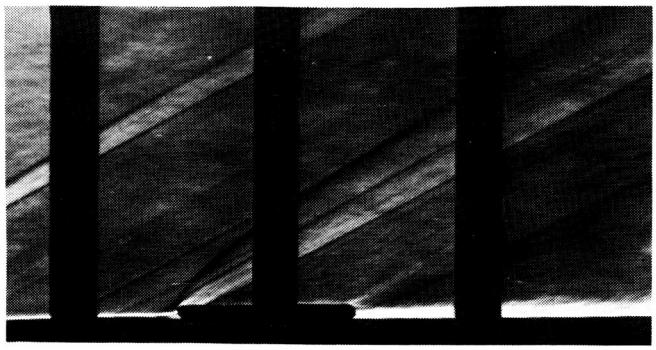

$y/d = 0.500$

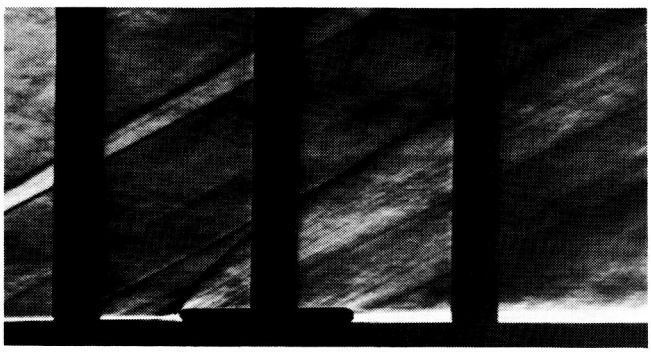

$y/d = 0.125$

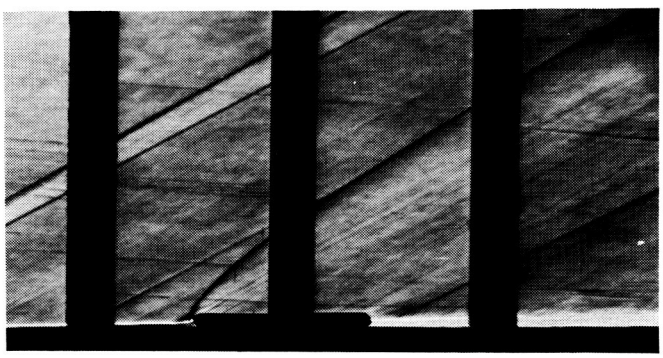

$y/d = 0.750$

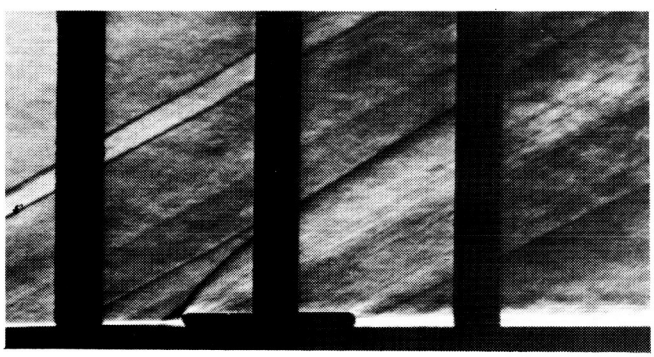

$y/d = 0.250$

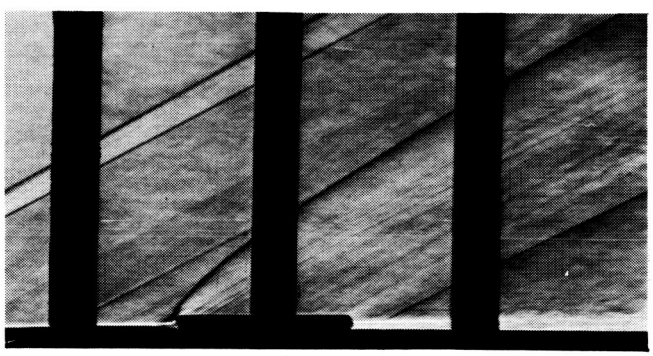

$y/d = 1.000$

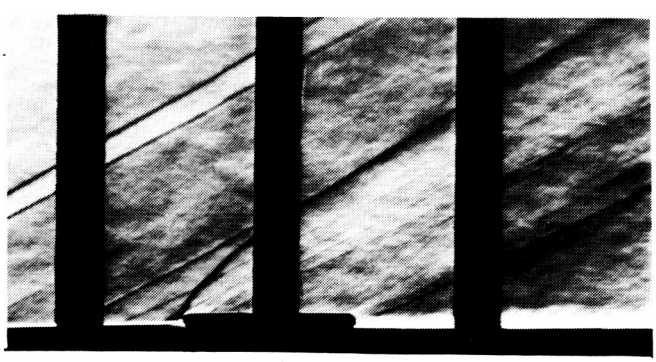

$y/d = 0.400$

(c) $M_\infty = 2.16$.

Figure 12. Continued.

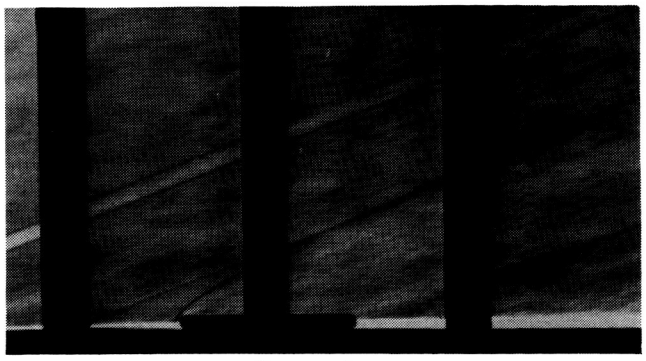

Store alone

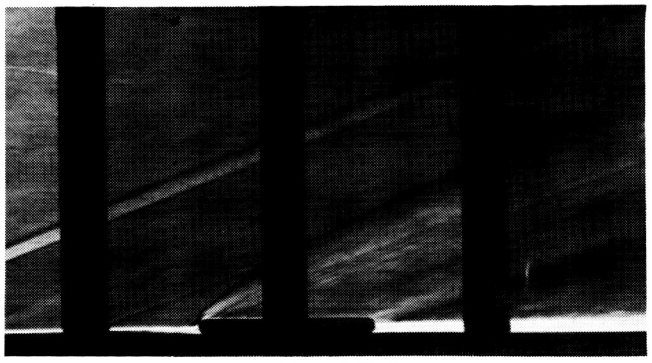

$y/d = 0.500$

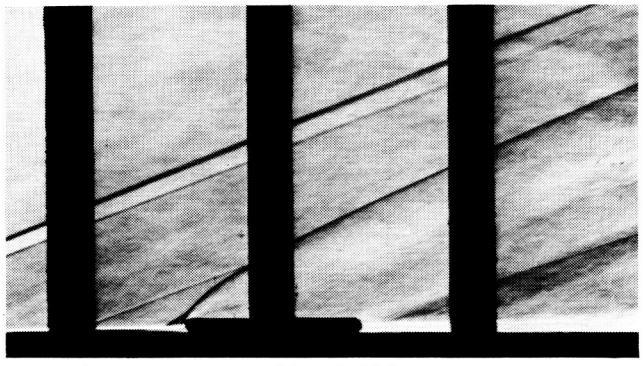

$y/d = 0.125$

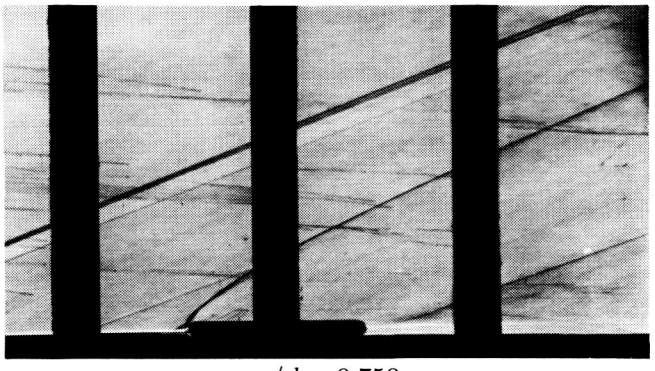

$y/d = 0.750$

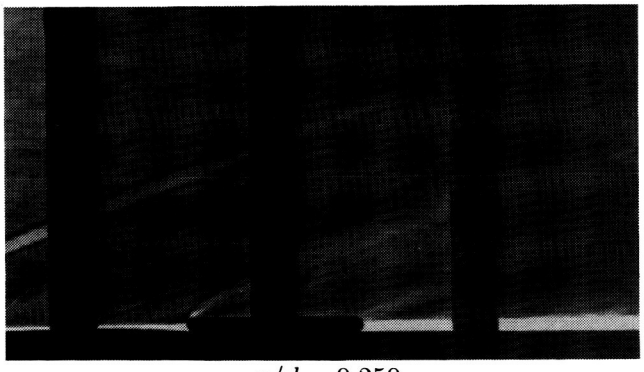

$y/d = 0.250$

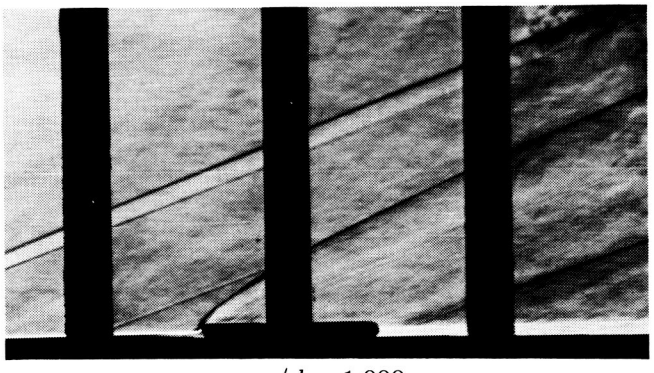

$y/d = 1.000$

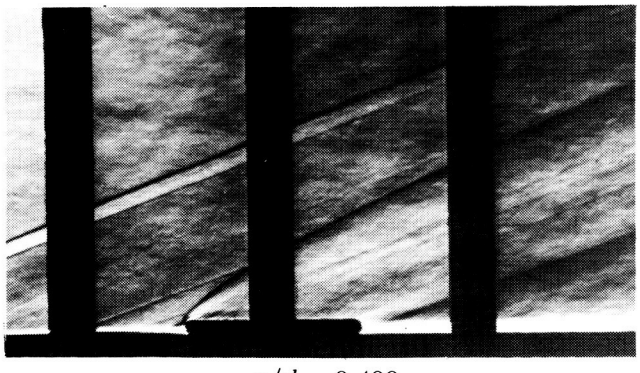

$y/d = 0.400$

(d) $M_\infty = 2.86$.

Figure 12. Concluded.

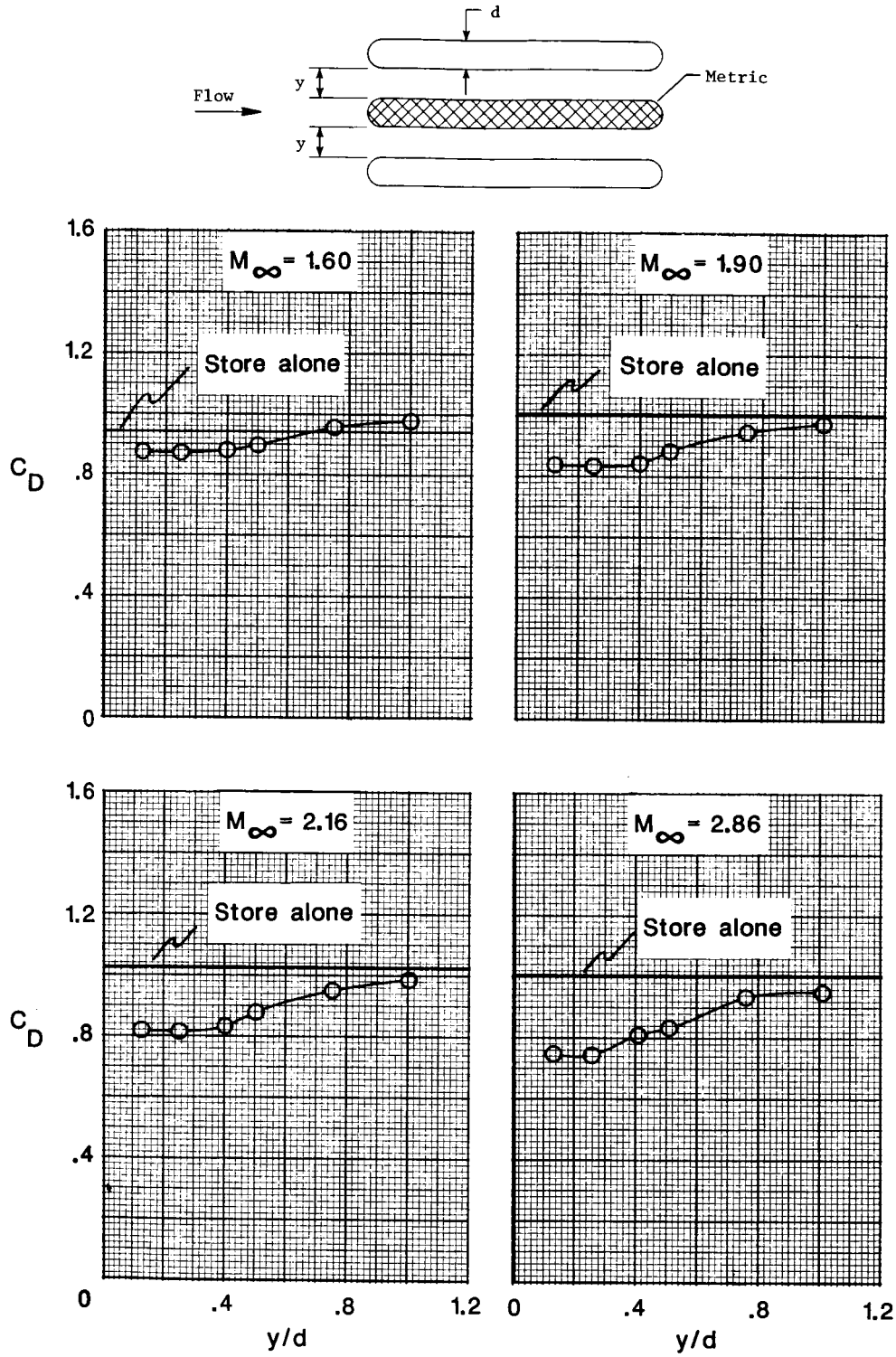

Figure 13. Lateral spacing effects for three-store arrangement with metric store in middle position.

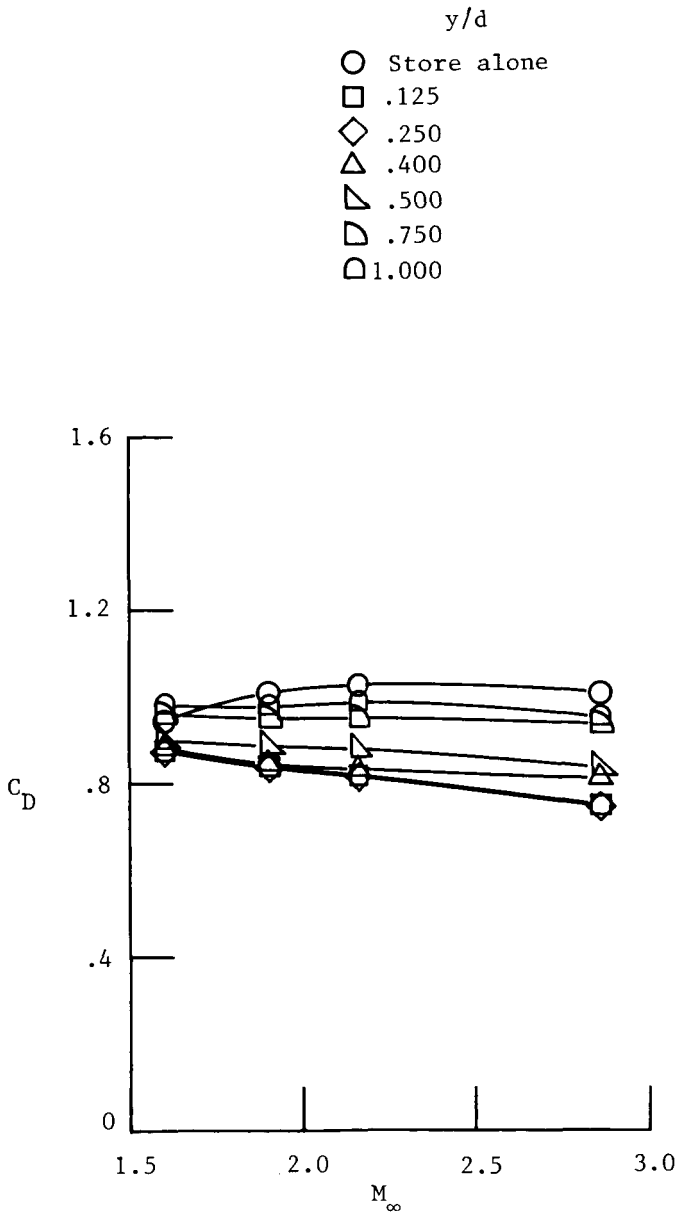

Figure 14. Mach number effects for three-store lateral spacing arrangement with metric store in middle position.

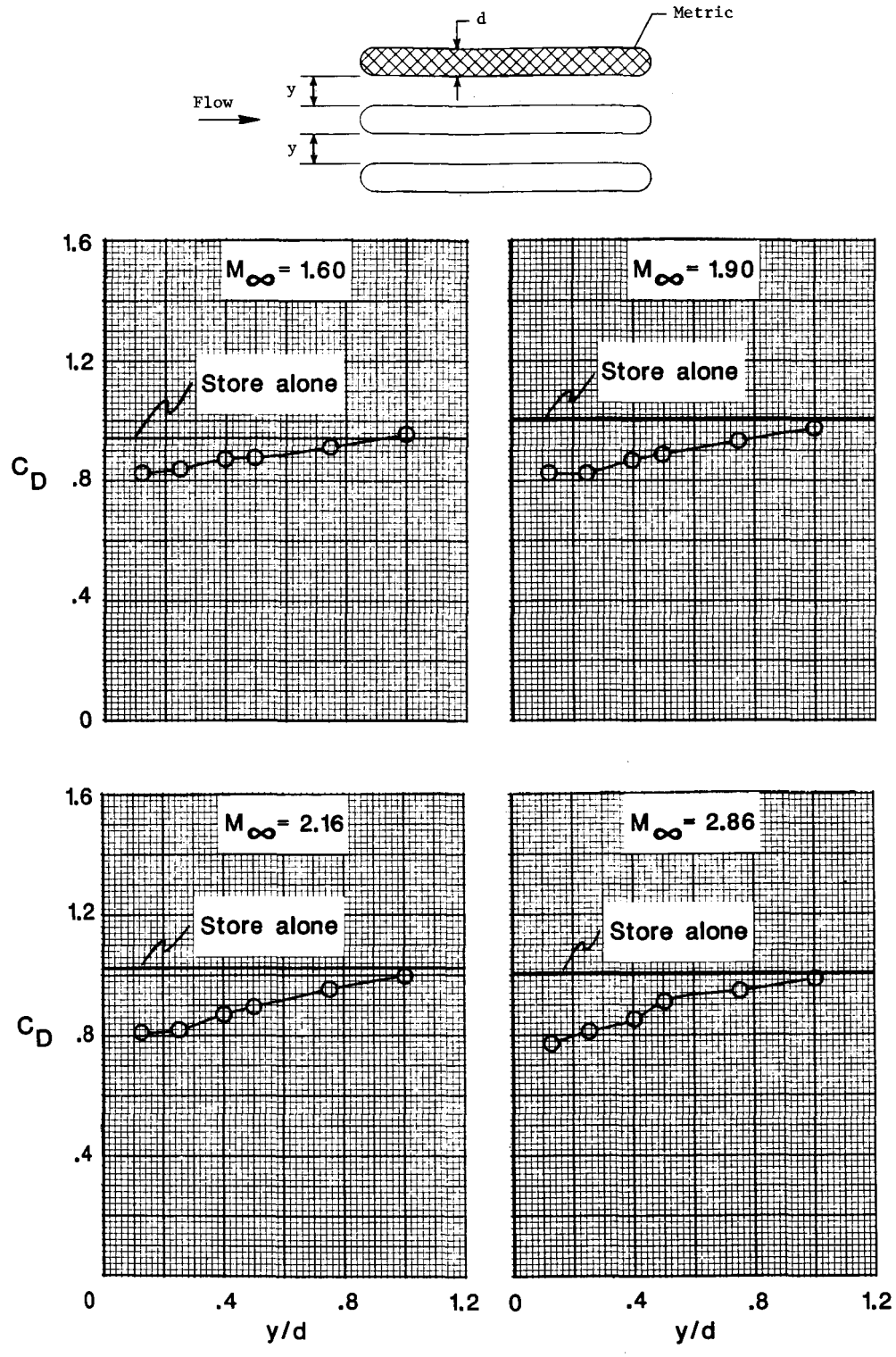

Figure 15. Lateral spacing effects for three-store arrangement with metric store in side position.

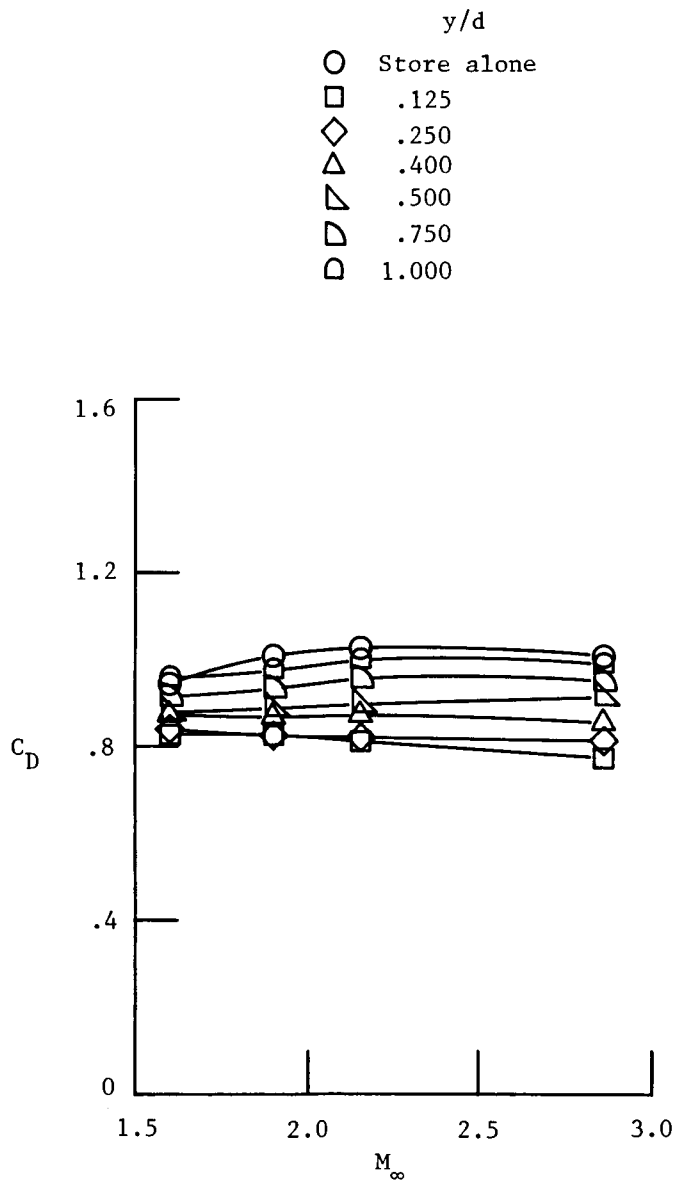

Figure 16. Mach number effects for three-store lateral spacing arrangement with metric store in side position.

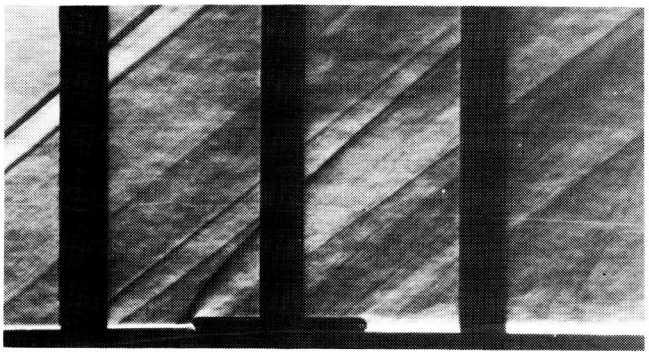

Store alone

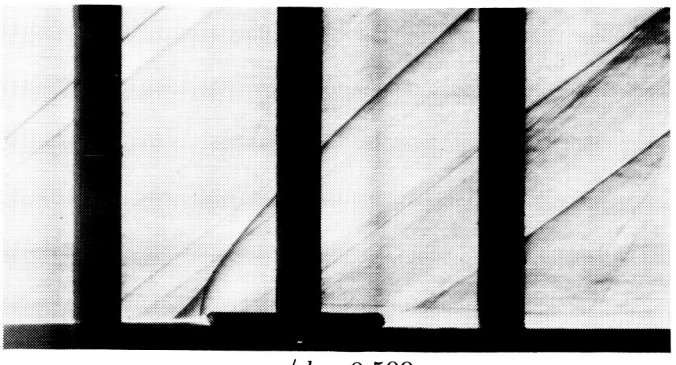

$y/d = 0.500$

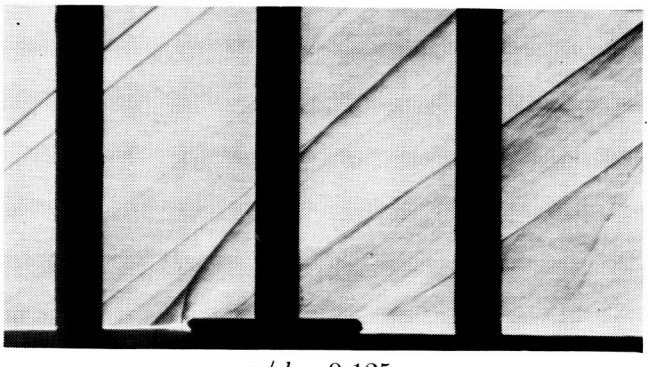

$y/d = 0.125$

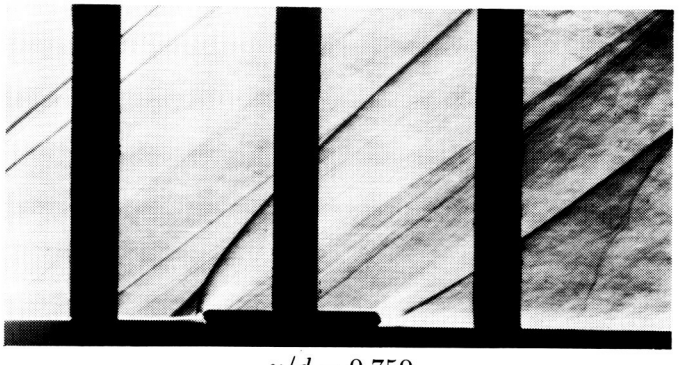

$y/d = 0.750$

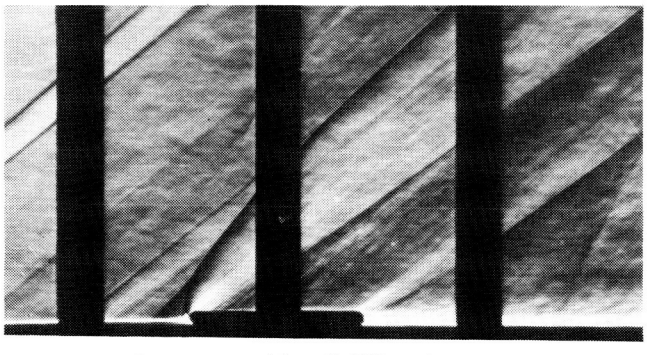

$y/d = 0.250$

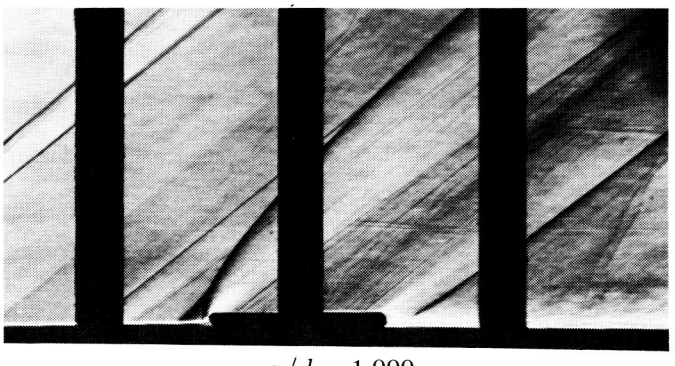

$y/d = 1.000$

$y/d = 0.400$

(a) $M_\infty = 1.60$.

Figure 17. Schlieren photographs of three-store lateral spacing arrangement.

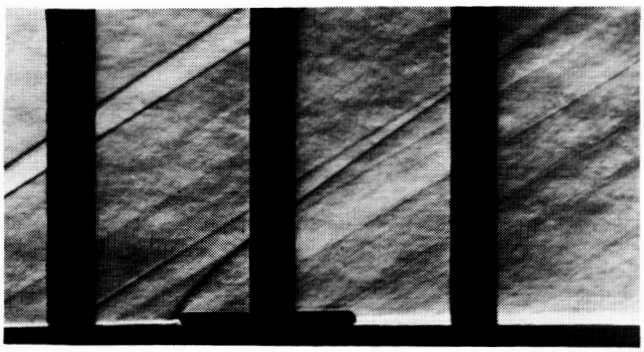

Store alone

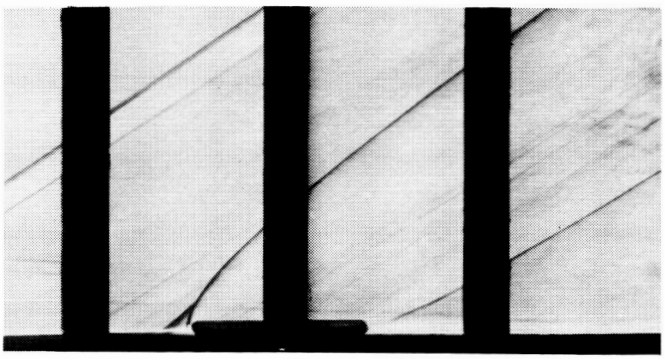

$y/d = 0.500$

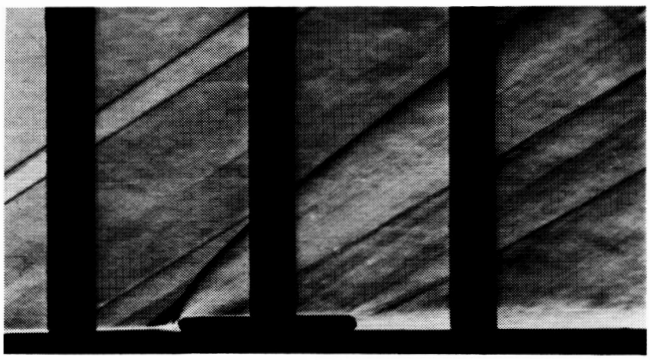

$y/d = 0.125$

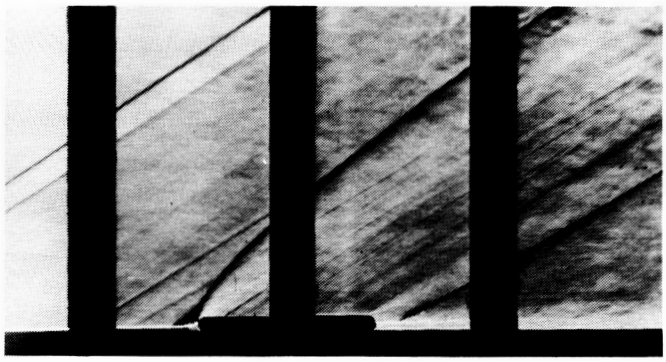

$y/d = 0.750$

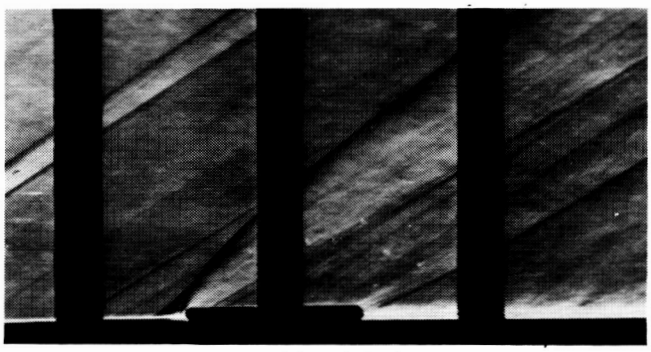

$y/d = 0.250$

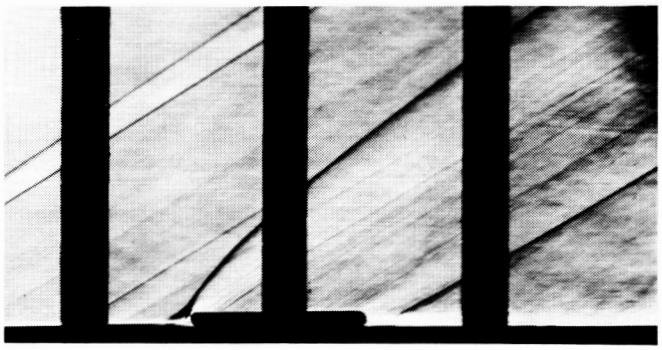

$y/d = 1.000$

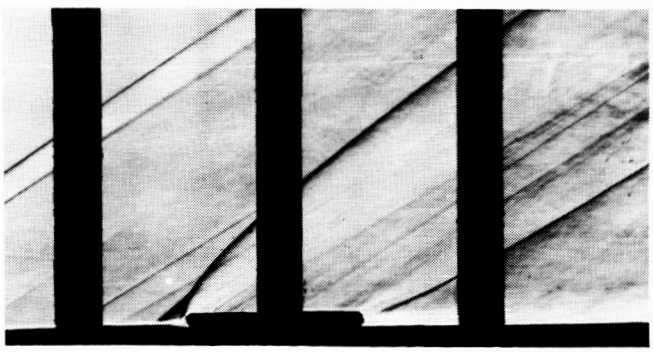

$y/d = 0.400$

(b) $M_\infty = 1.90$.

Figure 17. Continued.

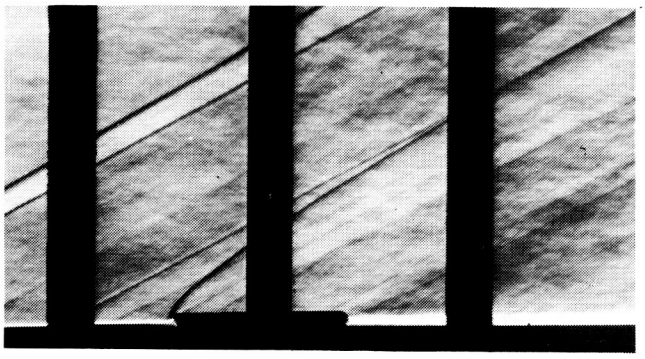

Store alone

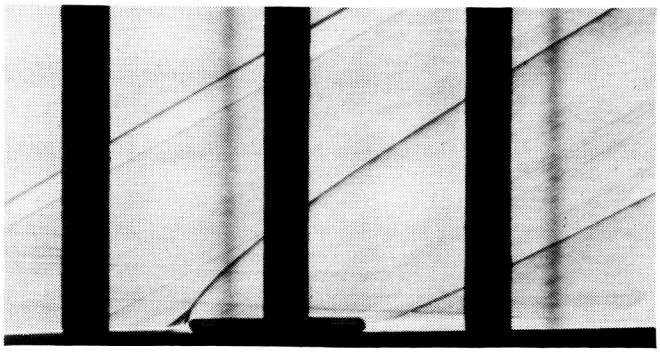

$y/d = 0.500$

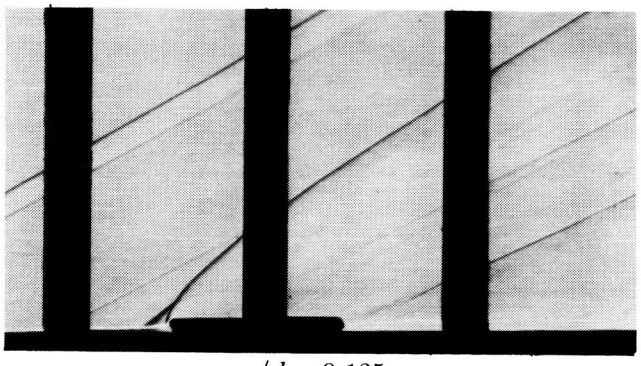

$y/d = 0.125$

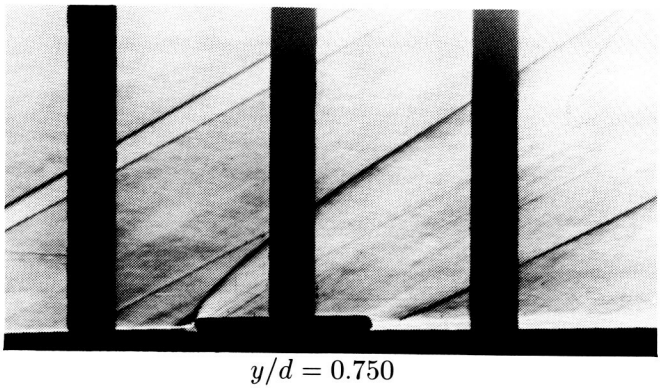

$y/d = 0.750$

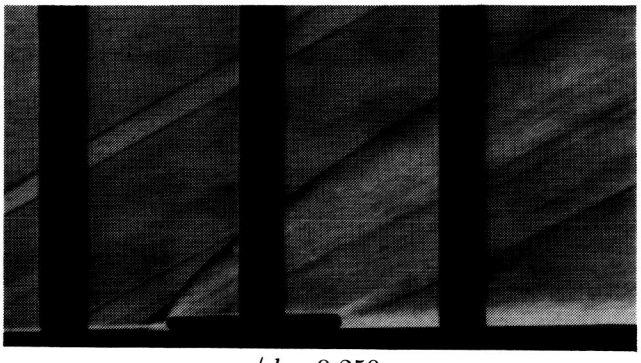

$y/d = 0.250$

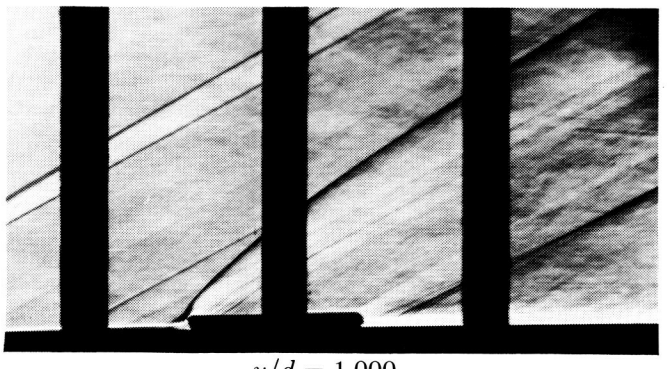

$y/d = 1.000$

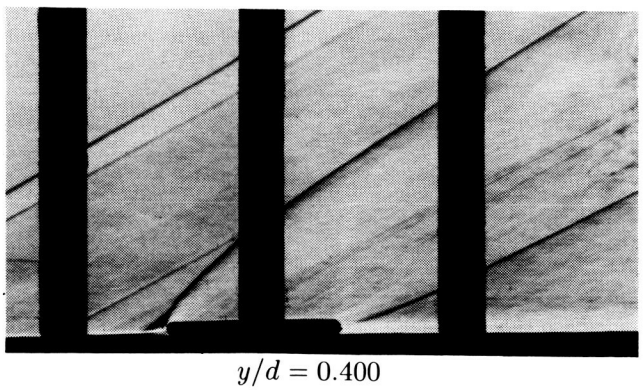

$y/d = 0.400$

(c) $M_\infty = 2.16$.

Figure 17. Continued.

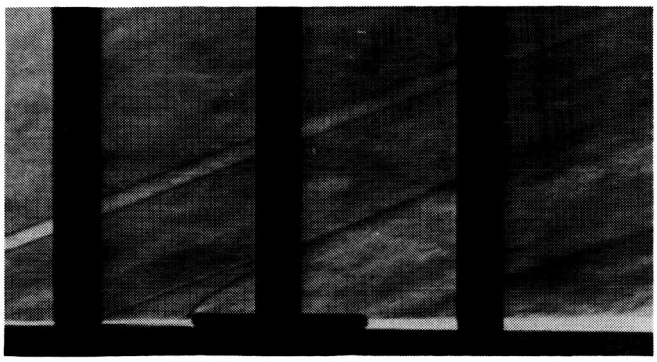

Store alone

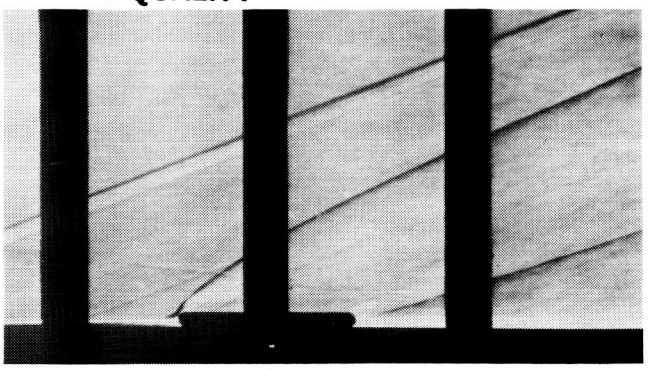

$y/d = 0.500$

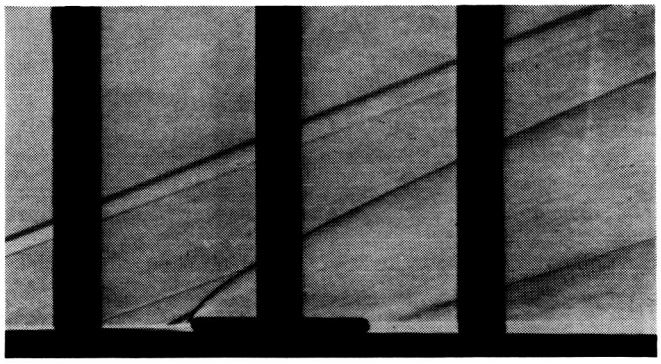

$y/d = 0.125$

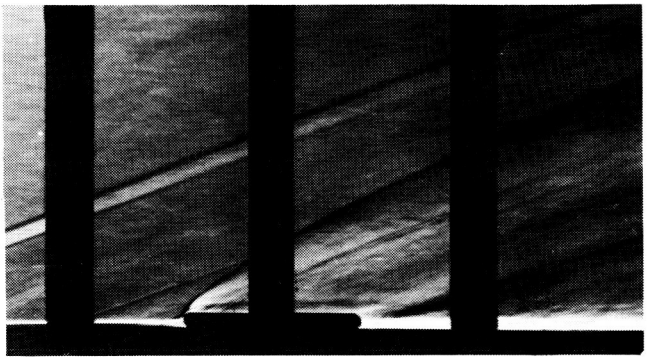

$y/d = 0.750$

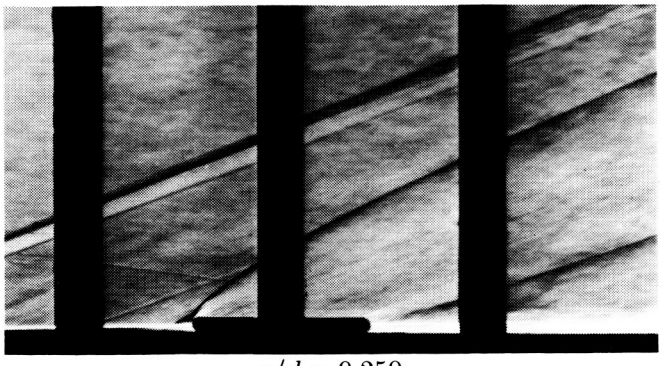

$y/d = 0.250$

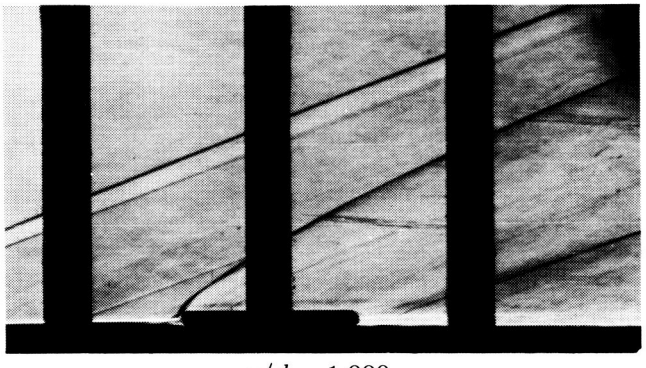

$y/d = 1.000$

$y/d = 0.400$

(d) $M_\infty = 2.86$.

Figure 17. Concluded.

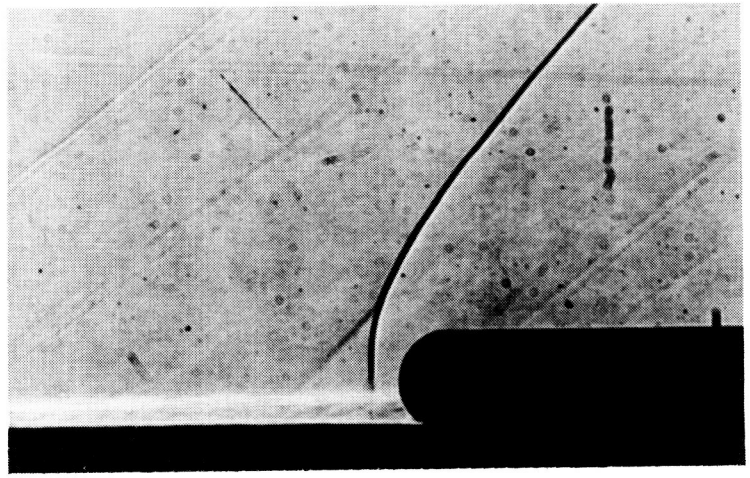

Store alone

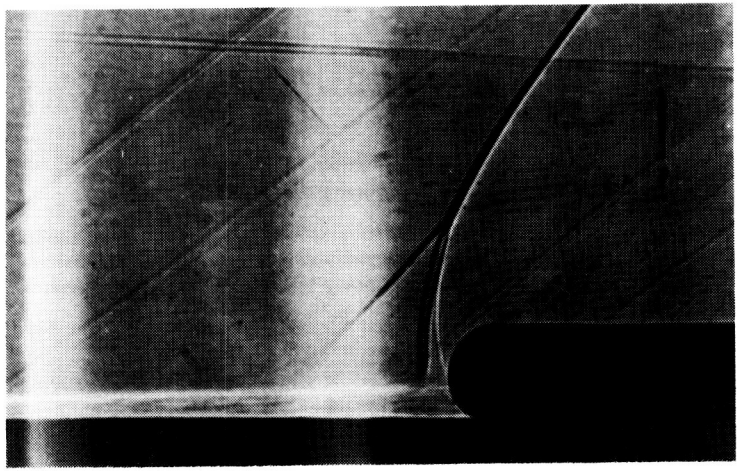

Two-store lateral spacing arrangement; $y/d = 0.750$

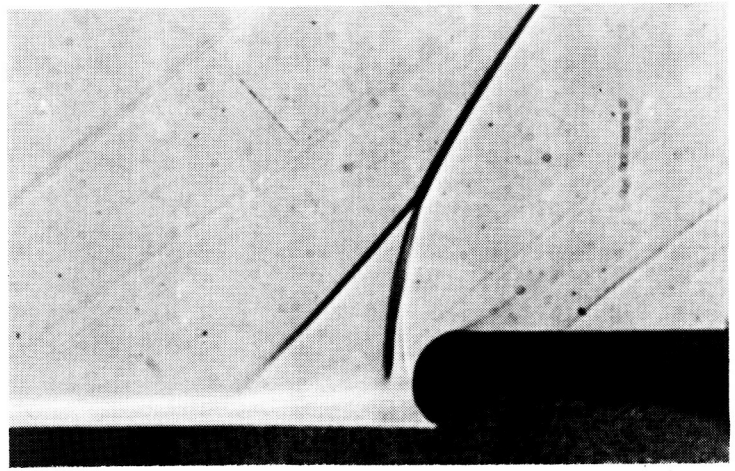

Three-store lateral spacing arrangement; $y/d = 0.750$

Figure 18. Shadowgraphs of store arrangements illustrating extent of boundary-layer separation.

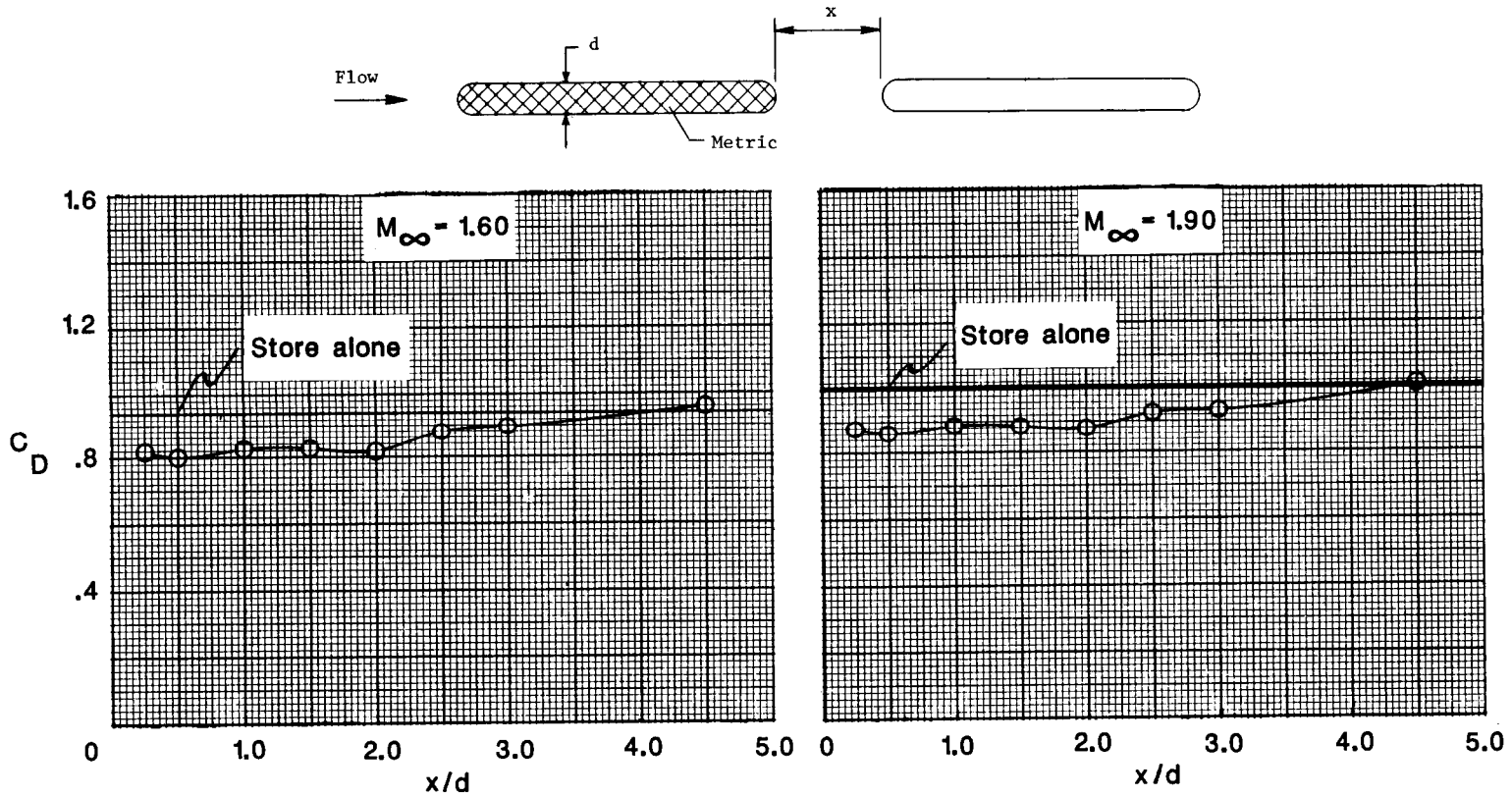

Figure 19. Tandem spacing effects for two-store arrangement with metric store in forward position.

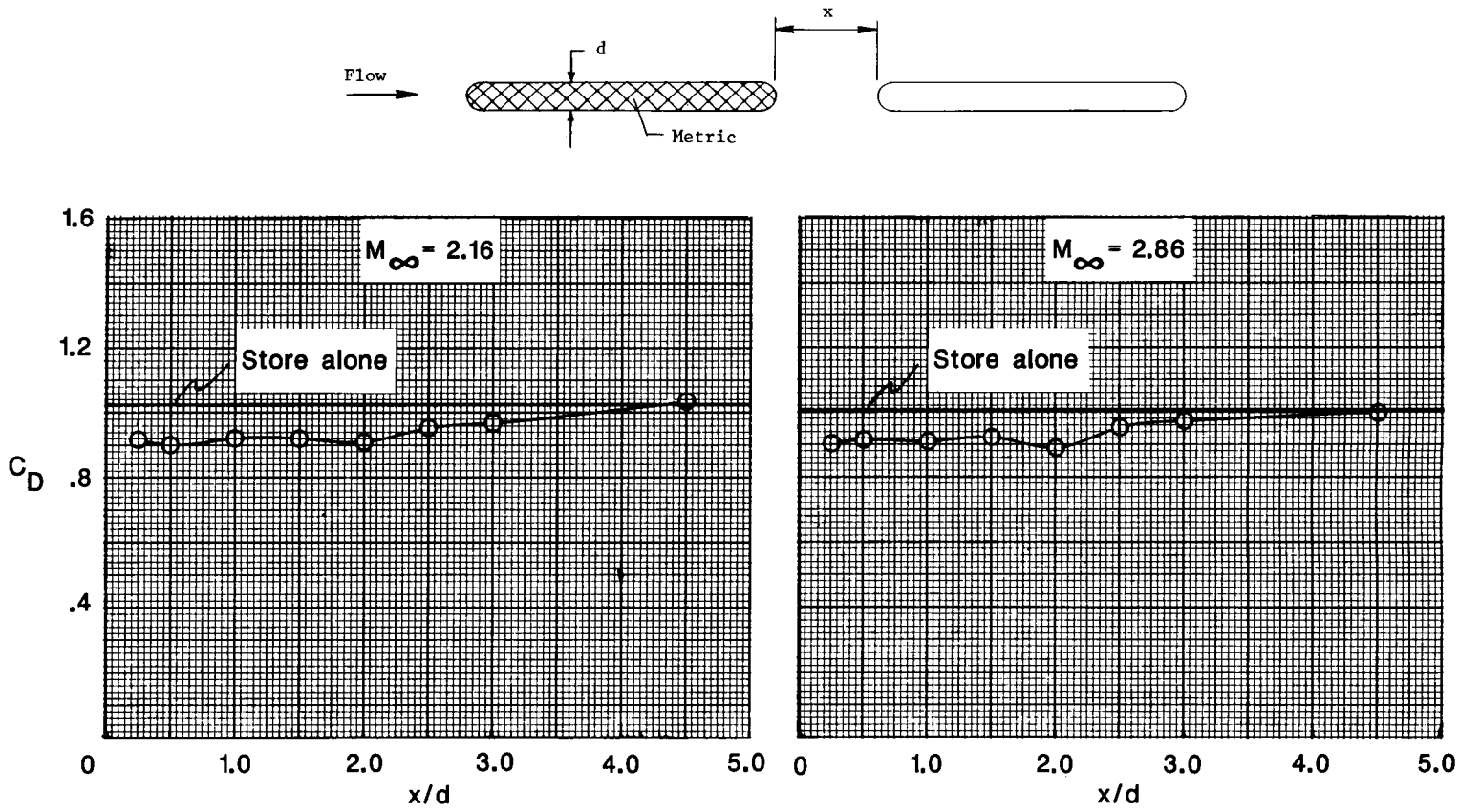

Figure 19. Concluded.

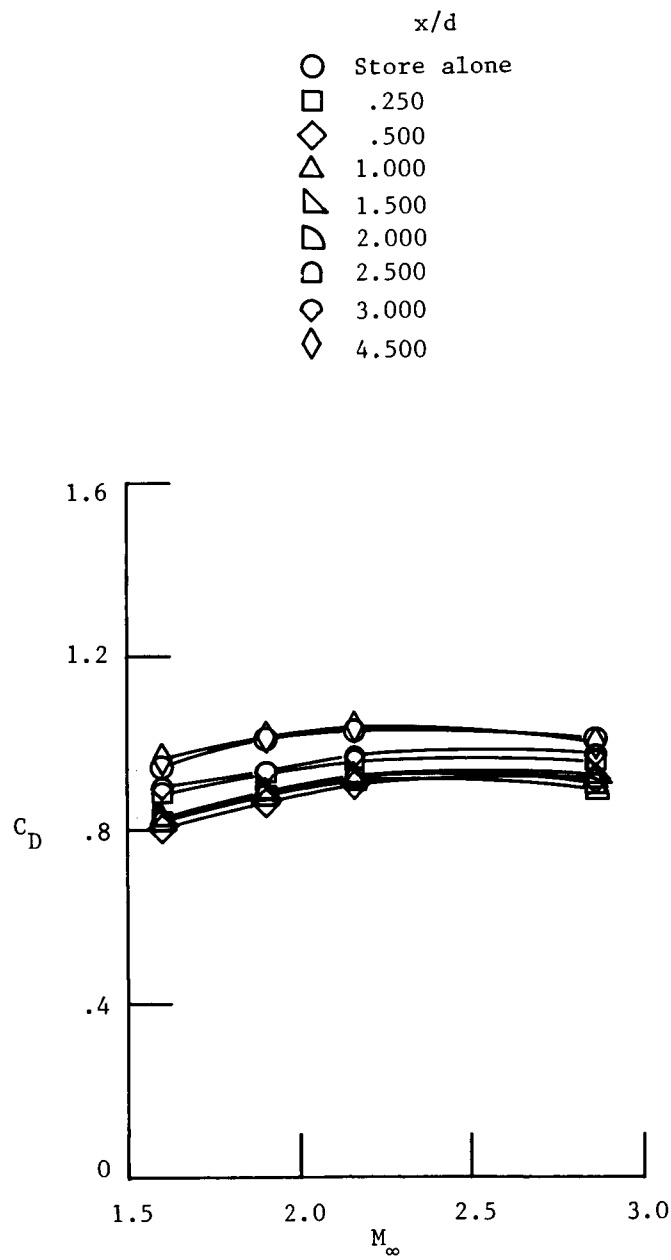

Figure 20. Mach number effects for two-store tandem spacing arrangement with metric store in forward position.

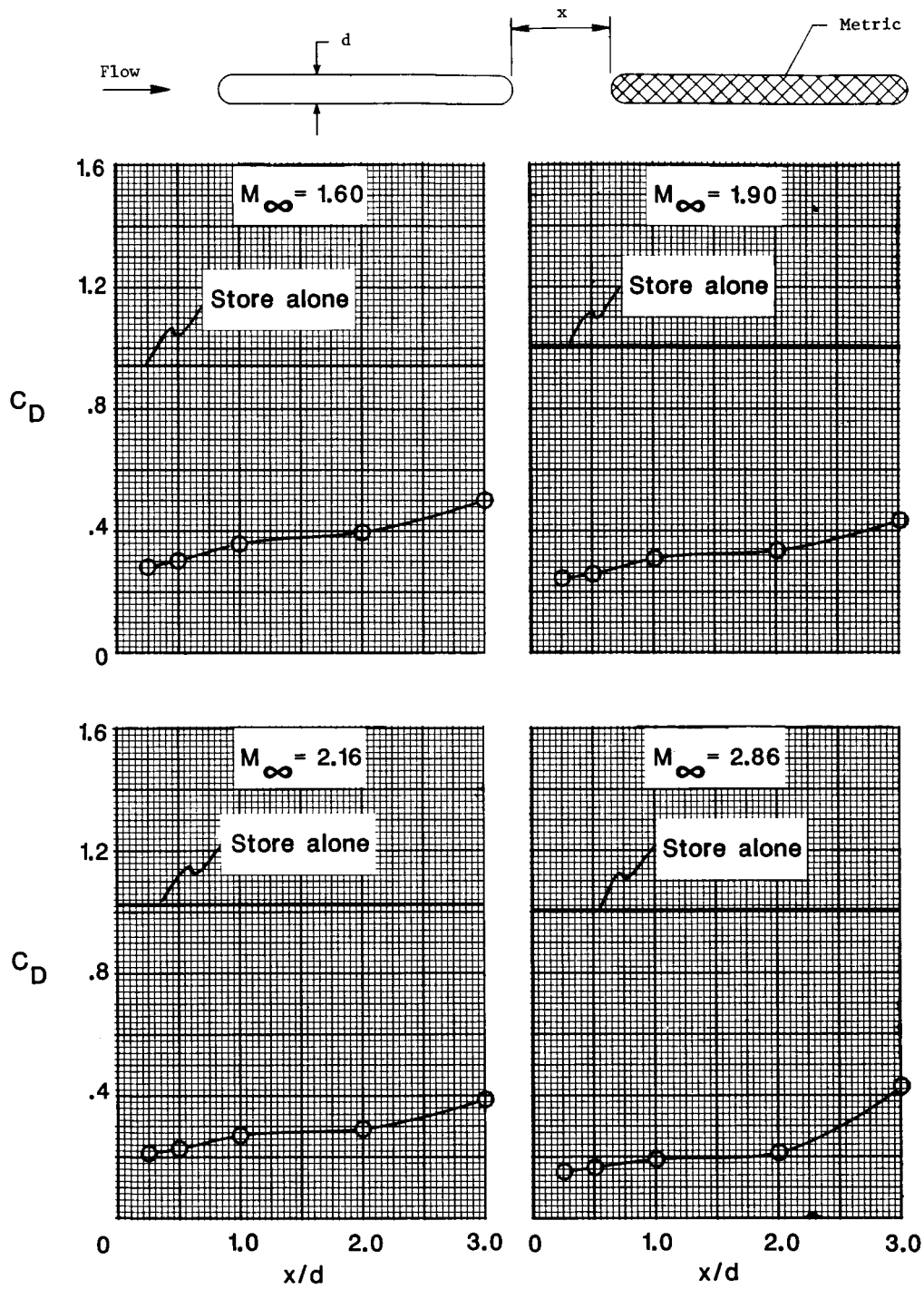

Figure 21. Tandem spacing effects for two-store arrangement with metric store in aft position.

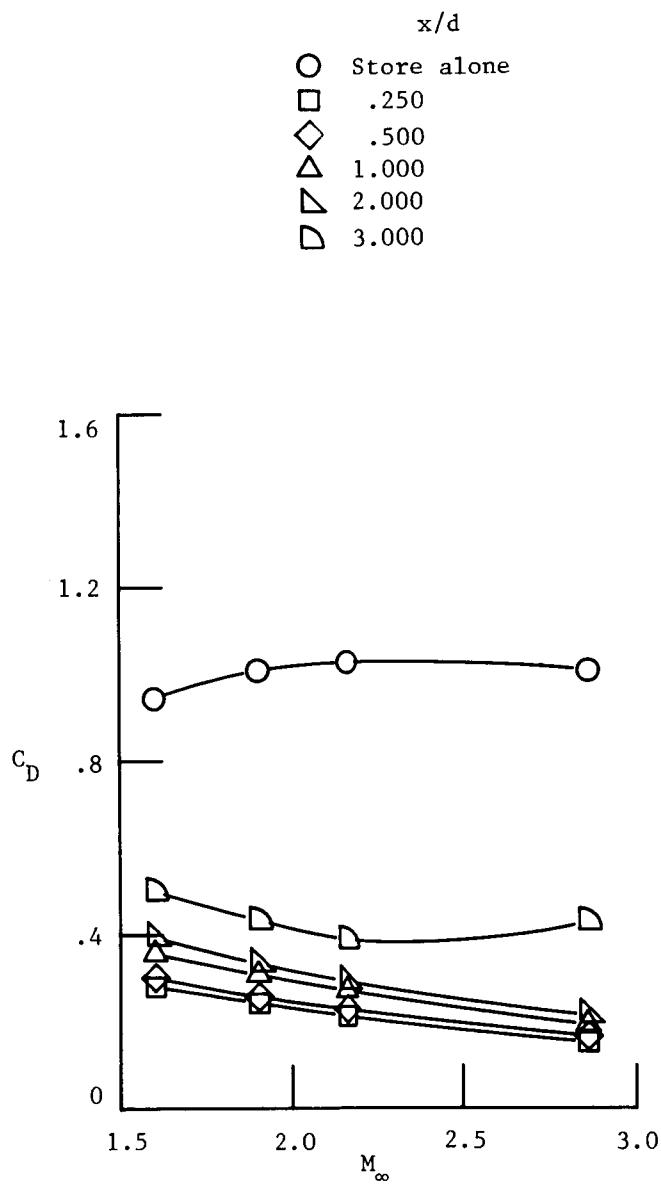

Figure 22. Mach number effects for two-store tandem spacing arrangement with metric store in aft position.

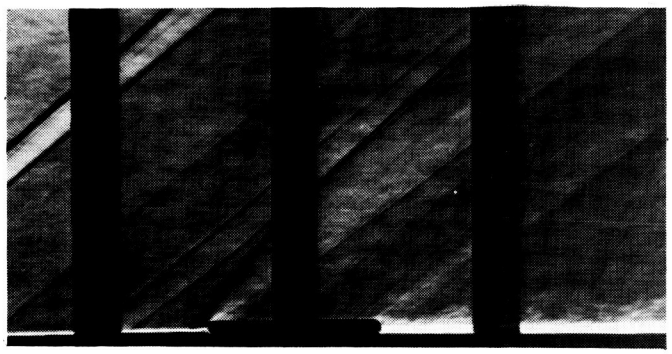

Store alone

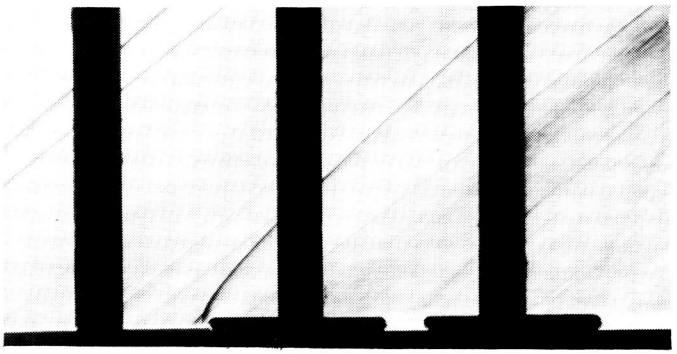

$x/d = 2.000$

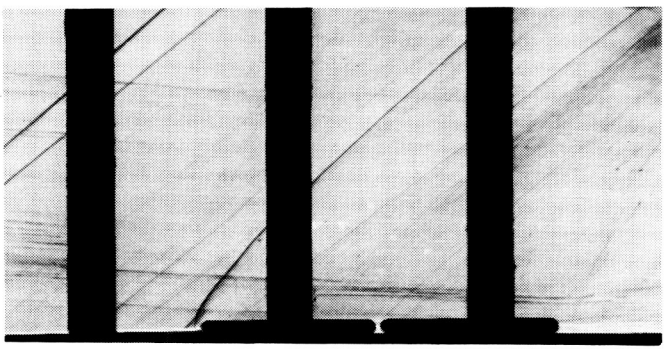

$x/d = 0.250$

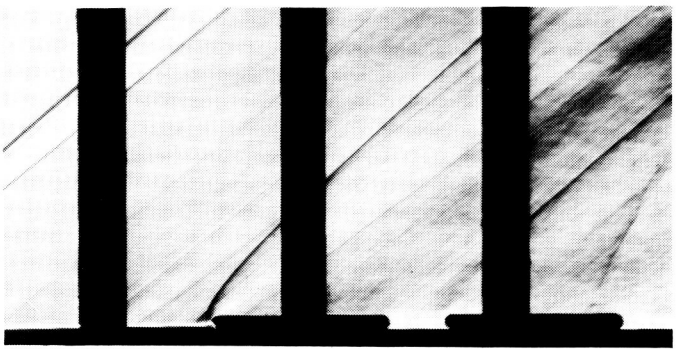

$x/d = 3.000$

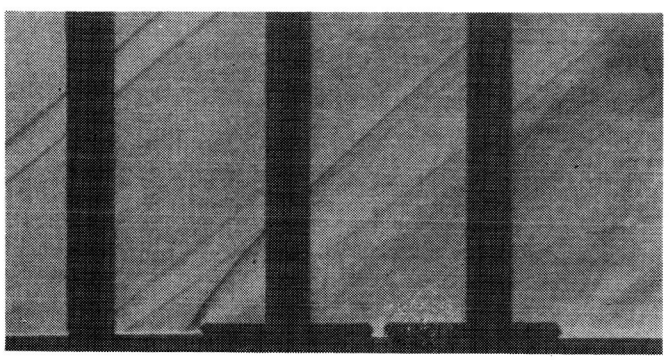

$x/d = 0.500$

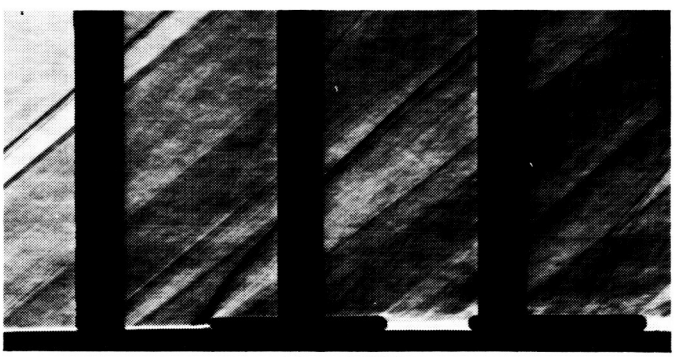

$x/d = 4.500$

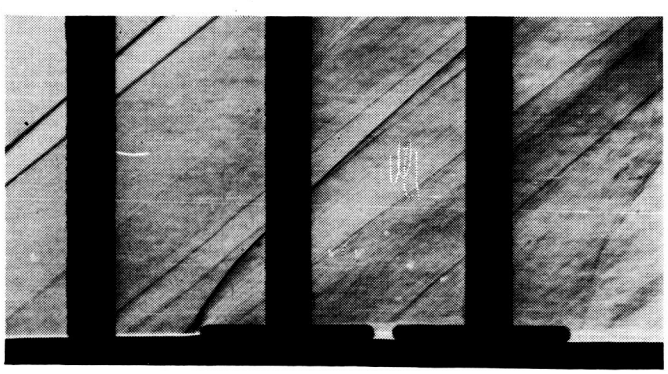

$x/d = 1.000$

(a) $M_\infty = 1.60$.

Figure 23. Schlieren photographs of two-store tandem spacing arrangement.

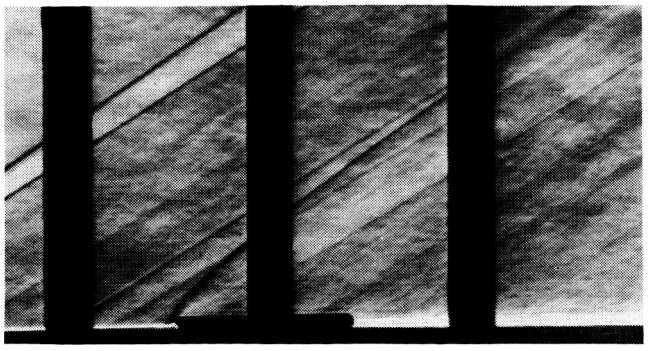

Store alone

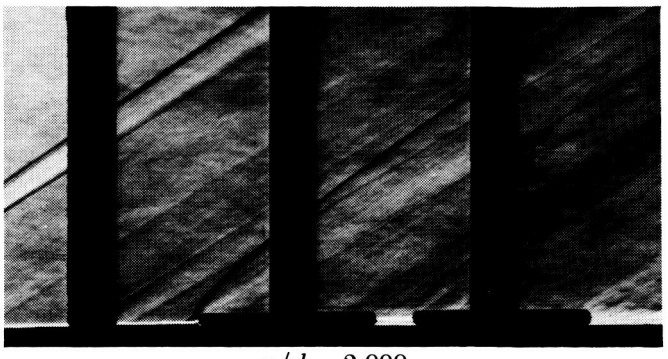

$x/d = 2.000$

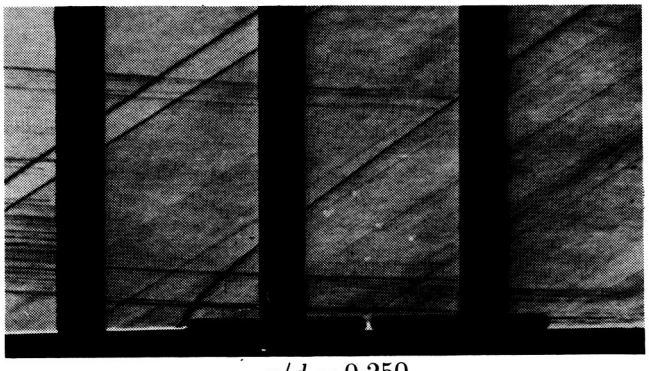

$x/d = 0.250$

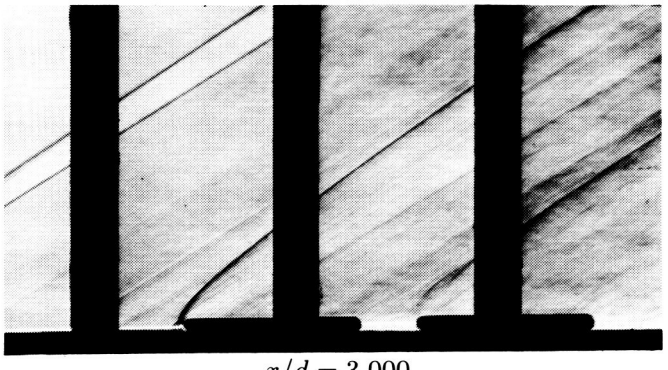

$x/d = 3.000$

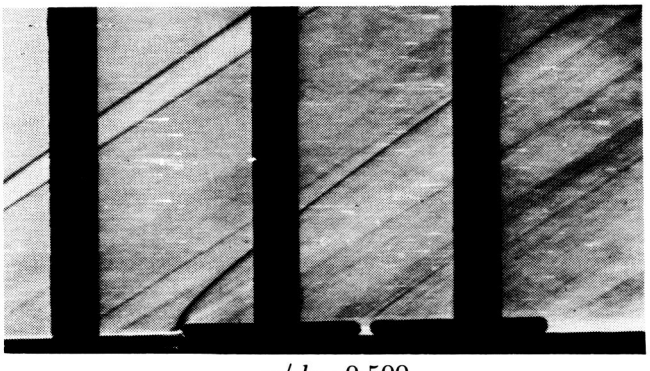

$x/d = 0.500$

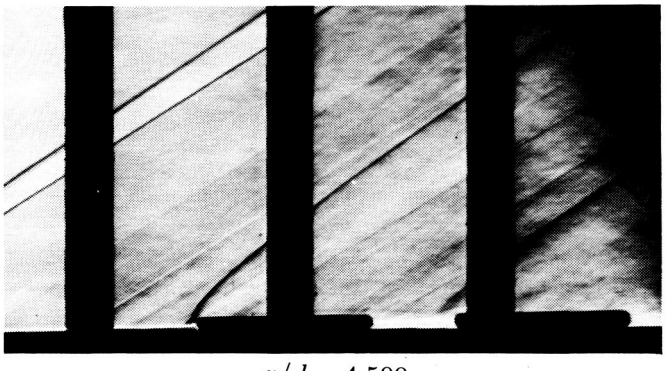

$x/d = 4.500$

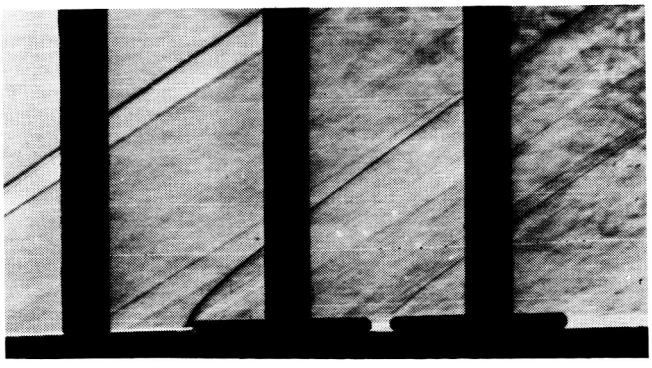

$x/d = 1.000$

(b) $M_\infty = 1.90$.

Figure 23. Continued.

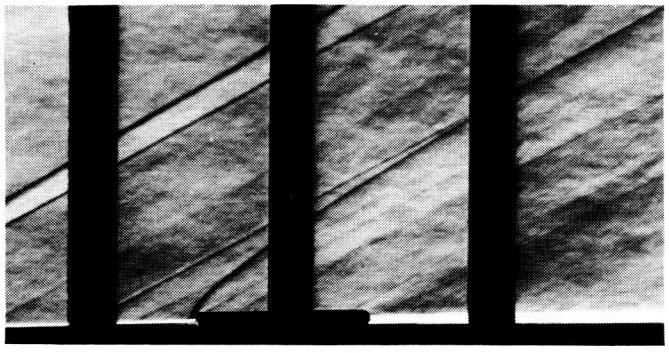

Store alone

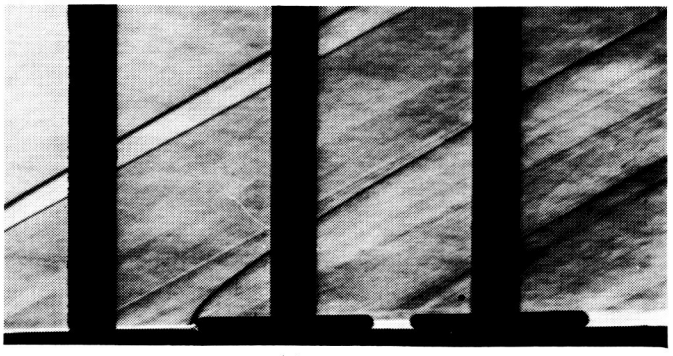

$x/d = 2.000$

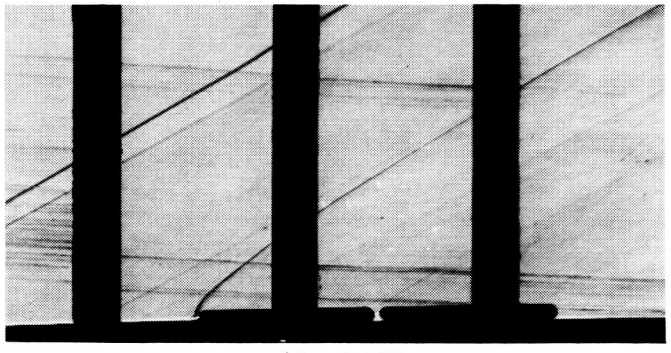

$x/d = 0.250$

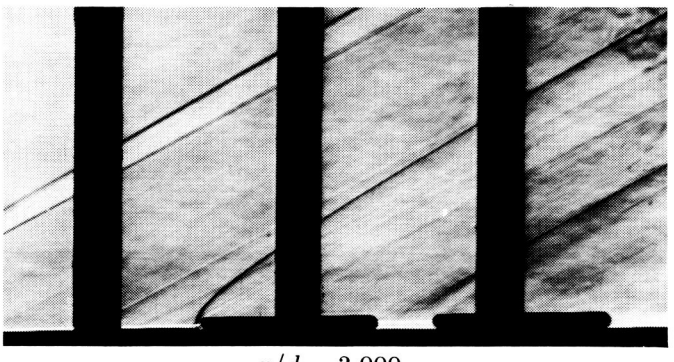

$x/d = 3.000$

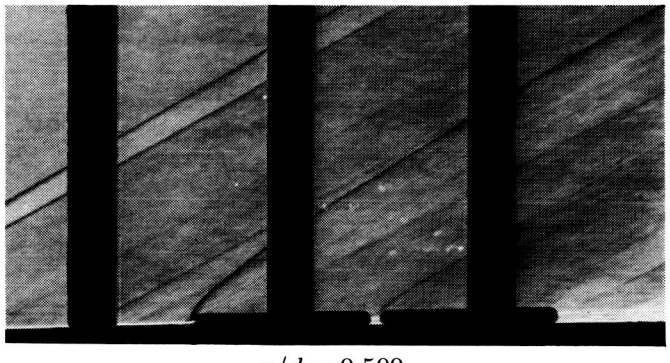

$x/d = 0.500$

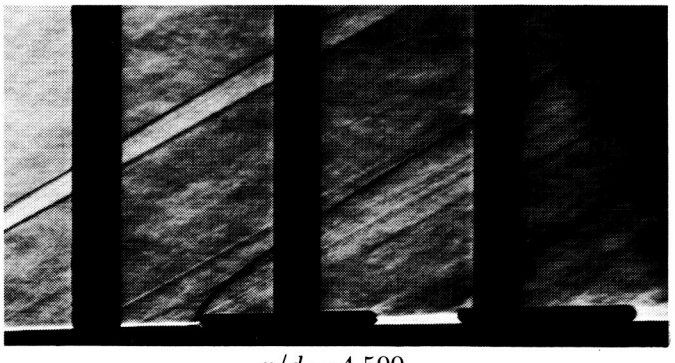

$x/d = 4.500$

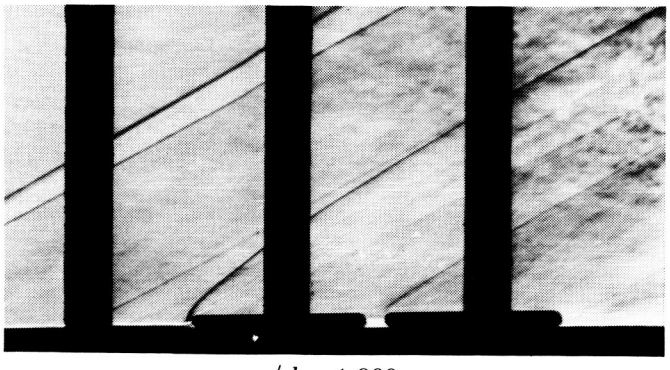

$x/d = 1.000$

(c) $M_\infty = 2.16$.

Figure 23. Continued.

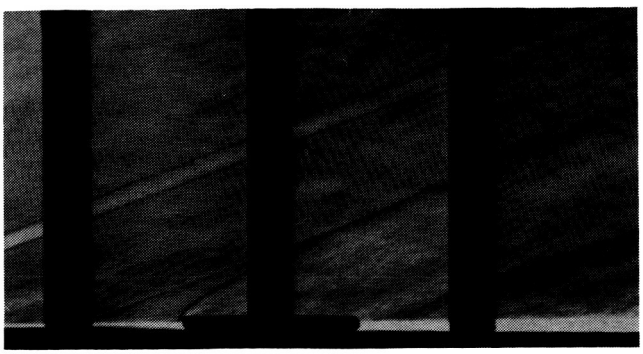

Store alone

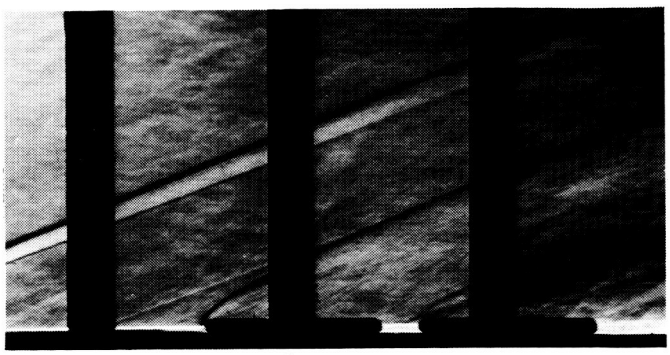

$x/d = 2.000$

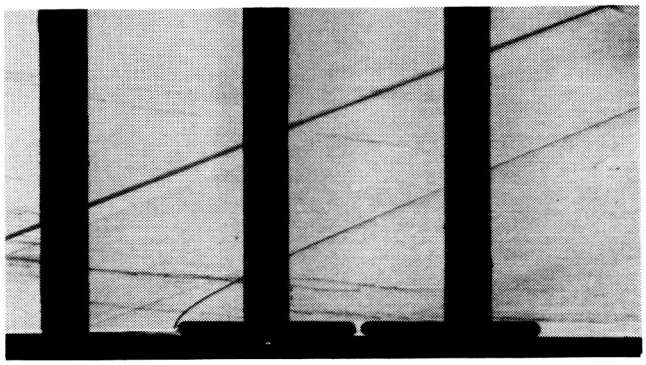

$x/d = 0.250$

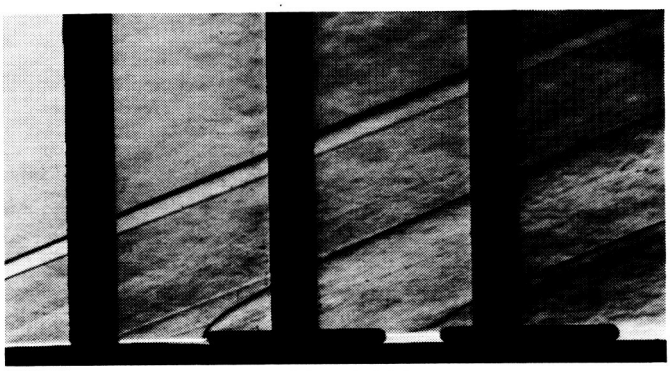

$x/d = 3.000$

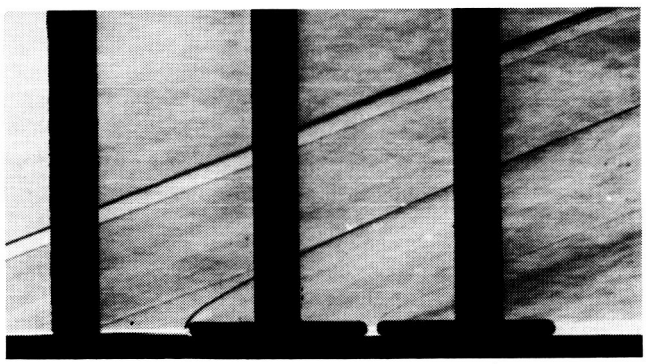

$x/d = 0.500$

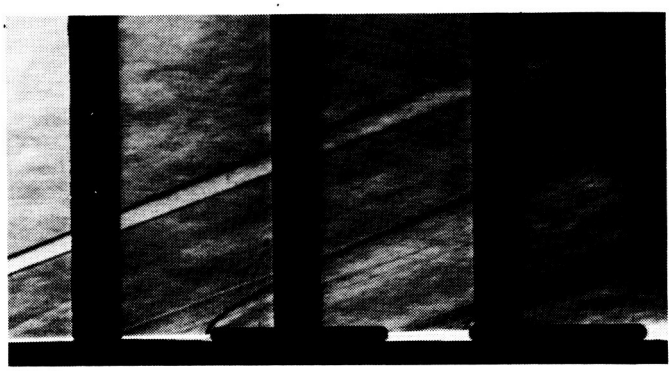

$x/d = 4.500$

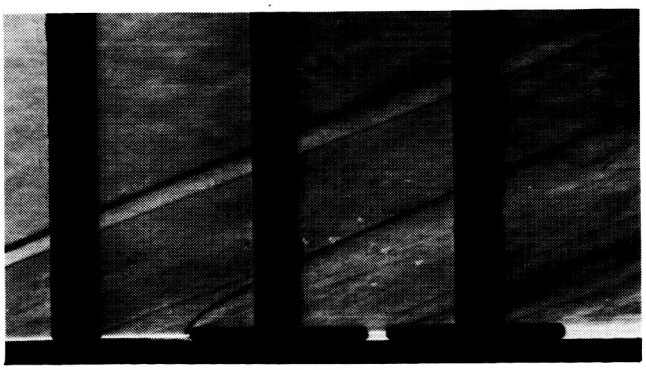

$x/d = 1.000$

(d) $M_\infty = 2.86$.

Figure 23. Concluded.

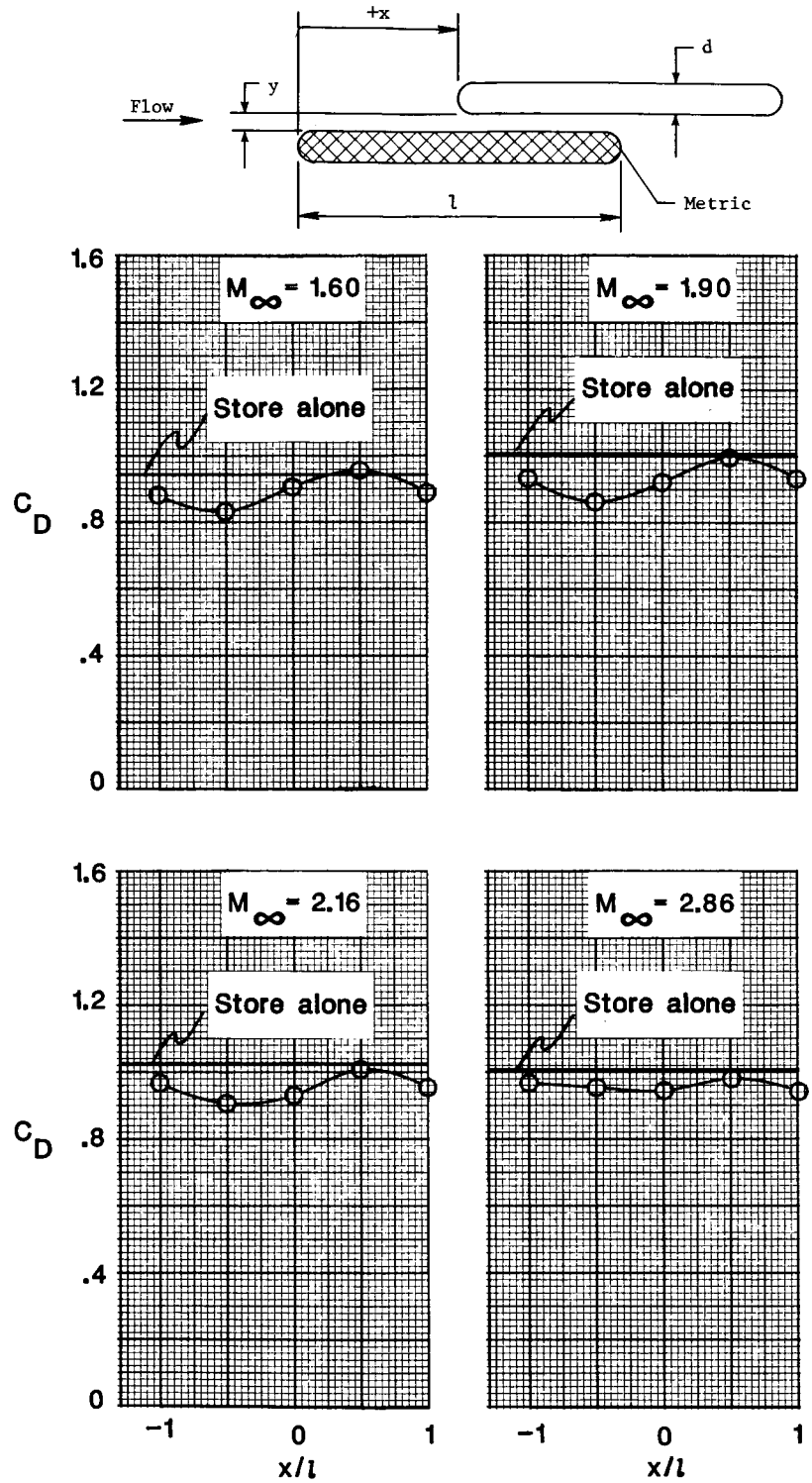

Figure 24. Staggered spacing effects for two-store arrangement. $y/d = 0.500$.

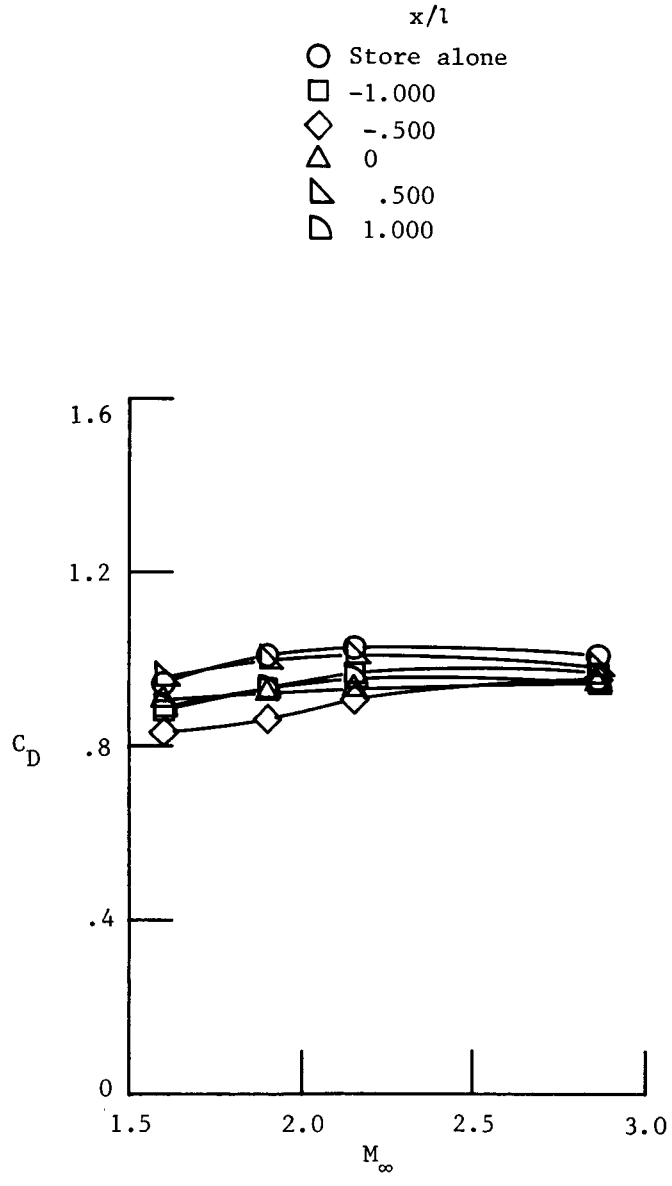

Figure 25. Mach number effects for two-store staggered spacing arrangement. $y/d = 0.500$.

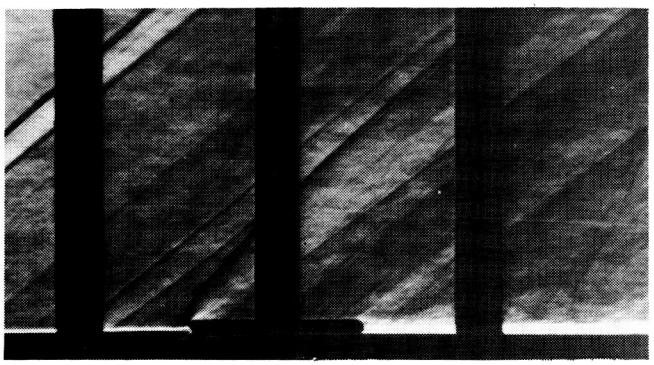

Store alone

NO DATA

$x/l = 0.000$

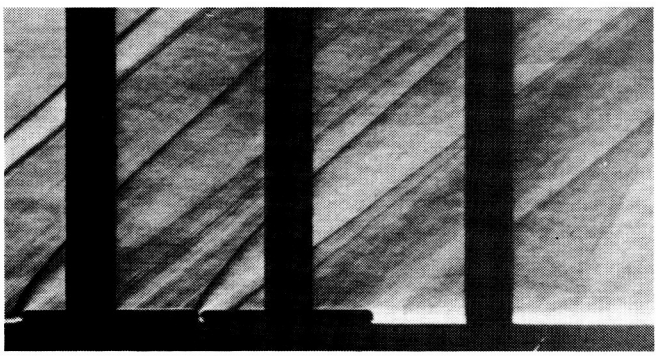

$x/l = -1.000$

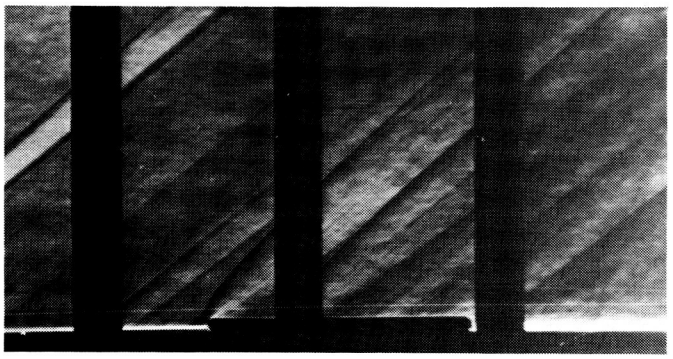

$x/l = 0.500$

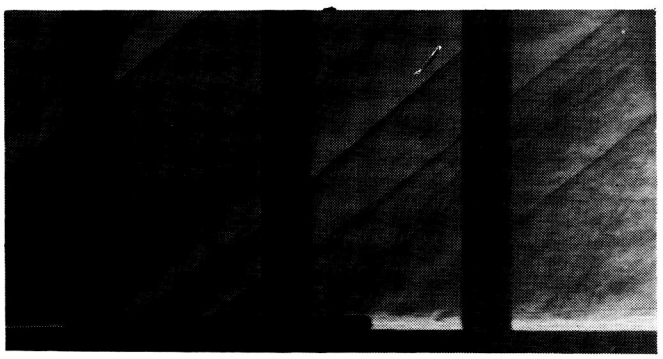

$x/l = -0.500$

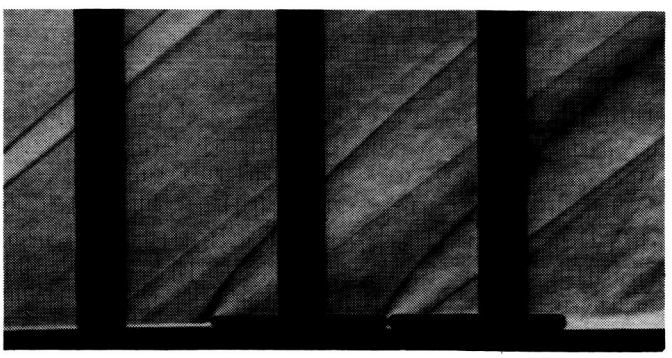

$x/l = 1.000$

(a) $M_\infty = 1.60$.

Figure 26. Schlieren photographs of two-store staggered spacing arrangement. $y/d = 0.500$.

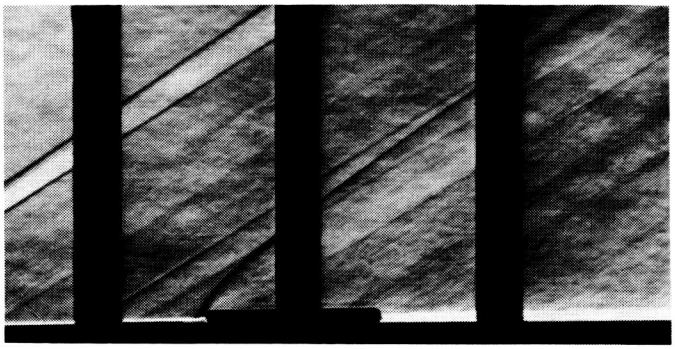

Store alone

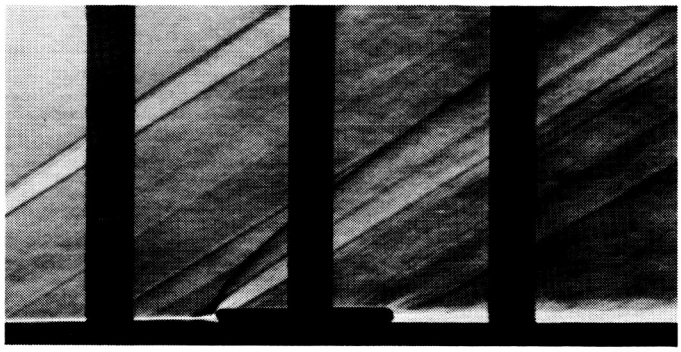

$x/l = 0.000$

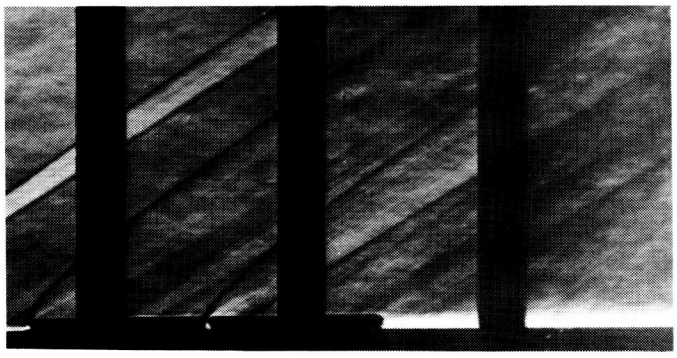

$x/l = -1.000$

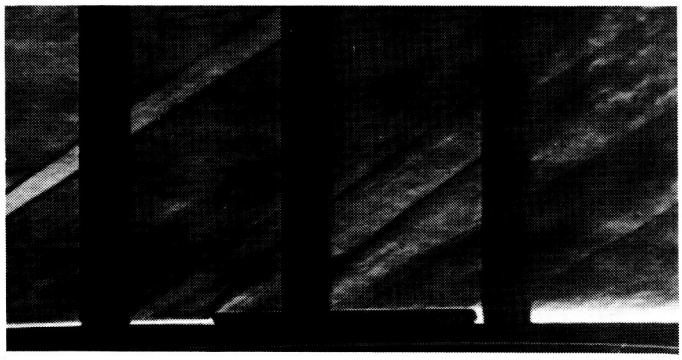

$x/l = 0.500$

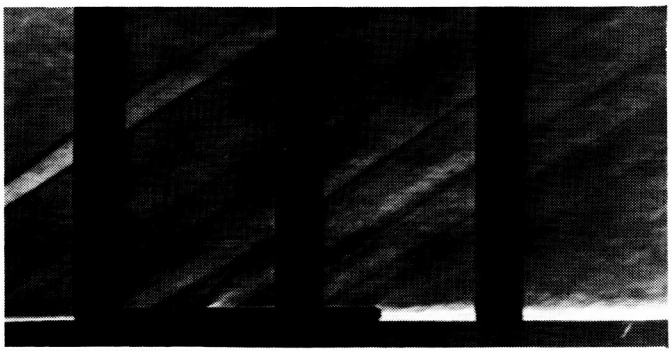

$x/l = -0.500$

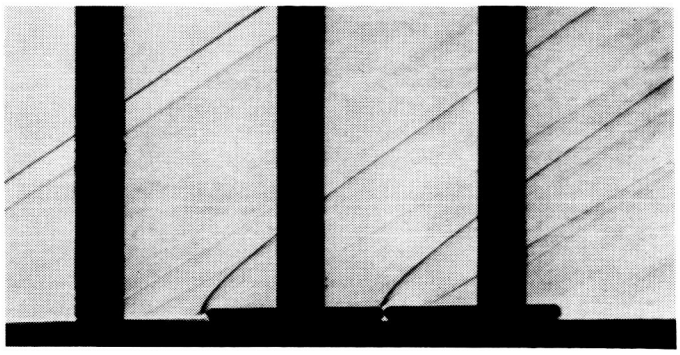

$x/l = 1.000$

(b) $M_\infty = 1.90$.

Figure 26. Continued.

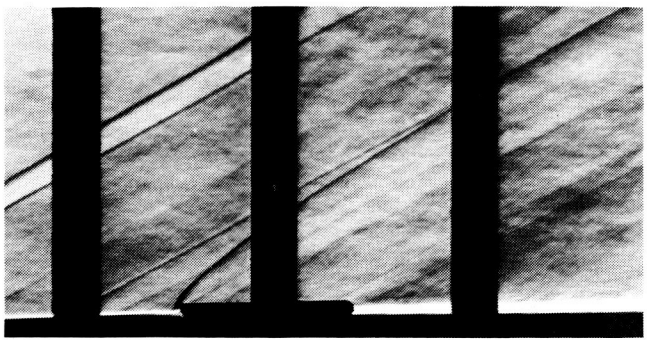

Store alone

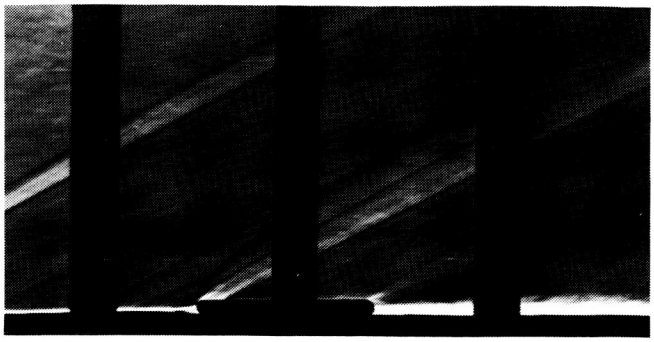

$x/l = 0.000$

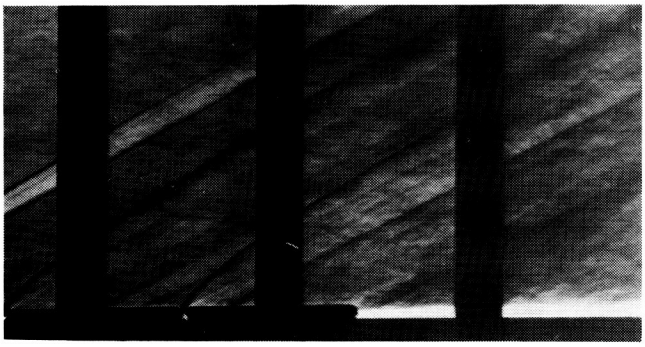

$x/l = -1.000$

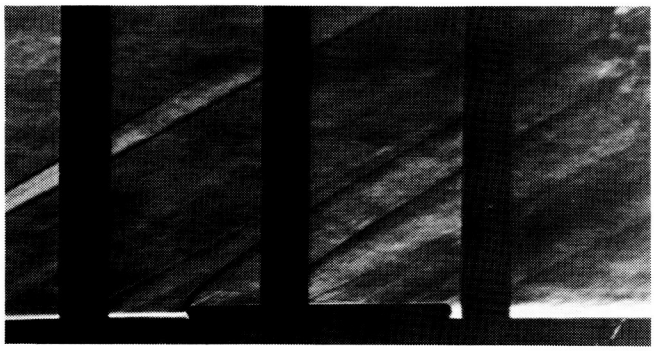

$x/l = 0.500$

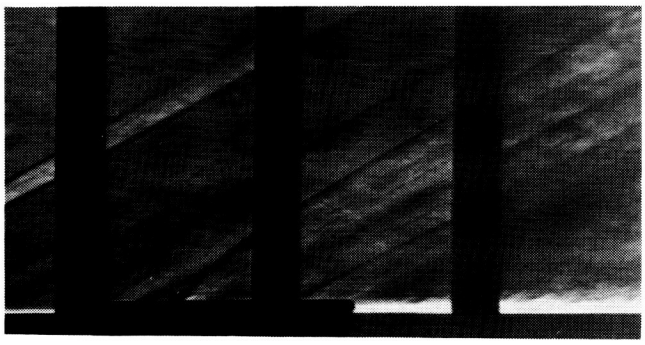

$x/l = -0.500$

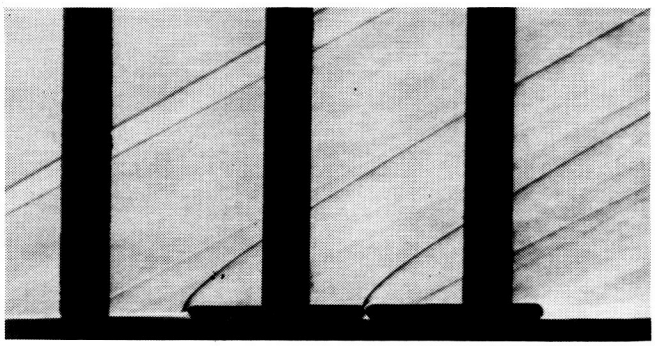

$x/l = 1.000$

(c) $M_\infty = 2.16$.

Figure 26. Continued.

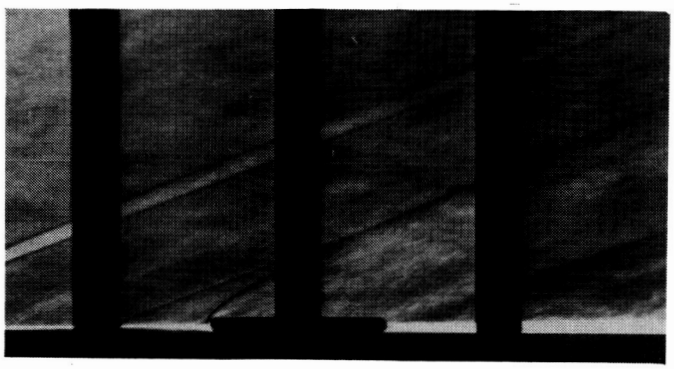

Store alone

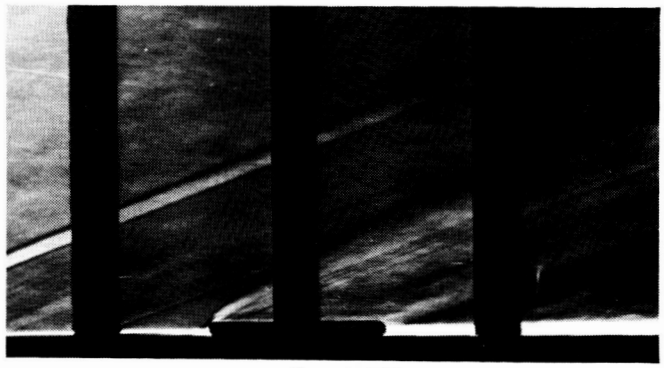

$x/l = 0.000$

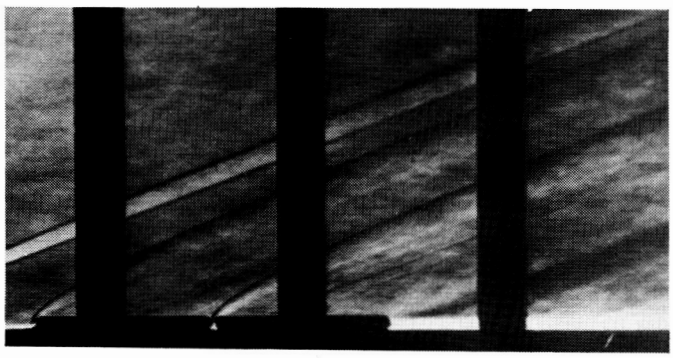

$x/l = -1.000$

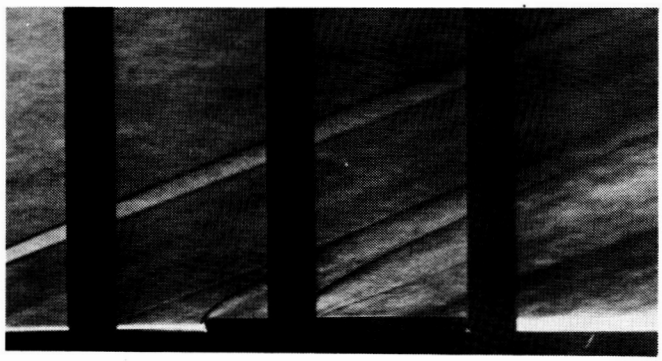

$x/l = 0.500$

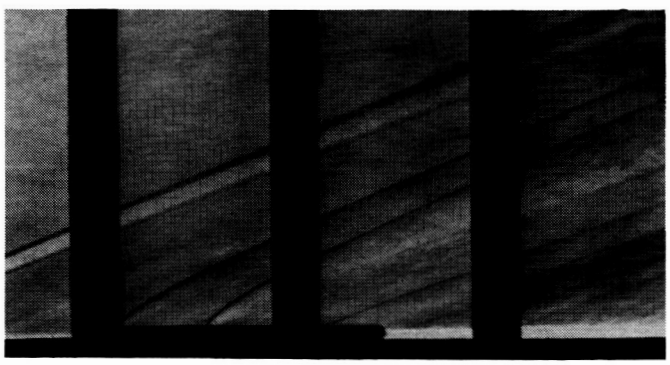

$x/l = -0.500$

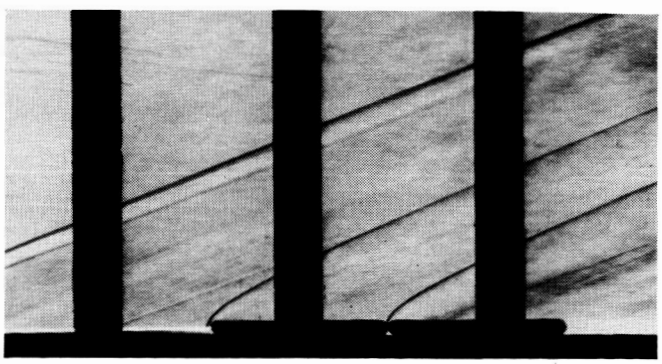

$x/l = 1.000$

(d) $M_\infty = 2.86$.

Figure 26. Concluded.

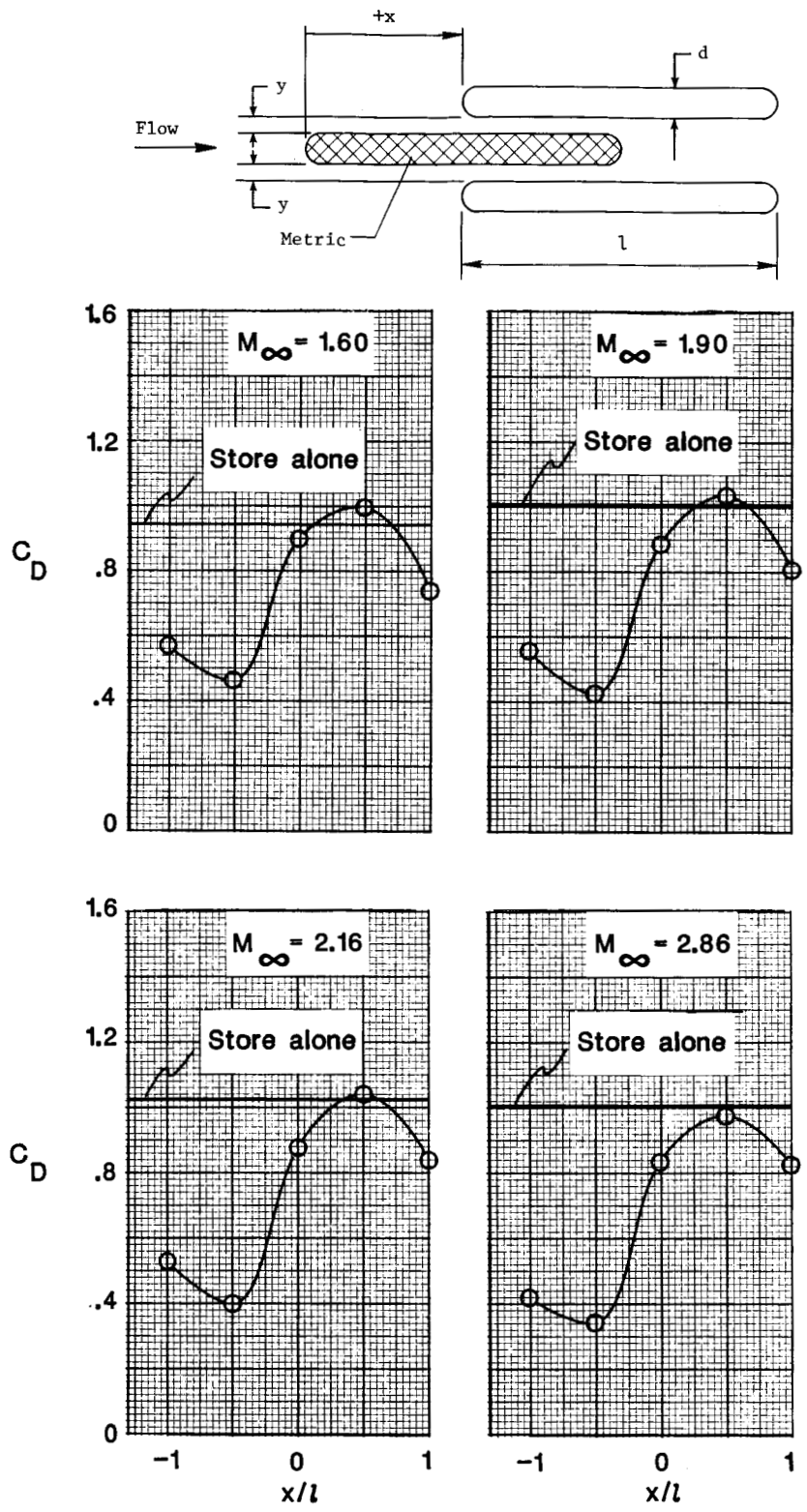

Figure 27. Staggered spacing effects for three-store arrangement with metric store in middle position. $y/d = 0.500$.

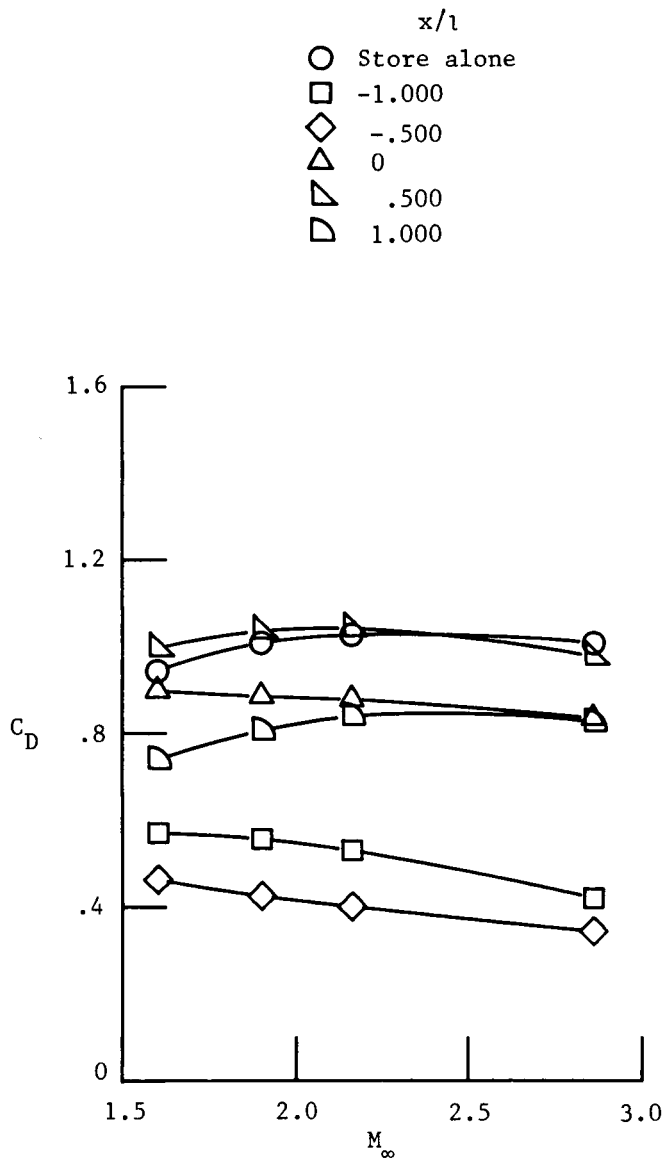

Figure 28. Mach number effects for three-store staggered arrangements with metric store in middle position.

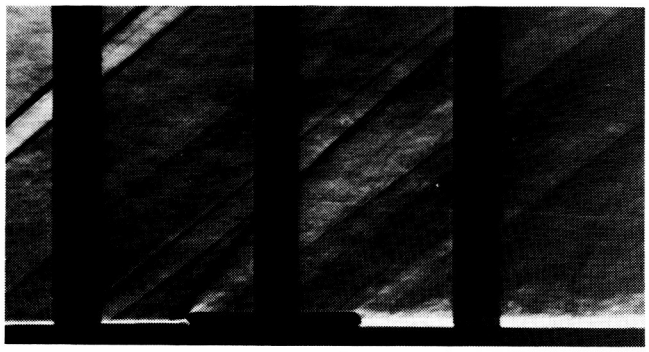

Store alone

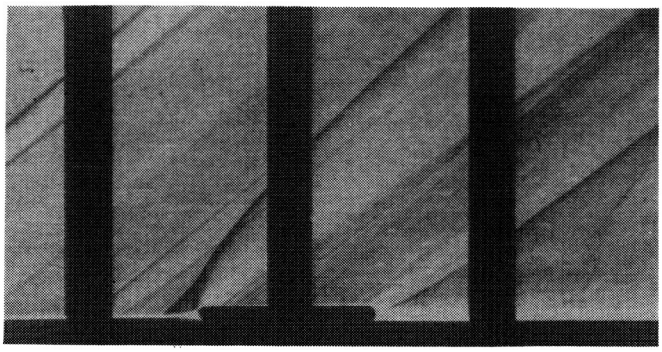

$x/l = 0.000$

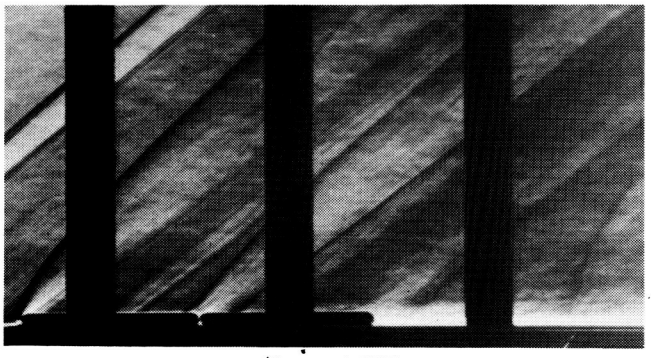

$x/l = -1.000$

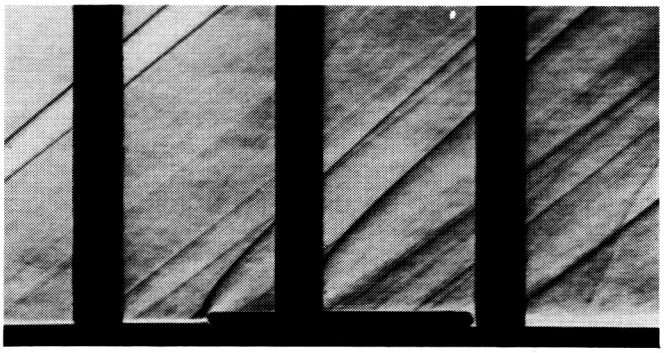

$x/l = 0.500$

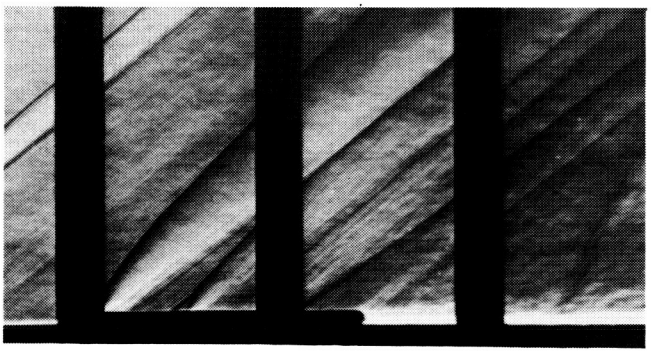

$x/l = -0.500$

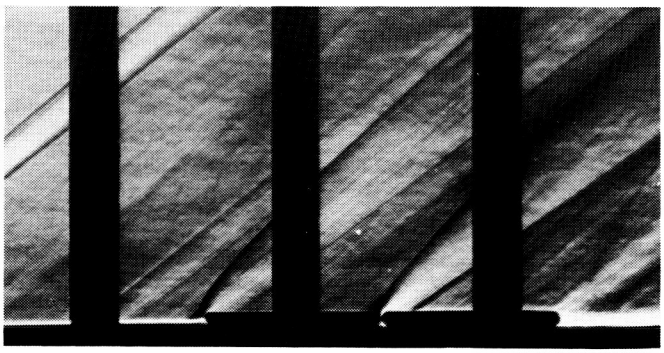

$x/l = 1.000$

(a) $M_\infty = 1.60$.

Figure 29. Schlieren photographs of three-store staggered spacing arrangement. $y/d = 0.500$.

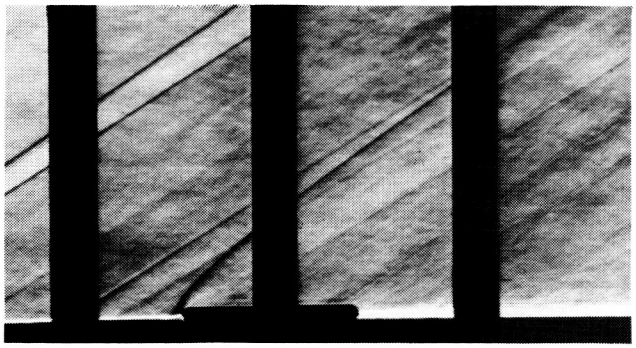

Store alone

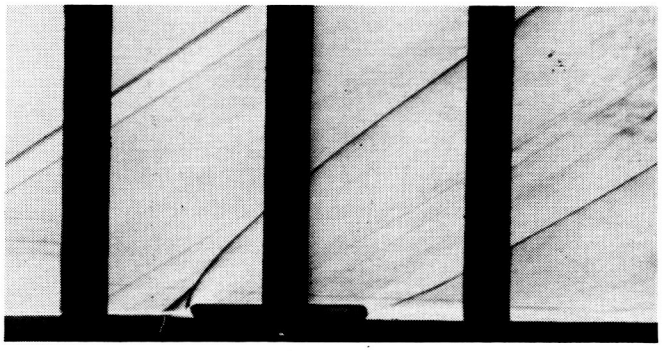

$x/l = 0.000$

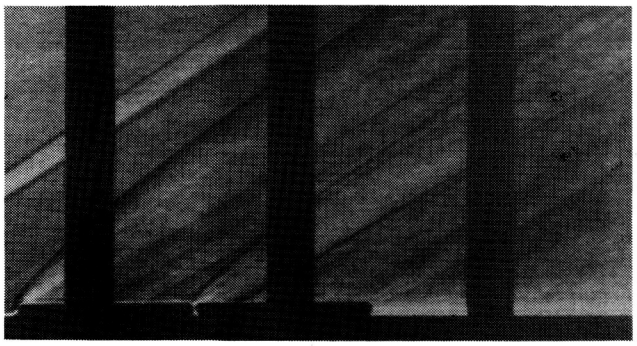

$x/l = -1.000$

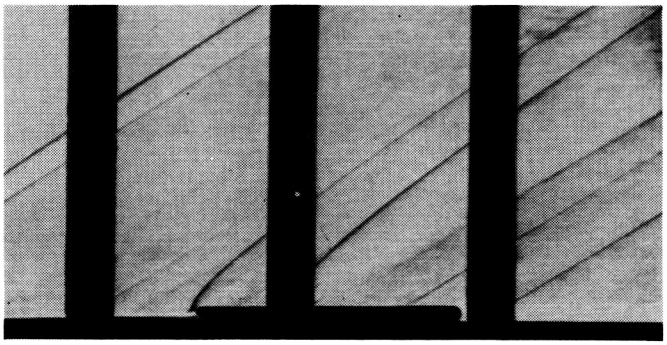

$x/l = 0.500$

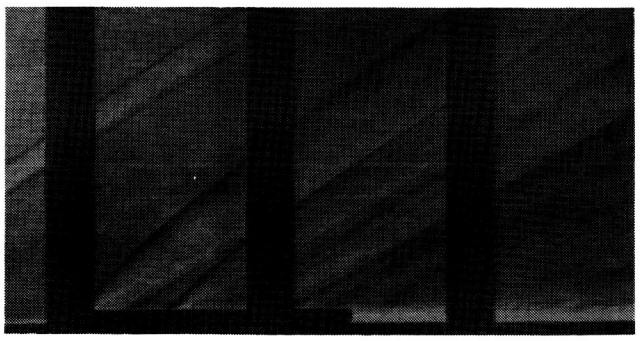

$x/l = -0.500$

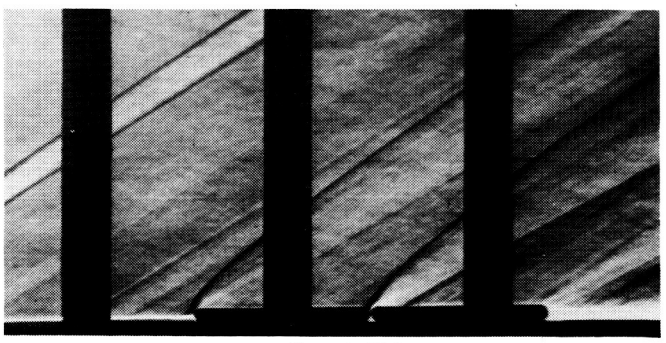

$x/l = 1.000$

(b) $M_\infty = 1.90$.

Figure 29. Continued.

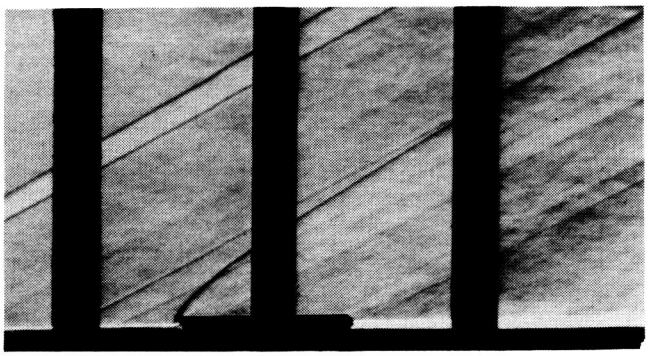

Store alone

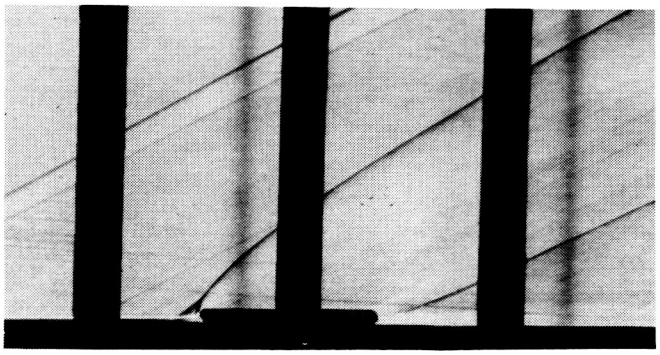

$x/l = 0.000$

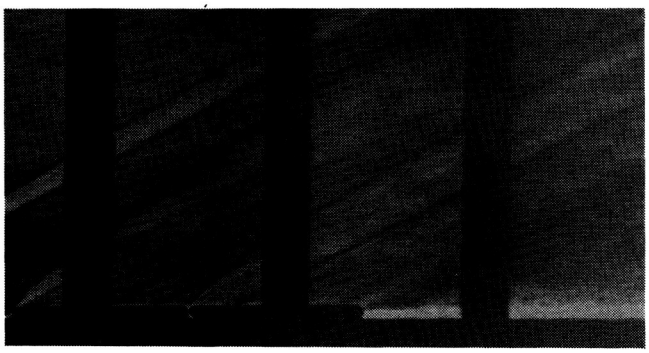

$x/l = -1.000$

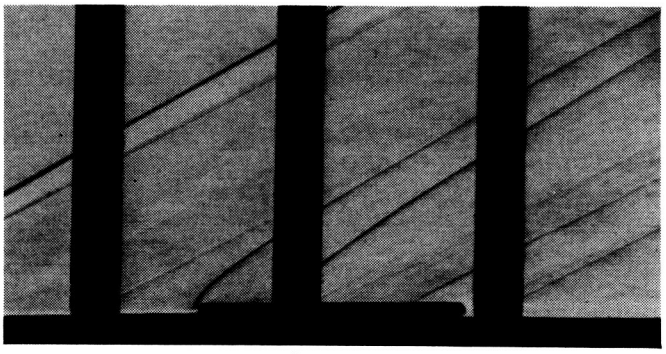

$x/l = 0.500$

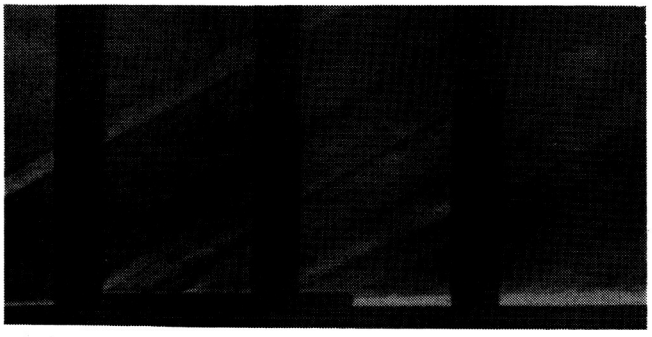

$x/l = -0.500$

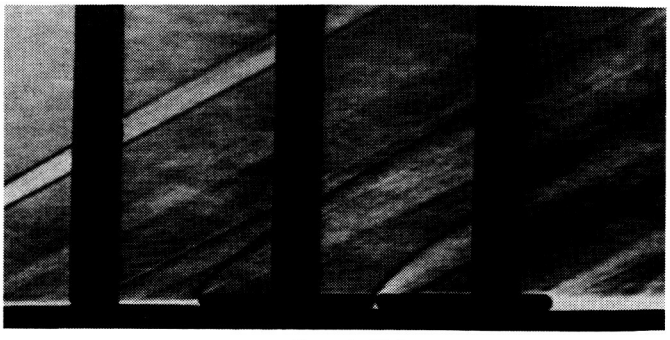

$x/l = 1.000$

(c) $M_\infty = 2.16$.

Figure 29. Continued.

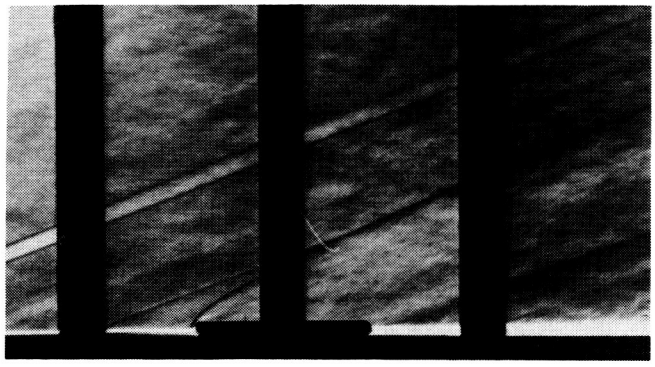

Store alone

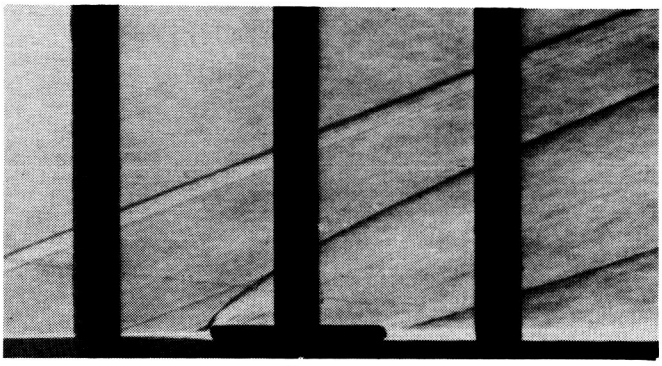

$x/l = 0.000$

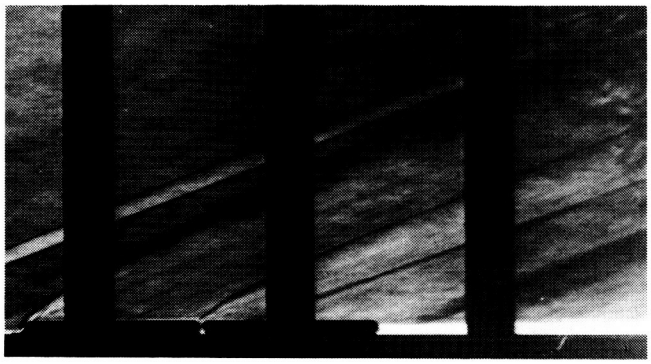

$x/l = -1.000$

NO DATA

$x/l = 0.500$

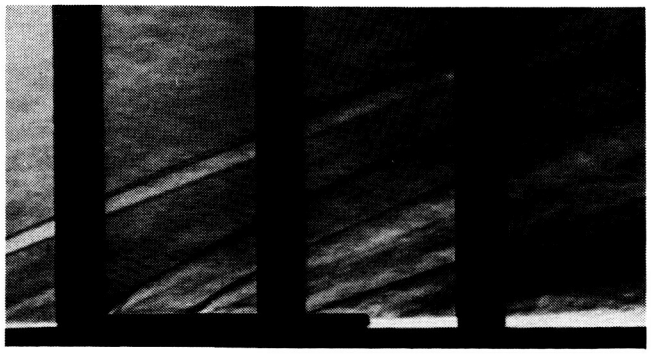

$x/l = -0.500$

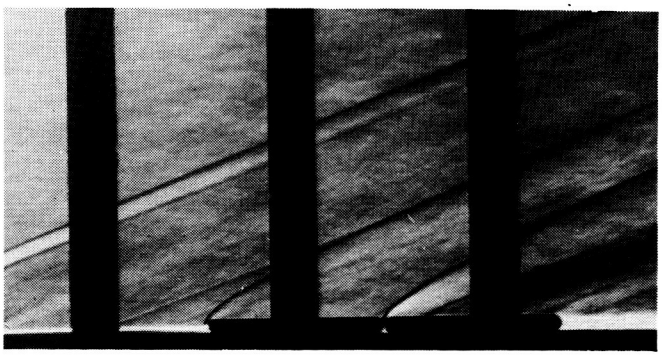

$x/l = 1.000$

(d) $M_\infty = 2.86$.

Figure 29. Concluded.

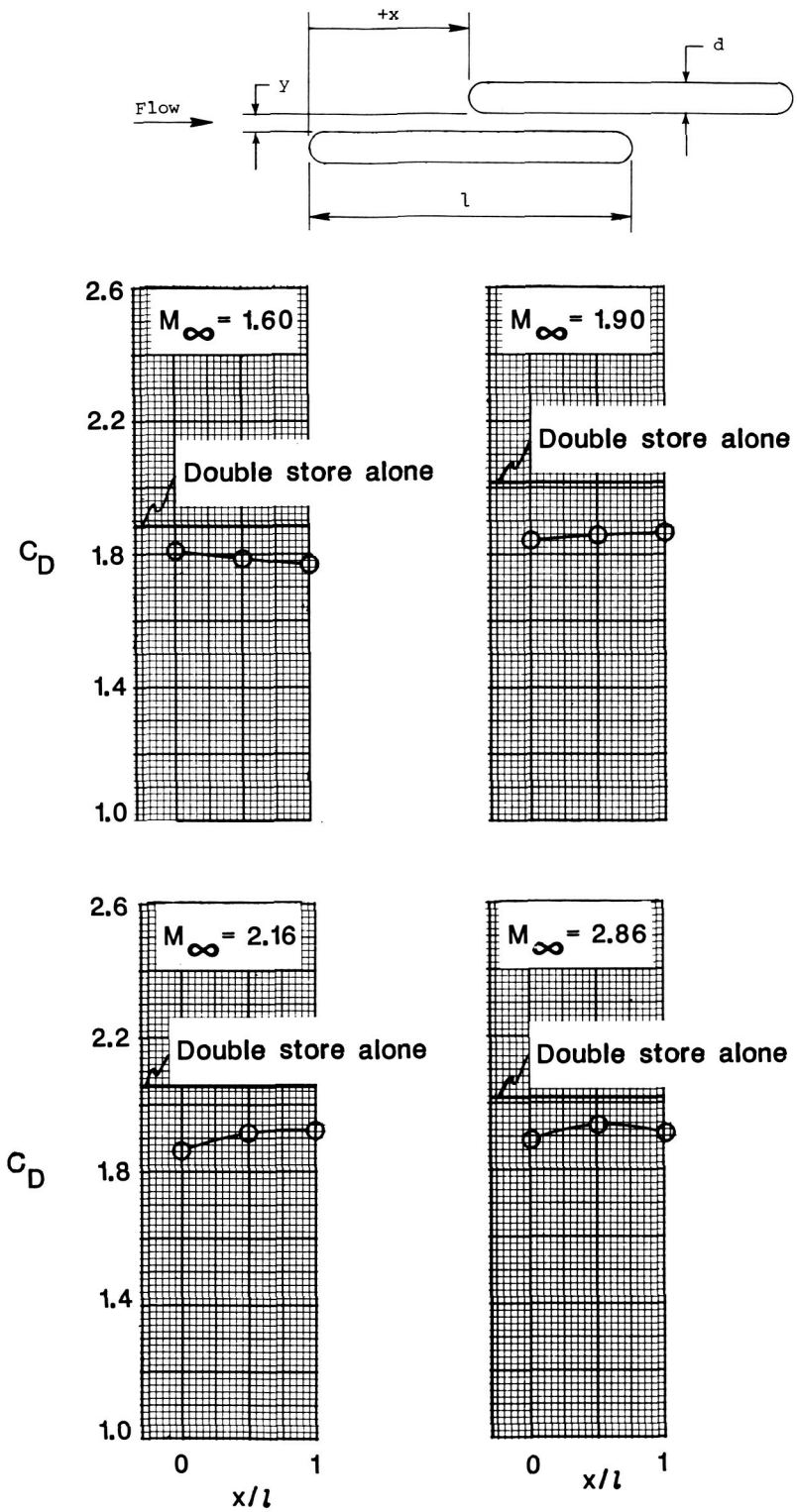

Figure 30. Total configuration drag of two-store staggered spacing arrangement.

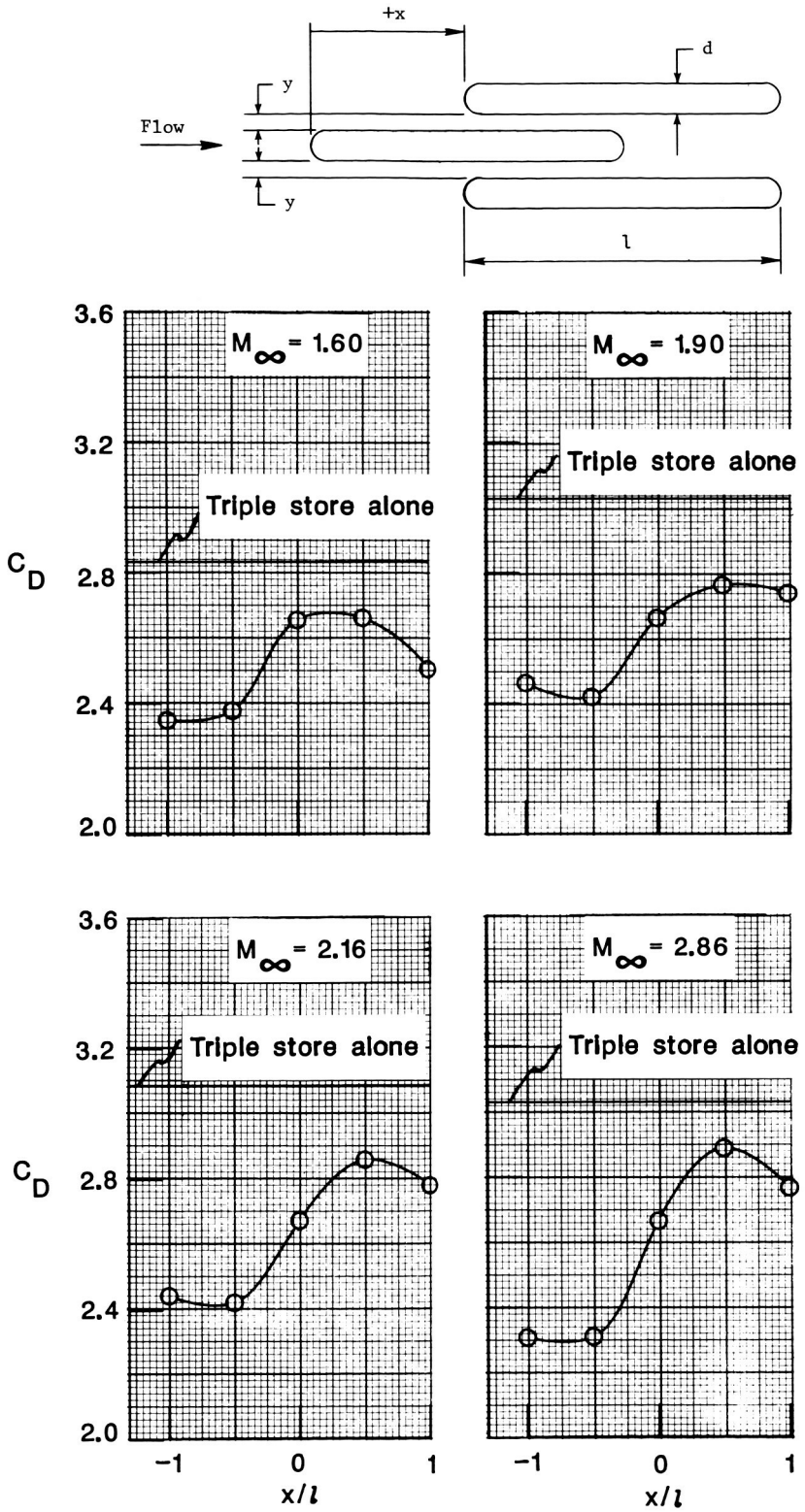

Figure 31. Total configuration drag of three-store staggered spacing arrangement.

NASA
National Aeronautics and Space Administration

Report Documentation Page

1. Report No.	2. Government Accession No.	3. Recipient's Catalog No.
NASA TP-2742		

4. Title and Subtitle	5. Report Date
Drag Measurements of Blunt Stores Tangentially Mounted on a Flat Plate at Supersonic Speeds	September 1987
	6. Performing Organization Code
7. Author(s)	8. Performing Organization Report No.
Floyd J. Wilcox, Jr.	L-16284
9. Performing Organization Name and Address	10. Work Unit No.
NASA Langley Research Center Hampton, VA 23665-5225	505-61-71-01
	11. Contract or Grant No.
12. Sponsoring Agency Name and Address	13. Type of Report and Period Covered
National Aeronautics and Space Administration Washington, DC 20546-0001	Technical Paper
	14. Sponsoring Agency Code

15. Supplementary Notes

16. Abstract

An investigation has been conducted in the Langley Unitary Plan Wind Tunnel to measure the drag of blunt stores (hemispherical noses and afterbodies) tangentially mounted in various arrays on a flat plate at nominal Mach numbers of 1.60, 1.90, 2.16, and 2.86 and at a nominal Reynold number of 2×10^6 per foot. The arrays consisted of two and three stores mounted in lateral, tandem, or staggered arrangements. The relative positions of the stores in the arrays were varied while the drag of only one store was measured to determine the effect of spacing on the store drag. Store-on-store interference was determined by comparing the drag of a single store with the drag of the store in an array. The results indicate virtually all arrangements and spacings which were tested had favorable store-on-store interference (drag reduction) across the Mach number range. Tabulated data, schlieren photographs, and shadowgraphs are included.

17. Key Words (Suggested by Authors(s))
Supersonic store drag
Store carriage drag
Store interference
External store drag
Tangent store carriage

18. Distribution Statement
Unclassified—Unlimited

Subject Category 02

19. Security Classif.(of this report)	20. Security Classif.(of this page)	21. No. of Pages	22. Price
Unclassified	Unclassified	66	A04

NASA FORM 1626 OCT 86

NASA-Langley, 1987

For sale by the National Technical Information Service, Springfield, Virginia 22161-2171